Universität Augsburg University

Plant-soil interaction and soil carbon turnover across geochemical and topographic gradients in African tropical montane forests

Inaugural-Dissertation zur Erlangung des naturwissenschaftlichen Doktorgrades (Dr. rer. nat.) der Universität Augsburg (Fakultät für Angewandte Informatik)

Vorgelegt von

Benjamin Bukombe

Augsburg 2023

First Reviewer: Prof. Dr. Sebastian Dötterl, ETH Zürich

Second Reviewer: Prof. Dr. Peter Fiener, Augsburg University

Date of oral exam: June 30th, 2023

Contents

Acknowledgements ii
List of figures iii
List of tables iv
List of equations v
Summary vi
Zusammenfassung viii
1. General introduction 1
1.1. Problem statement 3
1.2. Thesis objectives 5
1.3. Data and study area 6
2. Nutrient uptake and canopy chemistry in Afromontane forest ecosystems 11
2.1. Introduction 11
2.2. Material and methods 12
2.3. Results 14
2.4. Discussion 21
2.5. Conclusions 24
3. Carbon allocation, stocks and dynamics in distinct African tropical forest ecosystems 25
3.1. Introduction 25
3.2. Material and methods 29
3.3. Results 37
3.4. Discussion 45
3.5. Conclusions 52
4. Heterotrophic soil respiration and carbon cycling in African tropical forest soils 53
4.1. Introduction 53
4.2. Materials and methods 56
4.4. Results 61
4.5. Discussion 68
4.6. Conclusions 73
5. Synthesis and general conclusions 75
5.1. Main findings and synthesis 76
5.2. General conclusions 80
References 81
Appendices 99
Scientific contributions 121

Acknowledgements

This thesis was funded in the framework of Deutsche Forschungsgemeinschaft (DFG) Emmy Noether group through TROPSOC (project no. 387472333). Further financial support for writing this thesis was provided by the German Academic Exchange Service through the international office of Augsburg University. Field campaign and experiments were organized in collaboration with Université Catholique de Bukavu in the Democratic Republic of Congo and Mountains of the Moon University in Uganda. Part of the laboratory analyses was funded by the Soil Resources Group at ETH Zurich and the Department of Biogeochemical Processes at Max Planck Institute for Biogeochemistry, Jena. I thank you all for your support and collaboration. Special thanks goes to my thesis advisors "Sebastian Dötterl and Peter Fiener" for their support and guidance during my research project. This PhD project has been a great learning journey for me. I would like to thank my colleagues "Daniel Muhindo, Laurent Kidinda, and Mario Reichenbach" without you guys that field campaign could not be possible. I appreciate the friendship we built through our common projects. Special thanks goes to the TROPSOC team for their support in the lab and field work helpers who made the sampling campaign possible under difficult conditions. Thanks, to Landry Ntaboba Cizungu for his support during my field campaign and stay in DRC. Thanks to my fellow colleagues at the Water and Soil Resource Research Group (Anna, Florian, Joseph, Kathi, Raphael, and Tabea) for their feedback during our seminars. The "After-work beer time" has been one of the most entertaining moments I experienced in Augsburg. Special thanks goes to Anna Stegmann for her support during my studies and stay in Augsburg. I also thank all members of the Soil Resources Group at ETH Zurich for their support during my research visit and lab work at ETH. Special thanks goes also to Laura and Marina for their warm welcome and for hosting me during my visits to Zurich. I thank Marijn Bauters, the external reviewer of this thesis, I enjoyed working with you and I hope, we will keep this collaboration in the future. Thanks to Boris for hosting me during my research, visit at BOKU in Vienna and for helping with the organization of root monitoring. I would like to thank Laura Summerauer, Matt Cooper, and Jake Simpson for their valuable feedback on this thesis. I would like to thank my wife Hella, for her support and positive messages in difficult times as well as feedback while writing this thesis. Special thanks go to my dear friend and Brother Mutware Rugenerwa for making all TROPSOC campaigns possible. I thank you for facilitating field experiments and cross-border samples and equipment shipment. This PhD project was possible because of your incredible support.

List of figures

Figure 1. Framework and thesis outline: A Complete flow chart of the research project.…X
Figure 1.1. Overview of the study region and location of the study sites in central Africa 8
Figure 2.1. Concentration of major nutrients across geochemical regions.....16
Figure 2.2. Concentration of base cations across geochemical regions…….17
Figure 2.3. Pearson correlations between canopy chemistry and soil geochemical properties.19
Figure 2.4. Standardized effects size of (RC) as explanatory factors on leaf macronutrients. 20
Figure 3.1. C stocks of above- and belowground biomass across geochemical regions……..39
Figure 3.2. NPP and C allocation across geochemical regions.....41
Figure 3.3. rPCA of soil properties and their relation to NPP components.....42
Figure 3.4. Effect size of RC as explanatory factors on NPPlitterfall, NPPwood, NPProots..44
Figure 3.5. Relationship between tree growth indices.....46
Figure 3.6. Pearson correlations between geochemical soil properties and NPP C allocation.48
Figure 4.1. C:N ratio as points and specific potential respiration for non-valley positions. ...63
Figure 4.2. $\Delta^{14}C$ of bulk soil and respired CO_2 …. 65
Figure 4.3. Partial correlations between SPR and $\Delta - \Delta^{14}C$ controlling for soil depth……...68
Figure 5.1. Synthesis of the thesis with highlights of main topics covered and key findings..75
Figure S2.1.Canopy chemistry along topographic positions for the three geochemical ……99
Figure S2.2. Pearson correlations between canopy chemistry.....100
Figure S2.3. Biplot showing correlation between independent variables.....101
Figure S3.1. Contribution of each diameter class to the total number of trees per unit area….106
Figure S3.2. Species composition and similarities across geochemical regions…….107
Figure S3.3. NPP allocation for three components across regions and topography……...108
Figure S3.4. Correlations between NPP and NPP allocation……..109
Figure S3.5. C:N ratio of living leaves and litter layer for three geochemical regions……..110
Figure S3.6. Relative root biomass along soil depth for three geochemical regions……..111
Figure S4.1. Pearson correlation between $\Delta^{14}C$, SPR and soil available nutrient.…….116
Figure S4.2. Pearson correlation between $\Delta^{14}C$ and SPR…….……..……...117
Figure S4.3. Pearson correlation between SPR and sum of pedogenic oxides ……..….117
Figure S4.4. Pearson correlation between $\Delta^{14}C$ of respired CO_2 and SPR ……..…..118

List of tables

Table 4.1. Chemical composition of unweathered rock samples……56
Table 4.2. Biogenic and geogenic organic carbon contribution in the sedimentary region….65
Table 4.3. Results of three regression models for SPR and $\Delta - \Delta^{14}C$.……..…….....67
Table S2.1.Major nutrients in the canopy along topographic positions……102
Table S2.2.Results of the mixed effects models for canopy chemistry……103-104
Table S2.3.Rotated principal component analysis for canopy chemistry.....105
Table S3.1.Mineral soil properties of the three geochemical regions…….....112
Table S3.2.General plots information for all investigated sites.....……113
Table S3.3.Forest stands characteristics across geochemical regions……..…114
Table S3.4.Rotated principal components analysis for NPP and C allocation .....……...115
Table S4.1.Rotated principal component analysis for SPR and $\Delta^{14}C$…… ...119
Table S4.2.Overview of soil properties and fertility indicators assessed for SPR and $\Delta^{14}C$..120

List of equations

Eq.3. 1. NPP wood……..…....29
Eq.3. 2. Relative tree growth rate……..…...…29
Eq.3. 3. Wood turnover rate……..29
Eq.3. 4. Litter productivity……31
Eq.3. 5. Fine root productivity…….…....33
Eq.3. 6. Fine root turnover rate…….…....33
Eq.3. 7. NPP sum…….....33
Eq.3. 8. Carbon allocation into different NPP compartments……..…….33
Eq.4. 1. Fraction of C originating from biogenic vs geogenic organic C…….…..57
Eq.4. 2. Proportion of biogenic organic C…….……...59
Eq.4. 3. Proportion of geogenic organic C…….....59

Summary

Tropical forests play a central role in global carbon (C) cycles due to the high exchange rate of carbon between plants, soil, and the atmosphere. Nutrient availability in tropical forest systems controls these exchanges via their impact on tree growth, carbon productivity, and stocks. Research shows that local edaphic factors such as soil parent material and topography co-determine nutrient availability. However, the process knowledge of how tropical forests respond to changes in nutrients, the chemistry of the local parent material and topography, and the effect this has on C cycling between plants, soils, and the atmosphere remains unclear. This gap in knowledge obstructs the mechanistic understanding of the controls of C cycling in tropical forest systems. Furthermore, data for African tropical forests are scarce, as most research has focused mainly on Amazon and South Asia. This thesis tried to answer these questions and provided directions on where future research can focus.

This thesis is based on both experimental (field and laboratory) and observational studies at different sites in the Eastern Congo Basin and along the Albertine Rift Valley System. It has three major parts: (a) nutrient uptake and distribution in the canopy of African tropical forests, (b) C stocks, Net Primary Productivity (NPP), and NPP C allocation between plant compartments, and (c) soil potential heterotrophic respiration (SPR) and soil organic carbon (SOC) turnover rate in forests developed along geochemical and topographic gradients. Specifically, the thesis focused on three contrasting geochemical regions (mafic magmatic, felsic metamorphic, and a mixture of sedimentary rock but distinct from mafic and felsic. Throughout the thesis, the three regions are referred to as “mafic”, “felsic”, and “sedimentary).

Chapter 2 assessed canopy chemistry of 344 samples collected from different tree species growing on different parent materials and topographic positions. The data shows that tropical forest canopy chemistry shifts significantly when local soils and parent material geochemistry indicate fertility constraints, mainly due to low amounts of rock-derived nutrients. In contrast, topography did not affect canopy chemistry in the three investigated geochemical regions.

Chapter 3 assessed the effects that soil parent material and topography as drivers of soil fertility have on forest NPP, C allocation, and biomass C stocks and how they relate to SOC stocks. Here a combination of two years monitoring of vegetation growth and soil geochemical properties measurements were used. The thesis found that soil fertility parameters reflecting the local parent material are the main drivers of NPP and C allocation patterns in tropical

montane forests, resulting in significant differences in below to aboveground biomass ratio across geochemical regions. Topography did not constrain the variability in C allocation and NPP. Furthermore, SOC stocks showed no relation to C input in tropical forests. Instead, plant C input seemingly exceeded the maximum potential of these soils to stabilize C.

Chapter 4 assessed potential heterotrophic soil respiration and SOC turnover via lab-based incubation experiments. Here, depth explicit SPR and $\Delta^{14}C$ of samples originating from the three geochemical regions and topographic positions were measured under constant temperature and moisture conditions. The results revealed distinct patterns in soil respiration with soil depth and parent material geochemistry. The topographic origin of the samples was not the main determinant of the observed respiration rates and $\Delta^{14}C$. However, in situ soil hydrological conditions likely influence soil C turnover by inhibiting decomposition in valley subsoils.

Overall, the results of this thesis demonstrate that, even in deeply weathered tropical soils, parent material has a long-lasting effect on soil geochemistry that can affect (1) nutrient availability, and uptake, (2) NPP, and C allocation, ultimately affecting differently above and belowground biomass, (3) microbial activity, the size of subsoil C stocks and the turnover rate of C in soil. Therefore, soil parent material and its control on soil chemistry need to be taken into account to predict C fluxes and to understand C cycling in African old-growth tropical forest systems.

Zusammenfassung

Tropische Wälder spielen eine zentrale Rolle im globalen Kohlenstoffkreislauf aufgrund der hohen Austauschraten zwischen Pflanze, Boden und Atmosphäre. Die Nährstoffverfügbarkeit steuert über die Biomasseproduktion den Kohlenstoffaustausch und damit den Kohlenstoffspeicher. Aktuelle Forschungsergebnisse zeigen, dass lokale pedogene Faktoren, wie das Ausgangsgestein oder die Topographie, die Nährstoffverfügbarkeit des Bodens maßgeblich bestimmen. Es ist jedoch unklar welchen Einfluss unterschiedliche Ausgangsgesteine und topographische Gegebenheiten auf die Kohlenstoffaustauschraten tropischer Wälder haben. Damit die komplexen Kohlenstoffflüsse von tropischen Waldsystemen in globale Erdsystemmodelle eingebracht werden können, bedarf einer Verbesserung des Verständnisses der zugrundeliegenden Prozesse. Obwohl Afrika das zweitgrößte tropische Ökosystem der Erde beheimatet, ist der Großteil der Forschung zu tropischen Wäldern auf Amazonien und Südasien beschränkt. Hieraus resultiert eine kritische Wissenslücke im Verständnis von tropischen Ökosystemen Afrikas und deren Rolle im globalen Kohlenstoffkreislauf.

Diese Dissertation basiert auf umfangreichen Feldstudien und Laborarbeiten an unterschiedlichen Waldstandorten im östlichen Kongobecken, die sich durch unterschiedliche geochemische und topographische Standortbedingungen auszeichnen. Im Fokus der Untersuchung stehen: (a) die Nährstoffaufnahme und Nährstoffverteilung im Kronendach afrikanischer Tropenwälder, (b) die C-Speicherfunktion, die Nettoprimärproduktivität (NPP) und die C-Verteilung der NPP zwischen unterschiedlichen Pflanzenorganen und (c) die potenzielle heterotrophe Bodenatmung (SPR) und die Mineralisierungsraten des organischen Bodenkohlenstoffs (SOC). Die Arbeit konzentriert sich auf drei unterschiedliche geochemische Regionen (mafisch-magmatisch, felsisch-metamorph und ein Gemisch aus Sedimentgestein). Im ersten Hauptteil der Arbeit (Kapitel 2) wurde die chemische Zusammensetzung von Blättern (344 Proben) der Baumkronen untersucht. Die Blattproben wurden in allen Regionen an unterschiedlichen topographischen Hangpositionen von unterschiedlichen Baumarten entnommen. Die Analysen haben gezeigt, dass die chemische Zusammensetzung der untersuchten Blätter durch die geochemischen Eigenschaften des Bodens in der jeweiligen Region gesteuert werden. Im Gegensatz dazu hatten die unterschiedlichen topographischen Hangpositionen keinen Einfluss. Im zweiten Hauptteil der Arbeit (Kapitel 3) wurde der Zusammenhang zwischen dem Ausgangsgestein und der Topographie als wichtige Faktoren der Bodenfruchtbarkeit auf die NPP, C-Speicherung, Biomasse und SOC von tropischen

Wäldern untersucht. Im Rahmen der Studie wurde ein zweijähriger Feldversuch durchgeführt, welcher das Vegetationswachstums aufzeichnete und in Verbindung mit geochemischen Parametern des Bodens setzte. Es wurde gezeigt, dass die Parameter der Bodenfruchtbarkeit das lokale Ausgangsgestein widerspiegeln und die NPP und die C-Allokation in tropischen Bergwäldern steuern. Es konnte kein Einfluss der Topographie auf die C-Speicherung oder NPP erkannt werden. Zudem wurde kein Zusammenhang zwischen dem SOC-Speicher und C-Eintrag gefunden, stattdessen übersteigt der pflanzliche C-Input scheinbar das maximale C-Sequestrierungspotenzial der Böden im Untersuchungsgebiet. Im letzten Hauptsteil der Arbeit (Kapitel 4) wurden die SPR und der SOC-Umsatz tropischer Waldböden durch ein Inkubationsexperiment in kontrollierter Laborumgebung untersucht. Dabei wurden tiefenspezifische Bodenproben aus den geochemisch unterschiedlichen Regionen, die wiederum von unterschiedlichen topographischen Hangpositionen stammen inkubiert. Die Temperatur und Bodenfeuchte während der Inkubation entsprach dabei ungefähr der Jahresmitteltemperatur und einer mittleren Bodenfeuchte an den Entnahmestandorten. Gemessen wurden sowohl SPR als auch $\Delta^{14}C$ Alter. des bei der Mineralisierung entstandenen CO_2. Es zeigte sich, dass die Bodenatmung trotz vergleichbarer Klimabedingungen und Vegetation Unterschiede in Abhängigkeit von der Bodentiefe und der Geochemie des Ausgangsgesteins aufwies. Erneut hat die topographische Hangposition keinen Einfluss auf die Respirationsraten und das $\Delta^{14}C$. Es ist allerdings möglich, dass im Gelände durch topographiebedingte Unterschiede in der Bodenfeuchte vor allem im Unterboden, gewissen Unterschiede im C-Abbau bestehen, die mit einem Laborexperiment nicht detektierbar sind. Es ist allerdings möglich, dass im Gelände durch topographiebedingte Unterschiede in der Bodenfeuchte vor allem im Unterboden, gewissen Unterschiede im C-Abbau bestehen, die mit einem Laborexperiment nicht detektierbar sind. Im Rahmen der Dissertation konnte gezeigt werden, dass selbst in tief verwitterten tropischen Böden das Ausgangsmaterial einen langanhaltenden Einfluss auf: (1) Nährstoffverfügbarkeit, Nährstoffaufnahme und Baumkronenchemie, (2) NPP, C-Allokation und unterirdische Biomasse, sowie (3) mikrobielle Aktivität, , C-Umsatz im Boden und damit C- Speicherung im Boden hat. Damit wird offensichtlich, dass das Ausgangsgestein und dessen Auswirkung auf die Bodenchemie, selbst bei den tiefgründig verwitterten Böden der Tropen, berücksichtigt werden muss, wenn die Bedeutung afrikanischer Tropenwaldsysteme im globalen C-Kreislauf betrachtet wird. Ausgangsgestein und dessen Einfluss auf die Bodenchemie müssen Berücksichtigung finden, um C-Stabilisierungsmechanismen zu verstehen und die Rolle afrikanischer Tropenwaldsystemen im globalen C-Kreislauf vorherzusagen.

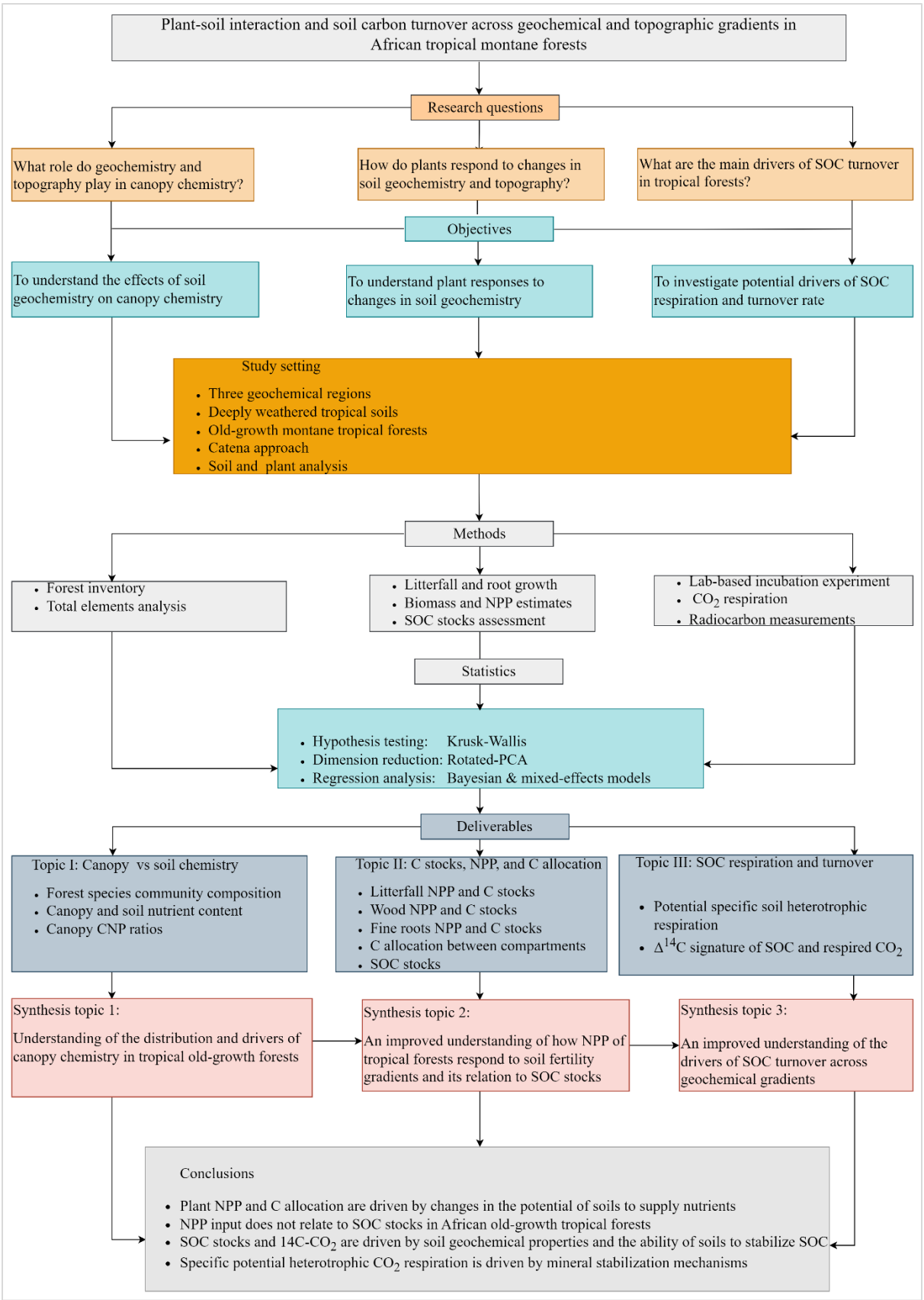

Figure 1. A complete flow chart of the thesis. From top to bottom: The figure highlights the title of the thesis, research questions, objectives, experimental settings, methods used to address each research question, deliverables of the thesis, achievements and general conclusions.

1. General introduction

Tropical forests and soils are a significant component of global biogeochemical cycling and are part of the complex interactions between ecosphere and atmosphere that affect the global carbon (C) cycle (Schmidt *et al.*, 2011). Despite the role of soils in regulating climate, much of the research on terrestrial C cycling over the past decades has focused on measuring aboveground plant productivity and the net exchange of C between the biosphere, and atmosphere, ignoring the role of soils in this process. Furthermore, despite its role in global C storage and cycling, belowground biomass is also the least studied among the plant biomass compartments (Ma *et al.*, 2021) potentially affecting the understanding of C cycling in terrestrial ecosystems. For example, studies on biogeochemical cycling suggest that annual plant productivity and C cycling between soils and the atmosphere are mainly driven by climate (Jiang *et al.*, 2020). Consequently, C estimates and predictions over the next century substantially vary between Earth System Models (ESMs) (Friedlingstein *et al.*, 2014). Such discrepancy and the wide range of estimates in ESMs signal a gap in understanding terrestrial C cycling and suggest that the controls on this process are poorly understood.

To understand tropical forests C cycling, it is necessary to consider the effects of local edaphic factors such as geology and topography as these factors play an essential role in soil formation processes, microbial activities, plant growth, and the overall ecosystem function. As such geology and topography can act and interact at different temporal and spatial scales to influence the soil-plant relationship and overall C cycling in tropical forest systems (Lewis *et al.*, 2013; Malhi *et al.*, 2013). However, to date, no study on the interrelationship of these controls and plants has been carried out in African tropical ecosystems. Among the dominant controls on C cycling, climate is the most studied and well-documented (Luo *et al.*, 2017, 2019; Jiang *et al.*, 2020). Much of the research on C cycling suggest that climate influences plant C stocks and NPP which in turn affect SOC stocks and turnover rate (Knapp & Smith, 2001; Gherardi & Sala, 2020). As such, in large-scale studies, SOC stocks are derived from aboveground biomass and plant NPP (Köchy *et al.*, 2015). However, studies carried out in other regions have shown that local edaphic factors are highly interlinked (Nadeu *et al.*, 2015; Hobley & Wilson, 2016) and that C cycling in tropical systems is controlled by a much more complex interplay of climate, topography, and local biogeochemical characteristics (Doetterl *et al.*, 2015; Luo *et al.*, 2019; Gherardi & Sala, 2020). It is noteworth the comparison of the effects of these factors. For example, mineral activity which is constrained by the mineralogy of the soil parent material

and soil weathering, together with biological activity, jointly exert a direct control over SOC, whilst climate exerts only minor and indirect control due to its impact on biogeochemical processes and matter flux (Tang & Riley, 2015). A recent study conducted at continental scale reported that on average 72 % of SOC in humid forest biomes is stabilized by soil organo-mineral interactions and occlusion by aggregation (Kramer & Chadwick, 2018). Topography through its control on water and soil fluxes as well as nutrient dynamics along slope gradients can influence C dynamics by altering C productivity, input, and turnover rate (Berhe *et al.*, 2012; Doetterl *et al.*, 2016). Hence, plants will likely respond differently to changes in topographic features and soil mineralogy derived from the parent material with unknown effect on long-term C cycling and storage in tropical forest systems.

Old-growth African tropical forests are among the largest terrestrial carbon (C) reservoirs and are characterized by high levels of biodiversity (Yude *et al.*, 2011). Available data shows that 89.3% of the total lowland humid and swamp forest area for Africa is in Central Africa, and 2.4% in Eastern Africa, with the Democratic Republic of Congo (DRC) accounting for 53.6% of Africa's lowland rainforest area (Malhi *et al.*, 2013). The first large-scale estimates for old-growth African tropical forests revealed that the mean aboveground biomass (AGB) is 395.7 Mg dry mass ha^{-1}, substantially higher than Amazonian values, with the Congo Basin and the adjacent forests region storing 429 Mg ha^{-1} (Lewis *et al.*, 2013). Despite this pivotal role in global C cycling, African tropical forests, especially the Congo Basin forests receive much less academic and public attention compared to the rest of tropical regions. Recently, White *et al.* (2021) reported that, between 2008 and 2017, the Congo Basin received only 11.5% of international funding compared with 55% for southeast Asia and 34% for the Amazon region. Nevertheless, the African tropical regions have witnessed an increase in research activities in the past few years (Malhi *et al.*, 2013; Hubau *et al.*, 2020; Cuni-Sanchez *et al.*, 2021), all predicting significant changes to both soil biogeochemical cycling and C fluxes between soils, plants, and the atmosphere. For example, recent advances in forests biogeochemistry reported high atmospheric nitrogen (N) and phosphorus (P) depositions in sub-Saharan Africa than in other tropical regions due to large amounts of frequent biomass burning originating from savanna and dry forests in North and South of the humid tropics (Bauters *et al.*, 2018, 2021). These fire-derived inputs will likely alter biogeochemical processes in the African rainforests with a substantial impact on C cycling. Furthermore, while tropical forests are known to be N and P-limited ecosystems, a recent study conducted in the Congo Basin found consistent Ca-limitation along succession gradients (Bauters *et al.*, 2022). However, the role soil

geochemistry such as rock-derived nutrients play in biogeochemical cycling in old-growth African tropical forests remains unclear.

1.1. Problem statement

African tropical forests are expected to experience significant changes in soil biogeochemical cycling and ecosystem-level carbon (C) fluxes between soil, plants, and the atmosphere (Lewis *et al.*, 2009; Cuni-Sanchez *et al.*, 2021). However, the effects of soil geochemistry on nutrient supply, biomass C stocks, NPP, and microbial SOC decomposition in old-growth African tropical forests are still poorly understood (Cuni-Sanchez *et al.*, 2021; Doetterl *et al.*, 2021b; Reichenbach *et al.*, 2021b; Kidinda *et al.*, 2022). This is specifically true for the understudied Congo Basin (Drake *et al.*, 2019; Doetterl *et al.*, 2021a; Bauters *et al.*, 2022). Consequently, most of the process understanding of biogeochemical cycling between soil and plant in the African tropics is often derived from global case studies or other tropical regions. Due to differences in their environmental settings and soil-forming processes, African tropical forest systems will likely react very differently to changes in soil characteristics compared to other forest systems. Hence, any changes in nutrients are, therefore, critical to understanding the soil-plant relationship and the functioning of African tropical forests ecosystems. Improving the process understanding of soil biogeochemistry and plant responses in the context of African tropical systems will help to better define and represent plant-soil interactions in large scale biogeochemical models.

1.1.1. Nutrient uptake and canopy chemistry in tropical forest systems

Canopy chemistry is an important component to understand how tropical forest ecosystems function (Norby *et al.*, 2017). It is a mediator of carbon (C) and nutrient cycling between soils and plants (Asner *et al.*, 2015). Changes in the concentration of nutrients in the leaves can greatly limit, enhance the overall plant productivity or alter soil nutrient cycling through soil-plant interaction processes (Hättenschwiler *et al.*, 2008; Reich *et al.*, 2009). As such, leaf stoichiometric ratios have been used to infer nutrient limitation in any ecosystem (Jobbágy & Jackson, 2004). Past and recent research all agree that canopy chemistry in tropical forest systems is controlled by a complex interplay of soil forming factors and ecosystem characteristics such as geochemistry of the local parent material, topography, and forest structure characteristics (Fyllas *et al.*, 2009; Asner & Mascaro, 2014; Asner *et al.*, 2015; Massmann *et al.*, 2022a). However, two major issues remain unresolved: first, most of the

understanding is greatly limited to C: N: P interactions, with little to no information about the rock-derived nutrient that shape plant growth (Han *et al.*, 2011; Tian *et al.*, 2019). As such, there is a need to mechanistically understand the influence that changes in soil geochemical properties has on canopy chemistry. Secondly, the interplay of soil geochemistry and canopy chemistry might be aggravated by the morphological characteristics of the landscape which further control nutrient and water fluxes along the slopes (Jucker *et al.*, 2018). Therefore, it is not clear how these landscape dynamics and interactions affect canopy chemistry in an African tropical forest system.

1.1.2. Carbon allocation in plants and soils of tropical forests

Carbon dynamics in tropical forests systems are often associated with climatic parameters, such as precipitation and temperature (Moore *et al.*, 2017; Tonin *et al.*, 2017a; Hofhansl *et al.*, 2020a), topographic patterns (de Castilho *et al.*, 2006; Malhi *et al.*, 2017) or to some extent anthropogenic disturbance (Riutta *et al.*, 2018; Ross *et al.*, 2021). However, recent studies have demonstrated that soil parent material co-determines nutrient availability more so than other factors (Augusto *et al.*, 2017a) with strong consequences for C cycling (Vitousek, 1984; Fernández-Martínez *et al.*, 2014; Wieder *et al.*, 2015). A lack of field data, especially in the African tropical ecosystem (Huang *et al.*, 2021a), limits the ability to assess how changes in parent material as a driver of soil geochemical properties influence C cycling and allocation in tropical forests. Topographic features such as terrain relief, slope, or curvature can strongly influence the heterogeneity of forest landscapes, ultimately altering local-scale variation in soil chemistry, and soil fertility (Tiessen *et al.*, 1994a; Chadwick & Asner, 2016; Xia *et al.*, 2016). For example, on ridges and steep slopes, nutrients and water limitation may favour species with traits that maximize environmental stress tolerance (Paoli, 2006; Heineman *et al.*, 2011; Holdaway *et al.*, 2011). In contrast, forests in alluvial valleys are shaped by competition for light, and generally develop taller, vertically stratified canopies (Paoli *et al.*, 2008; Banin *et al.*, 2012; Werner & Homeier, 2015), while also maintaining higher productivity and turnover rates (Aiba *et al.*, 2005a; Stephenson & van Mantgem, 2005; Quesada *et al.*, 2012). Furthermore, erosional processes could potentially lead to the resurfacing of subsoil or soil parent material that can lead to an increase (Porder *et al.*, 2007) or decrease in soil nutrients (Eger *et al.*, 2018; Doetterl *et al.*, 2021a,b). The way plants respond to these changes and the impact this has on SOC stocks remains unclear in African old-growth tropical forests.

1.1.3. SOC dynamics in tropical forest systems

Tropical forest soils represent a significant amount of global SOC stocks. However, SOC stocks are at stake of being lost due to the higher C turnover rate in these systems (Raich & Schlesinger, 1992). In the past few years, studies have shown that SOC dynamics is the result of a complex interplay of geochemistry, topography, climate, and biology (Doetterl *et al.*, 2015, 2018; Luo *et al.*, 2019; Haaf *et al.*, 2021; Kidinda *et al.*, 2022). For example, long-term chemical weathering in tropical systems has led to a significant increase of metal cations such as Fe, Al, and Mn that play an important role in stabilizing SOC (Reichenbach *et al.*, 2021). Consequently, about 72 % of SOC in humid forest biomes is stabilized by interaction with the mineral phase through soil organo-mineral interactions and occlusion by aggregation as recently demonstrated both at the global scale (Kramer & Chadwick, 2018) and regional scale (Reichenbach *et al.*, 2021). Furthermore, hydrological processes along topographic positions can greatly alter water and soil fluxes thereby affecting SOC dynamics (Berhe *et al.*, 2008). The interaction of soil geochemistry and topography is therefore central in order to understanding SOC exchange between soils and the atmosphere in the African tropical forests.

1.2. Thesis objectives

The aim of this thesis was to understand the effects of soil geochemistry and local topographic positions on canopy chemistry, above and belowground biomass productivity, C allocation strategies, and SOC dynamics in African old-growth tropical forests (Fig.1). Specifically, the presented work focused on understanding the effects that change in soil geochemical and topographic positions has on: (1) forest canopy rock-derived nutrients and CNP ratios. This objective is tight to the questions: (Q_1) what role do soils and topography play in plant nutrient uptake and canopy chemistry? Are canopy chemistry traits similar among forest stands developed on different soil parent material and topographic positions? (2) To understand the effects that change in soil geochemical and topographic positions has on plant biomass productivity, NPP, C allocation to litterfall, wood, and fine roots biomass, and how they relate to soil organic carbon stocks. This objective is tight to the following questions: (Q_2) how does change in soil properties driven by geochemistry of the parent material and topographic positions affect biomass productivity and C allocation between plant compartments and how do they relate to SOC stocks? (3) To understand the role geochemical soil properties and topographic positions of the local hillslopes play as drivers of specific potential soil heterotrophic respiration rate and C turnover in old-growth African tropical forests. This

objective is connected to question: (Q_3) how does soil geochemistry derived from the parent material interact with topography to influence SOC respiration and carbon turnover rate in tropical forest systems?

This thesis was centered on three main hypotheses: (H_1) canopy chemistry in old-growth tropical forests is driven by soil geochemical properties derived from parent material that shape rock-derived nutrients available for plant uptake. However, changes in water and nutrient availability due to topographic positions can shift canopy characteristics along the slopes. (H_2) Above and belowground NPP and C allocation in old-growth tropical forests are driven by soil chemical properties derived from the parent material that shape the availability of rock-derived nutrients for plant growth. Consequently, SOC stocks are positively correlated with belowground biomass and C input. (H_3) In old-growth tropical montane forests, soil geochemistry derived from parent material has a strong effect on potential heterotrophic SOC respiration and radiocarbon signatures compared to topographic positions. This is because soil mineralogy can drive both stabilization mechanisms and soil fertility. However, local topographic positions can influence soil carbon respiration and ^{14}C signatures through changes in hydrological features along slopes.

1.3. Data and study area

The data used and reported in this thesis has been collected as part of a larger project: "***Tropical soil organic carbon dynamics along erosional disturbance gradients in relation to variability in soil geochemistry and land use*** (TROPSOC)" (Doetterl *et al.*, 2021c). The data and the description are in an open-access database that contains spatially and temporally explicit data on soil, vegetation, environment, and land management collected from 136 old-growth tropical forest stands and cropland plots. The data were collected between 2018 and 2020 as part of monitoring and sampling campaigns in the eastern Congo Basin and the East African Rift Valley system. Note that, this thesis focused on forest sites only. General information such as plot establishment, soil sampling, and vegetation monitoring are described below and in appendices. Specific methods are described in the method section of each chapter.

Study sites are located in the Eastern part of the Congo Basin and along the East African Rift Valley system along the border between the Democratic Republic of the Congo (DRC), Uganda, and Rwanda, in three forested national parks (Fig. 1.1), each situated in a distinct geochemical region (Schlüter, 2006). Study sites in the DRC are located in Kahuzi-Biéga National Park (-2.31439 ° S; 28.75246 ° E) and were developed on mafic magmatic rocks.

Study sites in Uganda are located in Kibale National Park (0.46225 ° N; 30.37403 ° E) and were developed on felsic metamorphic rocks. Study sites in Rwanda are located in the Nyungwe National Park (-2.463088 ° S; 29.103834 ° E) and were developed on sedimentary rocks with a wider mixture of geochemical properties distinct from the mafic and felsic rocks (Doetterl *et al.*, 2021a,b).

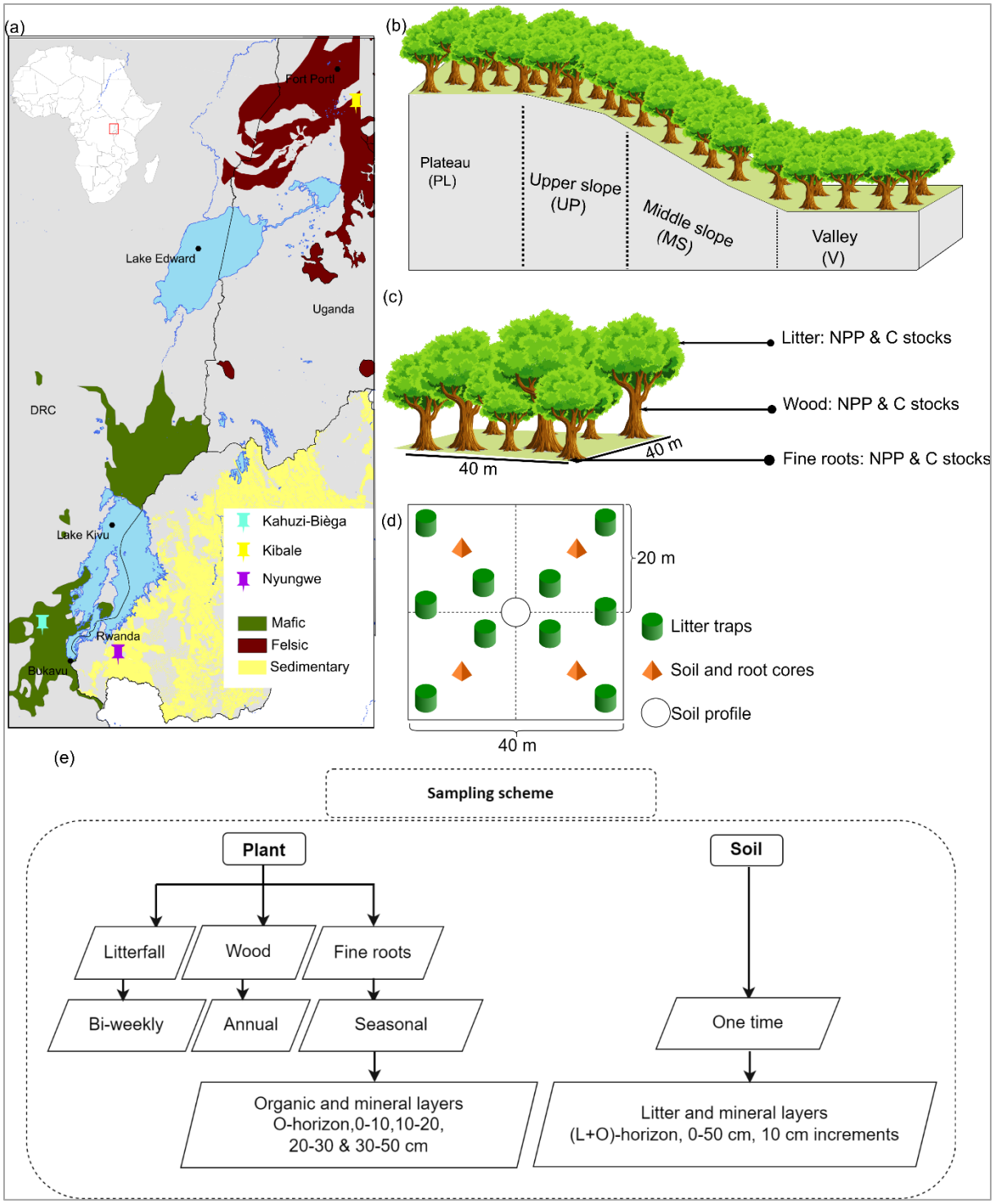

Figure 1.1. Overview of the study sites with respect to major investigated factors. (a) geochemical regions and corresponding geologies, (b) topographic positions following a catena approach, (c) NPP and C stock compartments investigated in this study and (d) Setup of litter traps and sampling design for soils and root cores, (e) sampling scheme, type of collected plant biomass and soil samples, temporal resolution as well as soil/root sampling depth intervals.

1.4.1. Climate and vegetation

The climate of the study region is classified as tropical humid with monsoonal dynamics (Köppen Af-Am). The mean annual temperature (MAT) at the study sites varies between 15.3 and 19.2 °C, and mean annual precipitation (MAP) varies between 1697 and 1924 mm (Fick & Hijmans, 2017). All forest sites are similarly developed and show the typical vegetation of tropical old-growth and primary forests (Nyirambangutse *et al.*, 2017; Imani *et al.*, 2017; Tyukavina *et al.*, 2018). A recent global forest age dataset supports that all forest stands in the investigated study area are 300+ years old-growth forests (Besnard *et al.*, 2021). Hence, based on the available information, and although historical disturbances cannot fully be excluded, there is strong evidence that all investigated forests are in fact old-growth.

1.4.2. Soil parent material

Study sites in the DRC are located in the Kahuzi-Biéga National Park where soils (alic Nitisols(ochric), alic Nitisols (vetic), and mollic Nitisols (ochric)) have developed from nutrient rich, mafic magmatic rocks, a result of volcanism in the East African Rift System (Schlüter, 2006), further referred to as mafic region. In Uganda, study sites are located in the Kibale National where soils (sederalic Nitisols (ochric), haplic Lixisols (nitic), and luvic Nitisols (endogleyic)) have developed from felsic magmatic and metamorphic rocks of intermediate nutrient content, referred to as felsic region. Study sites in Rwanda are located in the Nyungwe National Park where soils (haplic Acrisols (nitic), acric Ferralsols (vetic), and acric Ferralsols (gleyic)) have developed from a mixture of nutrient poor sedimentary rocks, referred to as sedimentary region. These sediments are mostly dominated by quartz-rich sandstone and schist layers spanning along the Congo-Nile divide (Schlüter, 2006). Soils in the three study regions were deeply weathered (> 2 meters) with homogeneous properties in subsoil horizons and no bedrock could be reached at any slope position. Soils were described and analyzed extensively across the three geochemical regions, separately for each topographic position and depth-explicit (Doetterl *et al.*, 2021a).

1.4.3. Plot setup across geochemical and topographic gradients

In each slope catena, four topographic positions were established in March 2018 within each of the three geochemical regions, under closed-canopy forests following an international, standardized protocol for C allocation and cycling assessments in tropical regions (Matthews et al., 2012): flat plateaus (3 - 5 %), upper slope (9 - 15 %), middle slope (45 - 60 %), and valley/foot slope (1 - 3 %) of slope steepness with an average slope length (plateau to valley plots) of (70 ± 56 m) in mafic, (149 ± 125 m) in felsic and (101 ± 103 m) in the sedimentary region (Table S3). At each topographic position, three replicate plots of 40 m x 40 m in size were established, resulting in a total of 36 plots. Each experimental plot was further subdivided into four 20 m x 20 m subplots in order to structure and distribute the replicate sampling of soil and root cores as well as the activities performed during forest inventorization evenly across the plot. Note that in January 2019, due to security concerns at the beginning of the monitoring activities in the mafic region, four plots (two plateaus, one upper slope, and one middle slope) were abandoned and four additional plots were re-established in the nearby area of the remaining original plots with similar vegetation, topographic, and geochemical features. This resulted in a reduced set of eight plots in the mafic region and a total of 32 plots, allowing for root and litter monitoring at all topographic positions. Furthermore, topographic indices relevant for distinguishing differences in the local landscape dependent variation in water and nutrient availability were derived from a 30m x 30m SRTM void filled DEM (NASA SRTM, 2013). The calculated topographic indices included the topographic position index (TPI), topographic wetness index (TWI), slope length, steepness factor (SL-factor), slope inclination (slope), stream power index (SPI), terrain aspect (aspect) and curvature.

1.4.4 Soil sampling

At the time of plot installation, as part of the TROPSOC project soil samples were collected following a catena approach with three 40 m × 40 m plots (field replicates). Four replicate soil cores per plot (one in each subplot) (See Fig 1.1d) were taken in a depth-explicit way in 10 cm increments up to 1 m soil depth and combined as composites per plot. In addition, one soil profile pit was dug to a depth of 1m in the center of one of the three replicate plots (Fig. 1.1d) per topographic position in each geochemical region. These soil pits were dug and described according to the FAO guidelines (FAO, 2006).

2. Nutrient uptake and canopy chemistry in Afromontane forest ecosystems

2.1. Introduction

Tropical forests play a substantial role in the global biogeochemical cycling (Canham, 1988; ter Steege *et al.*, 2006). The functionality of tropical forests, however, depends on canopy chemistry. As such, canopy chemistry is an important component of the plant to understand how tropical forest ecosystems function because it is a mediator of carbon (C) and nutrient cycling between soils and plants (Asner *et al.*, 2015). Canopy nutrients including nitrogen (N), phosphorus (P), potassium (K), calcium (Ca), and magnesium (Mg) are essential for plant ecophysiological processes such as photosynthesis, plant growth, and resistance to environmental stress (Marschner, 1986). An altered availability of these nutrients to leaf assimilation can ultimately limit the net primary productivity (NPP) of a forest or alter important plant-soil interactions through decomposition (Hättenschwiler *et al.*, 2008; Reich *et al.*, 2009a). In turn, the canopy chemical composition signals forest's nutrient status as well as tree growth and performance of a forest ecosystem (Poorter & Bongers, 2006). As such, leaf stoichiometric ratios have been historically used to infer nutrient limitation (Jobbagy & Jackson, 2004). Recent studies show that canopy chemistry is controlled by a complex interplay of geochemistry, topography, and forest structure characteristics (Fyllas *et al.*, 2009; Asner *et al.*, 2015; Massmann *et al.*, 2022a). However, most inferences and understanding of canopy chemistry and ecosystem functioning in tropical forests remain greatly limited to C: N: P interactions, ignoring other elements (Han *et al.*, 2005; Tian *et al.*, 2019). As such, there is a need for more detailed studies that explicitly link soil geochemical properties such as rock-derived base cations and potential soil cation exchange capacity (CEC) to canopy chemistry. Furthermore, the complexity of the potential interplay of soil geochemistry and canopy chemistry might be aggravated in tropical montane forests due to topographic controls on water fluxes (Asner *et al.*, 2015; Jucker *et al.*, 2018) and the removal of fertile topsoil through landslides (Guns & Vanacker, 2014). Research in other tropical systems has shown that topography can influence biogeochemical processes through its control on water fluxes, altering nutrient availability and dynamics along slopes, forest canopy structure, and species compositions (Lobo & Dalling, 2013; Jucker *et al.*, 2018). Furthermore, erosional processes could potentially drive resurfacing of former subsoil reflecting local parent material that can be both more (Porder *et al.*, 2007) or less depleted in soil nutrients (Eger *et al.*, 2018). While past studies have shaped the understanding of the role of elevation (van Loon *et al.*, 2014; Malhi *et al.*, 2017; Jucker *et al.*, 2018) on canopy chemistry, the interaction of local hillslopes

and the geochemistry of the parent material and their effects on canopy chemistry remains unclear.

The aim of this study was to disentangle the role of soil geochemistry and topography on shaping canopy chemistry in Afromontane forests. Canopy chemistry of forest communities was assessed in the three regions located in the western part of the East Africa rift system with contrasting soil parent material while including forest communities on different topographic positions – nested within each geochemical region. This study is centered around the following questions: (1) What role does soil geochemistry play as a driver of canopy chemistry in tropical old-growth forests? This question is connected to the hypothesis that canopy chemistry in old-growth tropical forests is mainly driven by soil geochemical properties derived from te soil parent material that control the type and content of nutrient uptake. (2) What is the role of topography as a driver of canopy chemistry in tropical old-growth forests? This question is connected to the hypothesis that topographic position affects soil nutrient status through lateral fluxes of soil material which in turn affect canopy chemistry.

2.2. Material and methods

2.2.1. Sampling canopy leaves and nutrient analyses

To assess the chemistry of living canopy leaves, during the short dry season (December, 2018 - January, 2019) six months after plot installation and inventory, sun-exposed shoots were sampled from the upper canopy of selected inventoried tree species. The sampling covered tree species that collectively make up 80 % of the standing basal area per plot following established protocols (Pérez-Harguindeguy *et al.*, 2013). Where sampling of upper canopy leaves was not possible, partially shaded leaves situated below the uppermost canopy were sampled. All fully-exposed, healthy-looking (i.e: without signs of herbivory) individual leaves and a minimum of 3 individuals per species were sampled. Further, a minimum of 5 and a maximum of 17 trees per plot were sampled. All leaf samples were oven-dried at 70 °C for approximately 72 hours, dry-weighed, and milled for later chemical analyses. Total Carbon (C) and nitrogen (N) analyses of leaf samples were measured in 1 g of ground subsamples using a dry combustion analyzer (Variomax C:N, Elementar GmbH, Hanau, Germany) with a measuring range of 0.2 - 400 mg g-1 biomass (absolute C or N mass in a sample) and reproducibility of < 0.5 % (relative deviation). The total elemental composition of the collected leave biomass was determined using inductively coupled plasma optical emission spectrometry (ICP-OES) (5100

ICP-OES Agilent Technologies, USA) for the determination of P, Ca, K, Mg and Na. For this, approximately 200 mg of sample material was placed in digestion tubes and boiled them for 90 minutes at 120 °C. Further, 15 ml of 65 % nitric acid (HNO3) were added using a DigiPREP digestion system (DigiPREP MS SCP Science, Canada). After 30 minutes of cooling, 3 ml of 30 % hydrogen peroxide (H_2O_2) were added to the plant sample, mixed, and heated for another 90 minutes at 120 °C. All extracts, including calibration standards, were cooled, mixed with nanopure water, filtered through 41 grade Whatman filters, and transferred into 50 ml PE-Tubes. PE tubes were rinsed three times with bi-distilled water to remove potential residues before the measurement of the extract. Note that the term canopy chemistry in this study refers to leaf (N, P, Ca, K, Mg, Na, C:N, C:P, and N:P) and canopy nutrient refers only to (leaf N, P, Ca, K, Mg, and Na).

2.2.2. Statistical analysis

In the first step, Kruskal-Wallis tests was used to assess whether there were significant differences in the distribution of canopy chemistry using data for individual tree species across geochemical regions and topographic positions within each geochemical region. Since the Kruskal-Wallis test does not explicitly show the differences between geochemical regions or topographic positions, a post-hoc pairwise comparison between groups was conducted using Dunn's test. To do this, first, tree species community weighted means (CWM) of canopy chemistry per plot were calculated using the proportion of community basal area to the total basal area of the plot as the weighting factor. Second, differences in CWM between geochemical regions, and then between topographic positions within each geochemical region were analyzed. The Kruskal-Wallis and Dunn's tests were conducted using the R package 'pgirmess' and "rstatix" (Giraudoux, 2021; Kassambara, 2021). Note that, CWM was selected over simple mean for two reasons. First to account for species abundance because abundant species are the ones playing a significant role in the forest structure and ecological functions. Second, to avoid the influence of rare species that may affects normal means while their ecological function is not significant. Consequently, this makes it easy to compare and interprete vegetation structure across sites.

In the second step, to quantify and compare the effect size and significance of geochemical regions (parent materials) and topography on canopy chemistry (separately for each canopy element), non-aggregated data for individual tree species sampled across all sites were analyzed using linear mixed-effects models separately for each canopy element following (Bates *et al.*,

2015). Because mixed effect models require that residual should follow a normal distribution and the fact that normality of the response variables was violated, a logarithmic transformation was applied on each canopy chemistry. All regression models were dignosed using the four diagnostic regression plots, namely: (1) Residuals vs Fitted plot, (2) Normal Q-Q plot, (3) Spread-Location plot and (4) Residuals vs Leverage plot.

For all mixed effect models, topographic positions and geochemical regions were set as fixed factors and tree species nested within the plot as a random factors. The marginal (R^2m) was calculated as an estimate for the variation explained by the fixed effects, following (Nakagawa & Schielzeth, 2013).

In the third step, using data aggregated at the plot level (CWM), linear regression models were used to identify which geochemical soil properties drive canopy chemistry in these tropical forests. Due to a large number of variables and a relatively small number of observations, a rotated principal component analysis (rPCA) for dimension reduction (Jolliffe, 1995) was conducted on a set of geochemical soil properties for the top 30 cm of mineral soil layers, before regression analyses. PCA analysis linearly combines the explanatory variables, while successively maximizing the variability of the explanatory variables and representing it as a set of new orthogonal and uncorrelated vectors. In addition to PCA, rPCA rotates the new axes using the "Varimax rotation method" (Kaiser, 1958) in order to achieve simple and interpretable rotated components (RC) as described by (Abdi & Williams, 2010). The retained rotated components (RCs) were then used as independent variables in the regression models for each canopy element. For these regression models, the R^2 was used as an estimate for the variation explained by independent variables (RCs). Finally, to assess the correlation between response variables and independent predictors, pairwise Pearson correlation coefficients and least square regression analysis were used. For all statistical tests, a p-values <0.05 was designated as significant. All statistical analyses were carried out with R software (R Core Team, 2020).

2.3. Results

2.3.1. Patterns of canopy chemistry along topographic and geochemical gradients

Kruskal-Wallis tests for pair-wise comparison between topographic positions showed that there was no significant difference (p-value ≤ 0.05) or consistent pattern in canopy chemistry was detectable in relation to the topographic position of plots in each geochemical region (Table

S2.2). In contrast, the three geochemical regions showed distinct patterns and differed significantly in terms of canopy chemical characteristics. For C content, the average plot canopy C concentration was higher in the sedimentary region (464.7 ± 8.3 $g.kg^{-1}$) compared to the felsic (466.2 ± 31.2 $g.kg^{-1}$) and the mafic region (489.5 ± 20.1 $g.kg^{-1}$) but the difference was not significant between the three geochemical regions (Fig. 2.1a). Canopy N content was significantly higher in the mafic region (32.5 ± 4.0 $g.kg^{-1}$), followed by the felsic (26.7 ± 3.1 $g.kg^{-1}$), and lower in the sedimentary region (19.6 ± 1.9 $g.kg^{-1}$) (Fig. 2.1b). Canopy P content was significantly higher in the mafic region (2.3 ± 0.5 $g.kg^{-1}$) compared to the felsic region (1.6 ± 0.5 $g.kg^{-1}$) and the sedimentary region (1.0 ± 0.3 $g.kg^{-1}$) (Fig. 2.1c). Similar to N and P concentrations, the canopy C:N:P ratios differed between the three investigated regions but the patterns took the opposite direction. Canopy C:N was significantly higher in the sedimentary (25.2 ± 3.2) compared to the felsic (17.6 ± 2.0) and mafic regions (14.5 ± 2.1) (Fig. 2.1d). Canopy C:P was significantly higher in the sedimentary region (496.66 ±111.11) compared to their counterpart felsic (323.1 ± 102.9) and the mafic region (208.5 ± 48.6) (Fig. 2.1e). Canopy N:P was also higher in the sedimentary (19.6 ± 3.6), compared to felsic (18.4 ± 5.5) and the mafic regions (14.4 ± 2.6), but the difference between the sedimentary and the felsic regions was not significant (Fig. 2.1f).

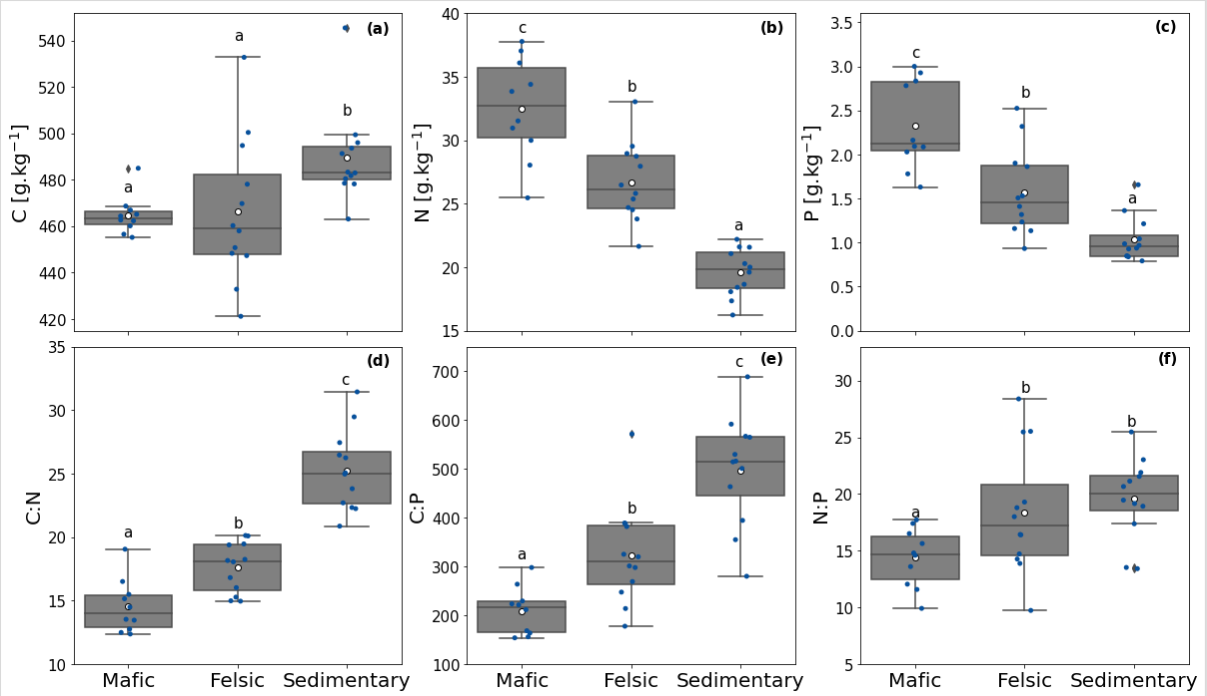

Figure 2.1. Kruskal-Wallis test results for community weighted concentration (n=10,12,12 for mafic, felsic, and sedimentary regions respectively) of major nutrients and their ratios in the canopy for the three investigated geochemical regions. (a) Leaf carbon content, (b) leaf nitrogen content, (c) leaf phosphorus content, (d) leaf carbon to nitrogen ratio, (e) leaf carbon to phosphorus ratio, (f) leaf nitrogen to phosphorus ratio. The white dot in the center of the box plot represents the mean value. The weighting factor is the proportion of community basal area to the total basal area of the plot. The black diamonds on top of the boxplots indicate communities that deviate from the overall average.

The concentrations of base cations in the canopy differed between the three geochemical regions (Fig. 2.2a-d), but their patterns were different compared to the ones of N, P, and the C:N:P ratios (Fig. 3.1b-c). Canopy Ca was significantly higher in the felsic region (11.0 ± 2.0 g.kg^{-1}) compared to the mafic (8.7 ± 2.2 g.kg^{-1}) and the sedimentary region (4.5 ± 0.8 g.kg^{-1}) (Fig. 3.2a). Canopy K concentration was higher in the mafic region (15.4 ± 5.3) compared to the felsic (14.7 ± 3.6 g.kg^{-1}) and the sedimentary (8.1 ± 3.4 g.kg^{-1}) regions. However, the difference between the mafic and the felsic regions was not statistically significantly different (Figure 2.2b). Mg content was significantly higher in the mafic region (3.95 ± 1.03 g.kg^{-1}) compared to the felsic (2.6 ± 0.7) and the sedimentary regions (2.0 ± 0.3 g.kg^{-1}) (Fig. 2.2c). Canopy Na was significantly higher in the felsic (0.1 ± 0.05 g.kg^{-1}) compared to the mafic (0.05 ± 0.02 g.kg^{-1}) and lower in the sedimentary (0.03 ± 0.01 g.kg^{-1}) regions (Fig. 2.2d).

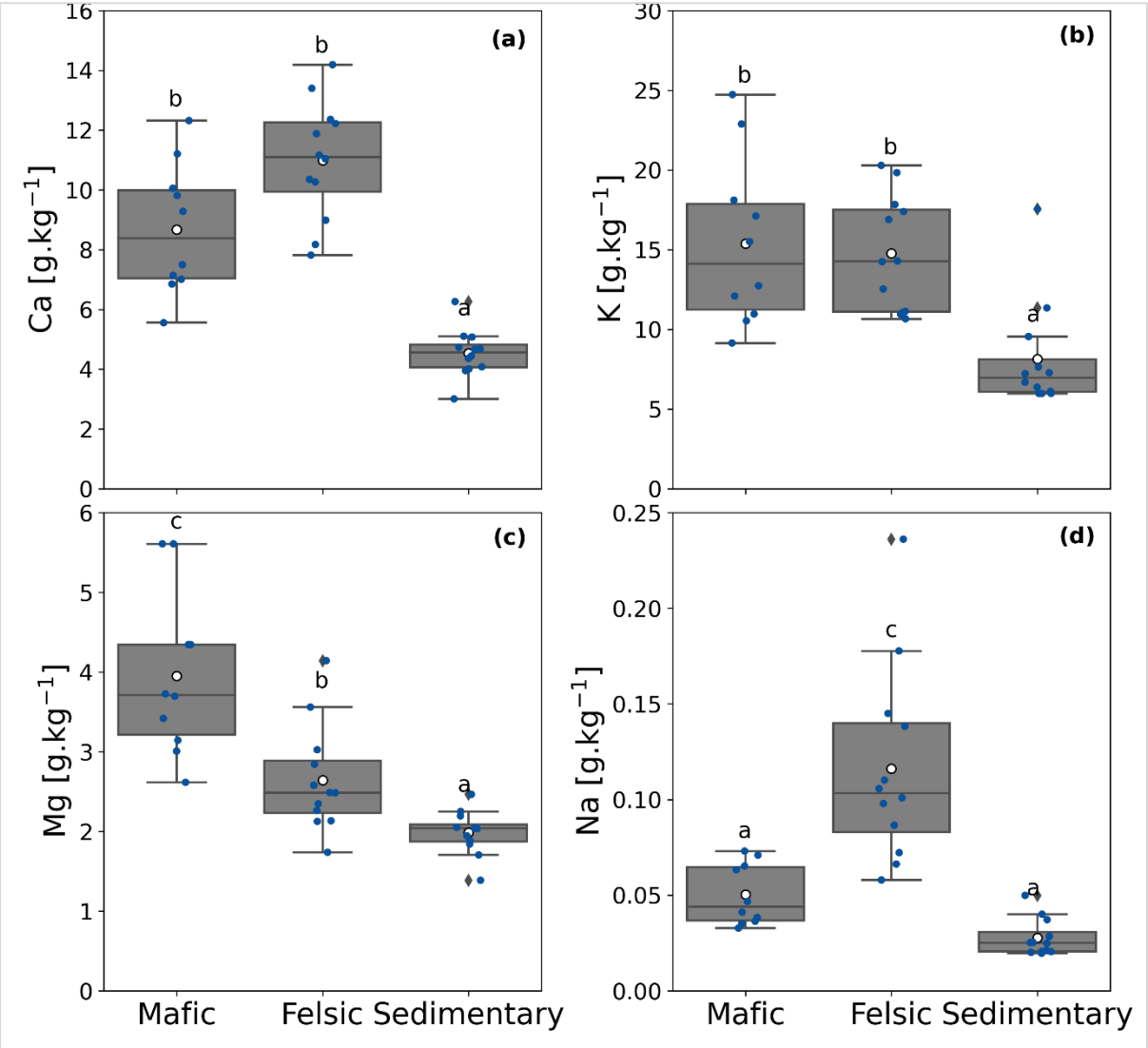

Figure 2.2. Kruskal-Wallis test results for community weighted concentration (n=10,12,12 for mafic, felsic, and sedimentary region respectively) of base cations in the canopy for the three investigated geochemical regions. (a) leaf calcium content, (b) the leaf potassium content, (c) leaf magnesium content, (d) leaf sodium content. The white dot in the center of the box plot represents the mean value. The weighting factor is the proportion of community basal area to the total basal area of the plot. The black diamonds on top of the boxplots indicate communities that deviate from the overall average.

2.3.2. Effects of soil geochemistry and topography on canopy chemistry

The results of the mixed-effects models using topography and geochemical regions as controls showed that for all investigated canopy elements, geochemical regions emerged as the most important factors, and their effects on canopy chemistry were significantly stronger than the effects of local topography positions (Table S2.3). Overall, the explanatory power of the fixed effects in mixed models, was higher in explaining canopy C:N:P compared to explaining

canopy base cations (Ca, K, Mg, and Na) (Table S3.3). For canopy N, the linear mixed effect model explained 30 % of the overall variance (marginal R^2). For canopy P, the model explained 30 % of the variance. For C:N, the model explained 32 % of the variance in the canopy C:N. For C:P, the model explained 38 % of the variance of canopy C:P. For N:P, the model explained 14 % of the variance in canopy N:P. For canopy Ca, the model explained 23 % of the variance. For canopy K, the model explained 21 % of the variance. For canopy Mg, the model explained 25 % of the variance. For canopy Na, the model explained 23 % of the variance in canopy Na (Table S2.3). Overall, when compared to the geochemical reference factor (i.e: the felsic region), the sedimentary region showed significant negative effects on canopy nutrients (N, P, Ca, K, and Na) whereas the mafic region showed significant positive effects on the canopy nutrients. In contrast, the sedimentary region showed significant positive effects on C:N, C:P and N:P ratios while the mafic region showed significant negative effects on these ratios (Table S2.3). Overall, no significant effects of local topographic positions on canopy chemistry were found in the investigated study regions (Table S2.3).

A bivariate analysis of the relationship between canopy nutrient concentrations and soil geochemical properties revealed a strong relationship between canopy chemistry and soil fertility indicators especially soil base cation stocks, exchangeable bases, and the soil CEC (potential and effective). Base cations (exchangeable and total) showed significant positive correlations with canopy nutrients and negative correlations with canopy C:N:P ratios (Fig. 3.3). Among all canopy elements, only Ca and Na exhibited a strong positive correlation with soil base cations and stocks but this was not the case for other elements (Fig. 2.3). Canopy C:N was mainly related to soil fertility, while canopy P and N:P were strongly correlated with total soil P (Fig. 2.3).

Canopy C:N:P ratios did not relate to the corresponding soil C:N:P. However, a weak negative correlation between canopy N and P and the soil C:N was observed. Significant correlations between clay content and canopy chemistry were observed, except for C and Na content. Furthermore, the results show weak to no correlations between sand, silts, and those elements representing canopy chemistry.

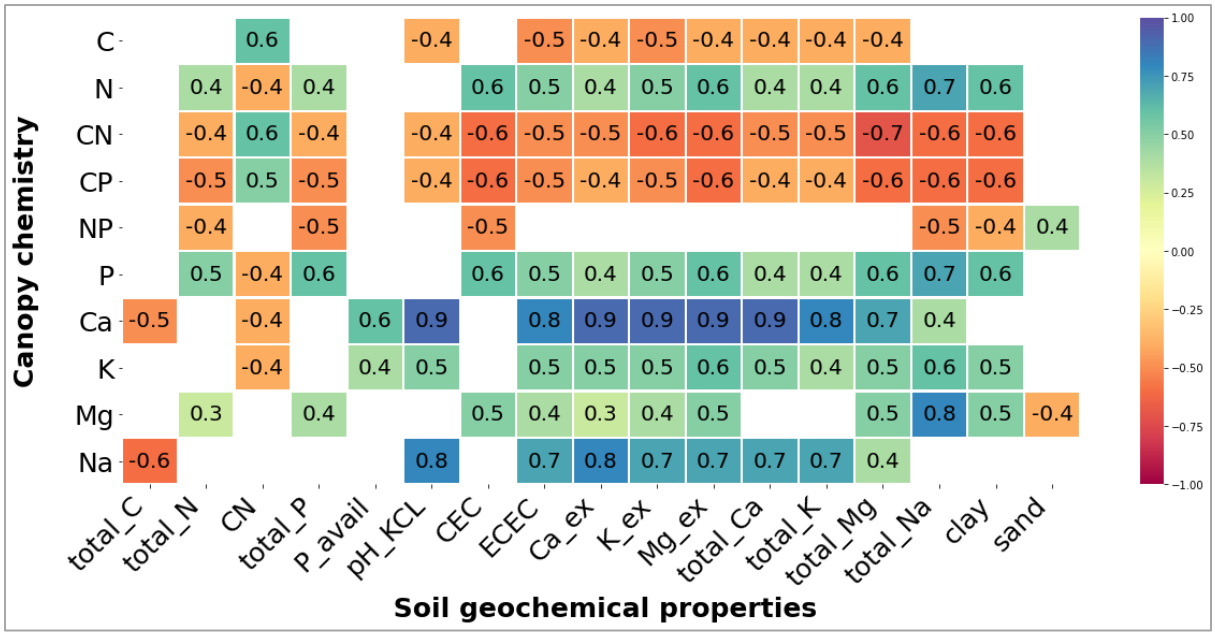

Figure 2.3. Pearson correlations between canopy chemistry (leaf carbon, leaf nitrogen content, leaf phosphorus content, leaf C:N ratio, leaf NP ratio, leaf CP ratio, leaf calcium content, leaf potassium, leaf magnesium content, and leaf sodium content) and soil geochemical properties (total carbon, total nitrogen, bioavailable phosphorus, clay content, silt content, sand content, pH, base saturation in potential cation exchange capacity (CEC), CEC, base saturation in effective cation exchange capacity (ECEC), ECEC, exchangeable magnesium, exchangeable calcium, exchangeable potassium, the sum of bases, exchangeable aluminum, total Ca, total K, total Mg, total Na, total reserve base and total P). Blank cells indicate non-significant correlations, p-value ≤ 0.05.

2.3.3. Mechanistic interpretation of explanatory variables and prediction of canopy Chemistry

The rotated principal component analysis resulted in four significant rotated components (RCs) (Table S2.4). Altogether the four RCs explained 84 % of the cumulative variance of the dataset. From the three rotated components, RC1 and RC2 explained about 60 % of the entire variance in the dataset and were related to soil exchangeable base cations and rock-derived bases (Table S2.4). Mechanistically, RC1 was interpreted as “Soil exchangeable bases and base cation stocks”. RC2 explained about 20% of the entire variance and was related to soil N, P, and CEC. RC2 was then interpreted as “Soil NP and nutrient exchange”. RC3 explained about 10 % of the entire variance within the dataset with the loading of independent predictors that relate to soil particle size distribution. Hence RC3 was interpreted as “Soil texture” (Table S2.4). Using linear regression models, the three rotated components explained a significant amount (39-80 %) of the variance observed in the canopy dataset for each canopy element. For canopy N, the three rotated components explained 76 % of the variance observed in the dataset. For canopy

P, the three rotated components explained 62 %. For canopy K, the selected components explained 46 %. For the canopy Ca, the selected components explained 82 %. For the canopy Mg, the selected components explained 42 %, while for the canopy Na, the selected components explained 63 % of the variance observed in the dataset. For the canopy C:N, the three rotated components explained 84 %. For the canopy C:P, the selected components explained 69 %. For the canopy N:P, the selected components explained 33 %.

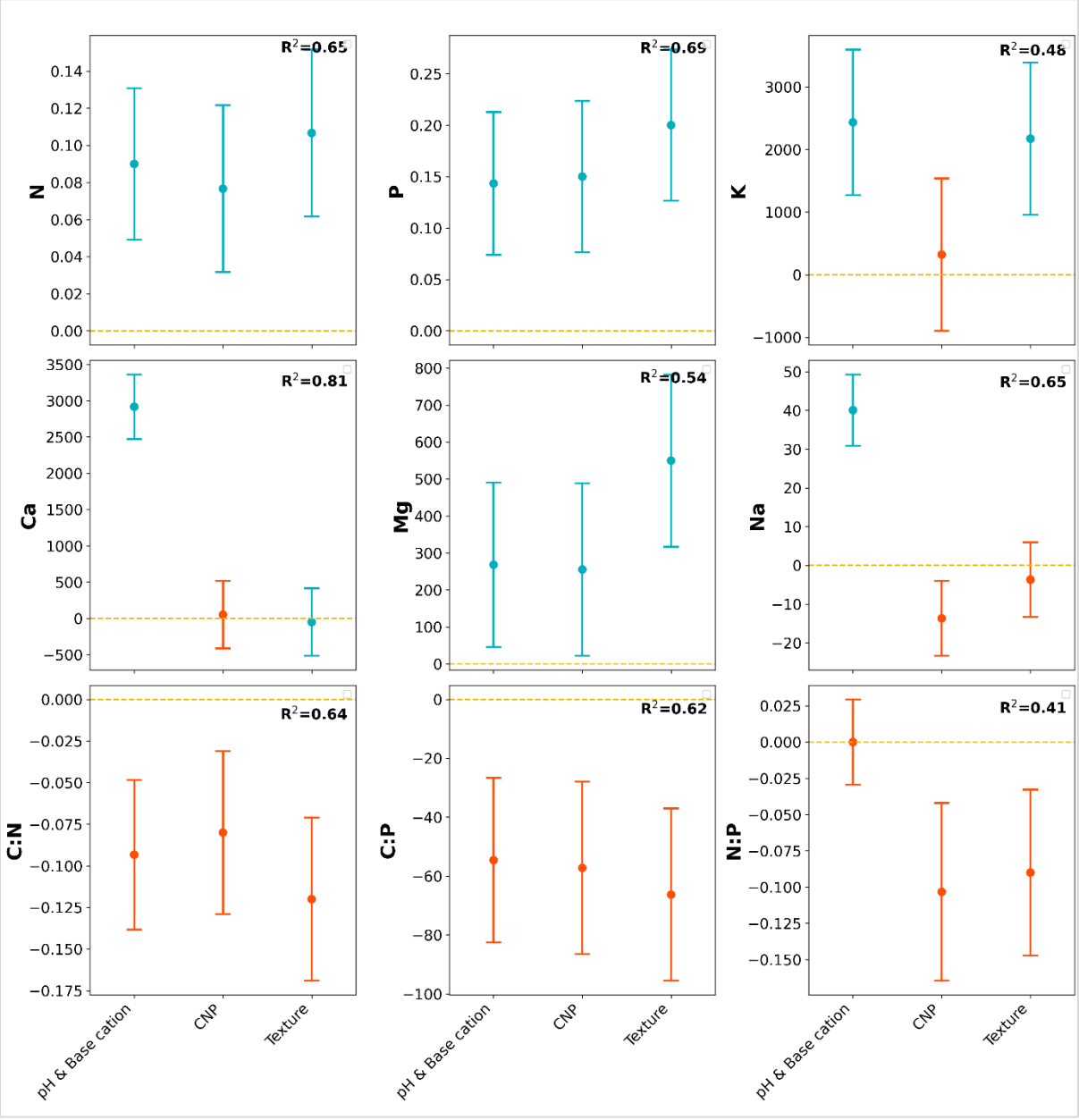

Figure 2.4. Standardized effects size of rotated principal components (RC) as explanatory factors on leaf macronutrients (nitrogen, phosphorus, potassium), base cations (calcium, magnesium, sodium), and C:N:P ratios (C:N, CP, NP). The estimated values indicate the mean effects size, the 95% confidence intervals of the estimates, and the R^2 values as results of the linear regression models.

2.4. Discussion

3.4.1. Local topography has a secondary role in explaining patterns of canopy chemistry

Throughout the three investigated geochemical regions of tropical African montane forests, local topography positions along hillslopes did not emerge as strong drivers of canopy nutrients (Table S2.2; Table S2.3). The pair-wise comparisons showed lower and non-significant differences in canopy chemistry along topographic positions within each region. For all canopy elements assessed in this study, the effects of topography were smaller and non-significant than the effects of geochemistry (Table S2.3). Consistent with these findings, similar results have been reported in other tropical regions. An assessment of the effect of slope gradients on canopy chemistry in the Amazonia region revealed that slope gradients did not have a detectable effect on canopy chemistry (Massmann *et al.*, 2022). These findings suggest that the lack of strong effects of topography (Table S2.3) is an indicator that lateral movement of soil and water in the study sites does not significantly influence soil nutrient dynamics which may lead to differences in canopy nutrients. Although it has been shown that topography can influence tropical forest structure as well as water and nutrient availability (Asner *et al.,* 2014; 2015; Jucker *et al.*, 2018), These findings provide evidence that topographic features at the hillslope scale are not driving canopy chemistry in the investigated study system. Furthermore, there was no indication that erosion has altered the soil landscapes in these study systems under intact tropical forest cover as it has been recently reported. (Wilken *et al.*, 2021). Recent studies on SOC turnover in the same regions as investigated here, have shown that the effect of topography is rather limited to differences related to hydrological conditions between the valley and non-valley positions of the local hillslopes (Doetterl *et al.,* 2021a; Reichenbach *et al.,* 2021). For the same sites, Doetterl *et al.* (2021a) reported deeply weathered soils along slope transects another indicator of little to no soil loss that could otherwise influence nutrient fluxes. The higher explanatory power of soil geochemical properties on canopy chemistry suggests that patterns in canopy chemistry are mainly driven by soil properties that relate to the regional parent material than local topography.

2.4.2. Soil geochemistry drives tropical forest canopy chemistry

Te results show that canopy chemistry in tropical montane forests relates closely to soil geochemistry. Using the three principal components extracted from the dataset (Table S2.4) in regression models, base cations availability and stocks explained most of the variance observed in the canopy chemistry in the study sites (Fig. 2.4). This was unexpected as deeply weathered tropical soils such as those found in the investigated study regions have been reported to acquire nutrients through organic matter recycling instead of weathering process (Cleveland et al., 2013). Forest stands in more fertile soils (mafic and felsic regions) showed higher canopy nutrients (P, Ca, K, Mg, and Na) concentrations compared to their counterparts forest stands in less fertile soils (sedimentary region) (Fig. 2.1; Fig. 2.2). Furthermore, the results revealed clear patterns in canopy C:N, C:P, and N:P ratios related to geochemical regions (Fig. 2.1d-f). C:N, C:P, and N:P ratios in canopy leaves widen as soil fertility decreases (Fig. 2.1d-f; Fig. 2.3). Consistently, data (Fig. 2.1b-c) showed that canopy N and P concentrations were about four and two times lower (for N and P respectively) in forest stands in low fertility soils of the sedimentary region compared to their counterparts in the mafic region, likely reflecting local soil properties. In line with these findings, studies conducted in the Amazon region reported a strong relationship between leaf N, P, Ca, and K and soil fertility with differences between low and high fertility sites (Fyllas *et al.,* 2009; Massmann *et al.,* 2022). Furthermore, a recent study conducted on a global scale reported a strong relationship between species composition and soil characteristics (Vallicrosa *et al.*, 2022b,a), and a strong relationship between canopy N:P and soil total P has been reported for lowland tropical rainforests (Massmann *et al.*, 2022a). But ecological studies have also often shown that canopy elemental compositions are driven by species and community compositions (Cardelús *et al.*, 2009). These findings are supportive of this interpretation as the plant composition across the study sites differ substantially (see chapter 3). However, the study results suggest that soil nutrient limitations in forest stands are the main factors driving canopy chemistry and that the establishment of plant species in canopy is likely driven by soil properties reflecting geochemical characteristics of the parent material. Nutrient ratios in canopy are adjusted to nutrient conditions in soils, demonstrated for example by the high correlation of NP, CP and C:N ratios between soils and canopy (Fig. 2.3, NP C:N and CP for soil). Furthermore, when controlling for the effects of tree species in the generalized mixed effect models, the results show that canopy nutrients tend to increase as forests shift toward nutrient-rich soils (i.e. mafic) and vice versa toward nutrient-limited soils (sedimentary). In contrast, canopy C:N, C:P, and N:P increased in forest stands developed on

nutrient-limited soils and decreased with soil fertility (Table S2.3). Unlike canopy nutrients, canopy C concentration was highest in the low fertility soils (sedimentary region) (Fig. 3.1a). Previous ecological studies argue that selective pressure on plant competition for resources including nutrients can result in a set of plant traits that are typically signs of resource conservation strategies (Ollinger, 2011; Grau *et al.*, 2017; Urbina *et al.*, 2021). Higher C concentration in low fertility soils suggest an adaptation mechanism for forest trees which reduce resource requirements while ensuring C stocks (Chapin *et al.*, 1986). Indeed, data showed significant negative correlations between canopy C and canopy N, P, Ca, and K (Figure S2.1). Consistent with these findings and interpretation, a study conducted in the same regions as investigated here, revealed that forest stands developed in sedimentary region reported lower annual C productivity compared to their counterparts in mafic and felsic regions while building significantly high amounts of C stocks (see chapter 3 for details). Therefore, these results provide strong evidence that soil geochemistry influences canopy nutrients and species communities alike which develop specific strategies to cope with nutrient limitations.

Despite its strong influence on nutrient availability, the contribution of soil parent material is often ignored in biogeochemical models for tropical systems (Augusto *et al.,* 2017). These findings suggest that soil geochemistry is likely a strong confounding factor in the species composition and canopy chemistry causal relationship. Changes in litter quality of canopy leaves then likely affect also nutrient cycling and plant-soil feedback, microbial as well as biogeochemical processes in tropical forests (Kaspari *et al.*, 2008; Bauters *et al.*, 2017; Kidinda *et al.*, 2022).

2.5. Conclusions

Canopy chemistry for Afromontane tropical forests was identified to be highly variable across geochemical regions and strongly correlated to soil chemistry. Soil chemical properties are likely to have strong confounding effects on forest species composition, litter quality and plant growth strategies. The revealed that in the three investigated geochemical regions, forest stands developed on fertile soils in mafic and felsic regions exhibit high canopy N, P, Ca, K, Mg, and Na concentrations compared to their counterparts developed on low fertile soils in the sedimentary region. Canopy C:N, C:P, and N:P as indicators of soil N and P status were high in forest stands of the sedimentary regions. Despite its relevance in global ecological models of tropical forest growth, topography did not influence canopy chemistry within each geochemical region, with local hillslope gradients being far less heterogeneous than local geochemical gradients. Altogether our results suggest that geochemistry of the soil parent material and its role on soil genesis are key factors to consider to improve our understanding of canopy chemistry and ecosystem function in tropical systems.

3. Carbon allocation, stocks and dynamics in distinct African tropical forest ecosystems[1]

3.1. Introduction

Tropical forests globally account for about 50% of the terrestrial vegetation carbon (C) stock and one-third of the global net primary productivity (NPP) (Lewis *et al.*, 2015), and are, therefore, important components of the global terrestrial carbon cycle (Beer *et al.*, 2010). Nested within, montane forests represent about 13 % (about 305 million ha) of the total coverage of tropical and subtropical forests (Salinas *et al.*, 2021) with African montane forests recently highlighted as an important but greatly underestimated and understudied C store (Cuni-Sanchez *et al.,* 2021). The conservation of old-growth tropical forest is key in any effort to mitigate global climate change. African tropical forests constitute a major part of this biome, with the Congo Basin tropical forests being second only to the Amazonian forests in both C storage (Dargie *et al.*, 2017; Cuni-Sanchez *et al.*, 2021) and as an active yet declining C sink (Lewis *et al.*, 2009a; Tchatchou *et al.*, 2015; Rammig & Lapola, 2021).

Research on identifying potential drivers for C dynamics in tropical forests have mostly focused on climatic parameters, i.e. precipitation and temperature (Moore *et al.*, 2017; Tonin *et al.*, 2017; Hofhansl *et al.*, 2020), topographic patterns (de Castilho *et al.*, 2006; Malhi *et al.*, 2017; Jucker *et al.*, 2018) or the effect of anthropogenic disturbance (Riutta *et al.*, 2018; Ross *et al.*, 2021). However, in many terrestrial ecosystems, soil parent material co-determines nutrient availability more so than other factors (Augusto *et al.*, 2017) with strong consequences for C cycling (Vitousek, 1984; Fernández-Martínez *et al.*, 2014; Wieder *et al.*, 2015). Due to a lack of observational data, especially in Africa (Huang *et al.*, 2021), it is unknown whether parent material through influencing soil geochemical properties has a substantial effect on C cycling and nutrient availability in tropical forests, especially, where long-term weathering has led to deeply developed, but often nutrient-depleted soils (IUSS Working Group WRB, 2015). The complexity of the potential interplay of soil geochemistry and plant C allocation might be aggravated in tropical montane forests due to topographic controls on heterogeneity of forest landscapes (Werner & Homeier, 2015; Jucker *et al.*, 2018). Topographic features such as terrain relief, slope, and curvature strongly influence local-scale variation in soil chemistry, hydrology, and microclimate (Tiessen *et al.*, 1994; Chadwick & Asner, 2016; Xia *et al.*, 2016).

[1] ***The content of this chapter has been published with minor changes as:*** Bukombe B, Bauters M., Boeckx P., Cizungu N. L., Cooper M., Fiener P, Kidinda L. K., Makelele I., Muhindo D. I, Rewald B., Verheyen K., Doetterl S. 2022. Soil geochemistry - and not topography - as a major driver of carbon allocation, stocks and dynamics in forests and soils of African tropical montane ecosystems. *New Phytologist. 236: 1676–1690*

As such, they directly constrain the conditions within which trees grow, driving environmental filtering, determining species habitat associations (Baltzer *et al.*, 2005; Russo *et al.*, 2008; Andersen *et al.*, 2014; Jucker *et al.*, 2018), and ultimately shaping the structure and composition of forest patches (Werner & Homeier 2015). For instance, on ridges and steep slopes, strong competition for nutrients and water favors species with life-history traits geared towards maximizing survival (Paoli, 2006; Heineman *et al.*, 2011b; Holdaway *et al.*, 2011b). In contrast, forests in alluvial valleys are shaped by competition for light, and generally develop taller, vertically stratified canopies (Paoli *et al.*, 2008; Werner & Homeier 2015), while also maintaining higher productivity and turnover rates (Aiba *et al.*, 2005; Stephenson & van Mantgem, 2005; Quesada *et al.*, 2012) Furthermore, erosional processes could potentially lead to a periodical "rejuvenation" of soil surfaces, leading to the resurfacing of former subsoil or soil parent material that can be either more (Porder *et al.*, 2007) or less depleted in soil nutrients (Eger *et al.*, 2018; Doetterl *et al.*, 2021b,a).

To date, the connection between drivers of C allocation and its relationship to the controls responsible for the build-up of soil organic carbon (SOC) stocks in tropical forest have rarely been investigated and never at the landscape scale from regions (>10000 km2) to catchments (> 10 km2) to local hillslopes (<1 km2). To attenuate this crucial gap in the understanding of C cycling in tropical African forests it is necessary to collect combined vegetation and edaphic data across topographic and geochemical gradients. Due to the wide extent of forest cover, difficult accessibility, limited field inventories and lack of long-term monitoring sites, efforts to estimate the distribution of tropical forest biomass C stocks and associated fluxes often rely on remote sensing techniques (Tyukavina *et al.*, 2013a; Xu *et al.*, 2017). This is why it is common practice in large scale modeling studies to use fixed ratios of shoot:root biomass/C allocation and apply allometric equations relating above to belowground biomass to estimate ecosystem C budgets (Mokany *et al.*, 2006; Cleveland *et al.*, 2013; Gherardi & Sala, 2020). As such, the potential impact of local edaphic parameters such as differences in soil geochemical properties and parent material on NPP allocation in tropical forests have often been ignored or considered of secondary importance (Moser *et al.*, 2011; Moore *et al.*, 2017). In part, this is due to the assumption that (i) nutrient cycling in deeply developed tropical soils should be largely decoupled from soil parent material (Augusto *et al.*, 2017; Doetterl *et al.*, 2021b,a) and that (ii) nutrients get recycled quickly in semi-closed systems with rapid turnover of organic litter by microbial decomposers and uptake into vegetation (Krishna & Mohan, 2017; Giweta, 2020).

However, there is reason to assume that differences in geochemical soil properties derived from parent material are likely to affect C dynamics in several ways. As such, the availability of rock-derived nutrients such as phosphorus (P), magnesium (Mg), calcium (Ca) or potassium (K) in soil depends on the concentration in the parent material source, the degree of weathering and (potential) depletion or enrichment of certain elements in soil (Quesada *et al.*, 2020). Nutrient limitations that vary with parent material (Augusto *et al*., 2017) may therefore drive the allocation strategies of tropical forests towards more efficient nutrient storage and uptake while minimizing leaching losses. Additionally, as a result of long periods of weathering, tropical soils are often enriched in iron (Fe) and aluminum (Al) oxyhydroxides compared to many (younger and less weathered) temperate soils (Khomo *et al.*, 2017). Fe- and Al-rich soils can typically form very stable (micro-)aggregates and complexes with organic matter (Bruun *et al.*, 2010; Torres-Sallan *et al.*, 2017). This provides a significant energetic barrier for microbial decomposers to overcome and can slow down organic matter turnover (Kleber *et al.*, 2021). Soil carbon stocks in tropical African forests have been shown to be determined predominantly by the potential of soils to stabilize carbon by these organo-mineral associations (Kirsten *et al.*, 2021b; Reichenbach *et al.*, 2021b). Recent studies from tropical African montane forests, for example, have demonstrated that geochemical soil properties related to the local parent material explain up to 75 % of variability in SOC stocks (Reichenbach *et al.*, 2021) and were significant in explaining soil C turnover under stable, warm-humid atmospheric conditions. Thus, drivers of NPP and the associated C fluxes in tropical forest systems remain unclear as they crucially rely on the complex interplay of soil formation and nutrient availability, topography, climate and biology (Yoo & Mudd, 2008). The objective of this study was to improve the mechanistic understanding of NPP and C allocation strategies in tropical forests along geochemical and topographic gradients and how they link to soil properties. This study presents the results of a two-year monitoring campaign on NPP components along topographic and geological gradients in African tropical montane forests. Specifically, this study aims to answer the following questions:

(1) What is the role of soil geochemistry as a driver of NPP and C allocation in tropical montane forests? Do similarly developed forests exhibit plasticity in their root:shoot C allocation and NPP depending on soil geochemical properties? This question is connected to the following hypothesis: Above and belowground NPP and C allocation in old-growth tropical forests are driven by soil chemical properties derived from its parent material that shape the availability of rock-derived nutrients for plant growth. Consequently, plant biomass and NPP should be

higher in forest stands developed on fertile soils than on low fertility soils. However, NPP allocation should react strongly to fertility differences in soil and forests growing on poor soils to invest more in root biomass production to mine sufficient nutrients for plant growth.

(2) What is the role of topography as a driver of NPP and C allocation in tropical montane forests? Topography should have a modifying effect on biomass production based on established paradigms (Werner & Homeier, 2015; Chadwick & Asner, 2016; Malhi *et al.*, 2017; Jucker *et al.*, 2018). Based on this earlier work, the study hypothesizes that changes in water and nutrient along hillslopes should shift above to belowground productivity favoring slow growing communities where water and nutrient become limited. Consequently, higher NPP fine roots and lower NPP litterfall and wood on slope positions should be expected. On plateaus and in valleys a competition for light favors fast growing communities. As a result, at plateau and valley positions, NPP litterfall and wood should be higher, and NPP fine root should be lower than on slopes.

(3) How closely are SOC stocks related to NPP and standing biomass C stocks in tropical forest soils? This question is connected to the following hypothesis: SOC stocks are mainly controlled by the amount of C productivity and allocation to belowground biomass. Therefore, SOC stocks should be higher in forest stands where root NPP and C allocation to roots is high, compared to forest stands where plants invest more in aboveground NPP components. To answer these questions, C stocks and C allocation for both above- and belowground biomass and soil were assessed in old growth forests across contrasting geochemical regions along the Albertine Rift in Eastern Africa. Using linear and non-linear models, the relationships of C allocation patterns among NPP components and C stocks to topography and soil (geo-) chemical properties were then determined.

3.2. Material and methods

3.2.1. Forest inventory and aboveground living biomass C stock

In 2018, full inventories of the forest tree species and aboveground standing coarse woody (further simply called "wood") biomass were conducted on all plots following Matthews et al. (2012). First, all living trees with a diameter at breast height (DBH; measured at 1.3 m aboveground) of ≥10 cm in each plot were identified. Second, two alpha diversity indices (species richness and H-Shannon) (Morris *et al.*, 2014) were calculate to get insight into aspects of species diversity across the investigated geochemical regions. Third, to estimate the wood biomass, stand-specific height-diameter (H:D) allometric relationships using a representative subset of plot-specific trees were constructed using modelHD included in R package 'BIOMASS' (Chave *et al.*, 2014; Réjou-Méchain *et al.*, 2017). For this, 20 % of all trees distributed across all DBH classes were selected for height measurement per plot. Depending on DBH class abundance, the heights of three to five individual trees per class were measured using a hypsometer (Forestry Pro II, Nikon, Japan). Wood biomass, i.e. stems and large branches, for each individual tree was then estimated using the allometric equation for moist tropical forests as described in Chave *et al.* (2014). For model parameterization, species-level averages of wood density (WD) were taken from the DRYAD database (Zanne *et al.*, 2009). Where species-specific WD data were not available, genus- or family-level mean WD values were used for the analysis. To calculate wood productivity, a re-census in 2020 was carried out. Note that inventorized dead trees in the first and second census were excluded as they do not contribute to the annual NPP. Wood NPP, the relative stem growth rate, and wood C turnover rate per plot were then calculated using the following equations:

$$NPP_{wood} = \left(\frac{\Sigma stem2 - \Sigma stem1}{\Delta t}\right) * a^{-1} \quad \text{(Eq. 3.1)}$$

$$RGR = \left(\frac{\ln(stem2) - \ln(stem1)}{\Delta t}\right) * 100 \quad \text{(Eq.3.2)}$$

$$\tau_{wood} = \frac{NPP_{wood}}{\text{Wood C stock}} \quad \text{(Eq. 3.3)}$$

Where NPP_{wood} is the wood net primary productivity of a plot (Mg C ha^{-1} $year^{-1}$), RGR the relative growth rate in (% $year^{-1}$), and is the biomass of individual stems for the first and second census, respectively, "a" is the plot area in ha, "Δt" is the time between the two censuses (2.0 - 2.4 years), and $\boldsymbol{\tau}_{wood}$ is the wood C turnover rate in (% C $year^{-1}$). To enable direct comparison with other studies on biomass assessment (see (Saatchi *et al.*, 2011; Kearsley *et al.*, 2013), the

study assumed that all standing wood biomass holds a C content of 50 % of dry biomass but acknowledge the uncertainty related to this since e.g. wood biomass C can vary between ~ 41 - 51 % of dry biomass (Martin & Thomas, 2011). To calculate standing wood C stocks, only data collected during the second census in 2020 were used. Wood C turnover rate was then calculated as a ratio of NPP_{wood} to wood C stock. In addition, C:N content and ratio of living, healthy-looking (without signs of herbivory), canopy leaves (sun-exposed shoots at outer canopy), sampled during the weak dry season of December 2018 – February 2019 were assessed following Pérez-Harguindeguy *et al.* (2013). Sampled leaves originate from at least 3 individual trees per species representing ≥80 % of the standing basal area per plot. Community-weighed means of C:N of canopy leaves were calculated using dried and homogenized samples at the plot level.

3.2.2. Litterfall productivity

For litterfall measurements, ten litter traps per plot were installed and distributed evenly across each plot and the subplots therein, for details of litter trap placement see Doetterl *et al.* (2021a). Traps, made of locally available charcoal sacks, had a diameter (d) of 60 cm and were installed at a height of 1.0 m. Litter samples were collected every two weeks for the period August 2018 to February 2020. In consequence, the strong rain and dry seasons were sampled once while the weak rain and the weak dry seasons were sampled twice, requiring to calculate weighted averages for each season. The collected litter included all organic residues collected by the traps; woody debris (d >2 cm) and dead animals were discarded. After each sampling, collected litter material was broken into small pieces, mixed and homogenised per plot. Material from all 10 traps per plot was pooled to obtain a composite sample per plot and taken to the laboratory the day of sampling, oven-dried (70 °C, 72 h), and subsequently weighed. Where mixing with hands was not possible due to the large surface area of leaves, an electric blender (1000 W; TYB-315) was used to homogenize the litter material. This resulted in a total of, on average, 45 pooled data points of litterfall per plot distributed over the monitoring period. then 10 g of well mixed litter material per data point were subsampled and milled using a PM 400 Planetary Ball Mill (Retsch, Germany) at 400 rounds per minute for C:N analysis. Litter C content was then measured on a 5 mg powdered litter subsample using dry total combustion (Variomax C:N, Elementar GmbH, Germany). Note that three replicates were measured on 20 % of the samples to assess the laboratory analytical error–showing a standard deviation of 5 % (Doetterl *et al.*, 2021c). To represent total litter production per plot, first the average daily litter productivity in each plot was calculated for season (i) using the equation below. Litter

productivity values for the seasons covered twice during sampling were first averaged before an annual average of litter productivity was calculated.

$$Lit_{dw(i)} = \frac{w}{a*n} \quad \text{(Eq. 3.4)}$$

Where $Lit_{dw(i)}$ is the average daily litterfall per season (i) (Mg ha^{-1} day^{-1}), w is the total dry weight (Mg) of the sample per plot, "a" is the area of the litter traps (ha), "n" is the number of days per sampling interval. The annual litter productivity $NPP_{litterfall}$ (Mg C ha^{-1} $year^{-1}$) was calculated from the averaged litter productivity of the considered four (equal length) seasons, as the sum of 365 days. Litter biomass C for each plot was calculated by multiplying the measured litter C content with the corresponding biomass productivity.

3.2.3. Root biomass and fine root production

Fine ($d \leq 2$ mm) and coarse ($d > 2$ mm) root biomass and fine root production were assessed from September 2018 to December 2019 on all plots, following depth-explicit sampling and standardized protocols (recently summarized by (Freschet *et al.*, 2021)). Prior to deciding on maximum sampling depth and depth intervals, root depth distribution was assessed to 1 m depth using soil profiles established at the center of a plot. This assessment revealed that fine root counts on the profile wall were most frequent in organic horizons and the upper 50 cm (data not shown), with approximately 90-97% of the root biomass evenly placed within the O horizon and the top 30 cm of mineral soil (see Fig. S3.6 for fine root biomass distribution to 50 cm depth). Belowground standing root biomass was thus sampled to a depth of 50 cm using a soil core sampler with 6.8 cm inner diameter (Vienna Scientific Instruments, Austria). Sequential coring took place once per season (every three months) where one soil core per subplot was sampled, resulting in a total of four cores per plot per season. More frequent sampling campaigns similar to litterfall monitoring were not feasible for logistic reasons. No cases of soil compaction as a result of the incremental sampling were observed. Cores were subsequently divided into five distinct depth layers: the organic O horizon, and four mineral soil layers from 0 – 10 cm, 10 – 20 cm, 20 – 30 cm, 30 – 50 cm. After transport to the laboratory, roots were separated into fine and coarse roots. To do this, each sample was rinsed within a sieve of 2 mm-mesh size positioned on top of a 1 mm sieve. The two sieves together were placed on top of a bucket to collect also the smallest roots fragments. Note that Coarse roots were not considered for further analyses as i) their spatial distribution is considered insufficiently covered by the sequential coring approach (Ostonen *et al.*, 2005; Yuan & Chen,

2013), and ii) the contribution of relatively slow coarse root growth and turnover rates to seasonal biomass productivity (using the DM method, see below) is considered minimal (McCormack *et al.*, 2015; Huang *et al.*, 2020). This can lead to an underestimation of the total NPP. However, fine roots' contribution to the terrestrial NPP range is 22 % - 40 % (Cordeiro *et al.*, 2020) with turnover being much faster than for coarse roots, making them an important but often unmeasured component of the carbon budget of forest ecosystems (Jackson, R *et al.*, 1997; Ostonen *et al.*, 2005). Therefore, as a dynamic carbon pool (fast growth and high turnover rate), fine roots are often seen as a major C input and contributor to SOC stocks (Lukac, 2012). Hence, for roots, this study reported only fine root biomass.

Thus, fine roots were separated into living and dead fractions based on criteria such as color, root elasticity, and the degree of cohesion of cortex, and stele–roots were i.a. considered living when root steles were bright and resilient (Ostonen *et al.*, 2005; Freschet *et al.*, 2021). The dry mass of fine roots per core, horizon/layer and living/dead fraction (± 0.01 g dwt) was determined after drying (70 °C, 72 h); standing fine root biomass C was calculated (Mg C ha^{-1}), assuming a C content of 50 % of dry biomass. Fine root productivity was calculated using the improved Decision Matrix (DM) method (Yuan & Chen, 2013) as a reliable method to determine fine root production when rapid turnover can be assumed (Fairley & Alexander, 1985; Assefa *et al.*, 2017; Freschet *et al.*, 2021). Briefly, to determine the fine root NPP, this method includes both (significant) changes in living and dead standing root mass between two sampling dates throughout the monitoring period. The collected fine root data per season were aggregated for each layer at the plot level. In brief, fine root biomass production (P_{root}) in (g) for 90 days for each sampling point and horizon/layer was then calculated taking into account variation in living (ΔL) and dead (ΔD) fine root mass between two consecutive sampling dates where P_{root} is equal to ΔL if $\Delta L > 0$ and $\Delta D < 0$. P_{root} is equal to zero if both ΔL and $\Delta D < 0$; see (Yuan & Chen, 2013) for details. In order to give all seasons, the same weight for the year 2018 and 2019, first daily averages of root biomass per unit area were calculated for each season using the following equation:

$$root_{season(i)} = \frac{P_{root}}{a*n} \qquad \text{(Eq. 3.5)}$$

Where $root_{season(i)}$ is the daily dry weight fine root biomass productivity per season (i) (Mg $ha^{-1}day^{-1}$), P_{root} is the root productivity (Mg) between two sampling dates per layer and plot, “a” is the area of a soil core for each layer (ha), “n” is the number of days each sampling interval

represented. Note that the DM method may underestimate fine root NPP owing to fine root losses through herbivory, secondary growth of fine roots, or decomposition of dead roots faster than the sampling interval (Lowatschek, 2021).

Similar to litter productivity, before calculating the annual root productivity, the four seasons were weighed equally. That is root productivity values for the seasons covered twice were first averaged to daily means before an annual average for root productivity was calculated. Similar to $NPP_{Litterfall,}$ annual dry weight fine root productivity NPP_{roots} (Mg C ha^{-1} $year^{-1}$) was calculated as the sum of the (averaged) seasonal root productivity. Fine root biomass C for each plot was calculated by assuming C content to be 50% of dry biomass (Lewis *et al.*, 2009a; Zhu *et al.*, 2017). Fine root turnover rate was calculated following (Gill & Jackson, 2000; Brunner *et al.*, 2013) (Eq. 3.6).

$$\tau_{fineroot} = \frac{NPP_{fineroot}}{\text{fineroot C stock}} \quad \text{(Eq. 3.6)}$$

3.2.4. Assessing biomass C allocation

NPP_{sum} was calculated as the sum of components (wood growth, litterfall and fine root production) for each forest plot using the following equation (eq. 3.7). Finally, the proportion of NPP_{sum} allocated into each component (x) was calculated using the following equation (eq. 3.8).

$$NPP_{sum} = NPP_{wood} + NPP_{litterfall} + NPP_{roots} \quad \text{(Eq. 3.7)}$$

$$Allocation_x = \frac{NPP_x}{NPP_{sum}} * 100 \quad \text{(Eq. 3.8)}$$

where NPP_{sum} is the total NPP (Mg C ha^{-1} $year^{-1}$). Note that the NPP_{sum} estimated in this study may be biased towards underestimation because it omits several NPP terms such as volatile organic emissions, and C allocation to root exudates and mycorrhizal symbionts for methodological reasons (Malhi *et al.*, 2017). Particularly, the amount of C allocation to tree root exudates and mycorrhizal symbionts can be substantial and strongly related to nutrient availability (Treseder, 2004; Hobbie, 2006; Aoki *et al.*, 2012; Doughty *et al.*, 2018)--creating some uncertainty in stands with medium- or low-nutrient availability (Buendia *et al.*, 2014). However, the calculation of NPP was based on three independent measurements (wood growth, litterfall, fine root production) covering major components of NPP (Vieira *et al.*, 2011;

Doughty *et al.*, 2018) allowing for an essential characterization of plant investment into root:shoot and root:leaf allocation.

3.2.5. C stocks of organic and mineral soil layers

As part of an extensive sampling campaign (Doetterl *et al.*, 2021a), organic soil litter layers (L horizon and O horizon) were sampled at eight points along the border distributed across all subplots and in the center of each forest plot at the time when soil sampling took place. At each sampling point, the thickness of the L and O horizons were measured with a ruler and then sampled within a 5 cm x 5 cm square. When the litter layers were thin (<0.5 cm), the sampling square was expanded to 10 cm x 10 cm to retrieve sufficient sample material. The nine samples of each layer were combined into one composite sample per plot. In the laboratory, samples were oven-dried (70 °C, 48-96 h) and weighed. To sample mineral soils, four one-meter soil cores were sampled per plot (one core per subplot) using a cylindrical soil core sampler for undisturbed sampling. For the purpose of this study, relating to the depth of sequential root coring (see below), only soil C data of the top 50 cm was used. Cores were separated into 10 cm increments and combined into depth-explicit composite samples per plot. For the organic litter layers (L and O horizons), C stocks were determined as the product of the litter mass per area and the litter C content. For mineral soil, total C was measured to 50 cm soil depth on 1 g of grinded soil samples using dry total combustion (Variomax C:N, Elementar GmbH, Germany) with the laboratory analytical error assessed in the same way as for litterfall (see above and Doetterl *et al.* (2021c)). Since no inorganic C was found in any of the investigated soils (Doetterl *et al.*, 2021b,a), total C was interpreted as SOC. C stock of the bulk soil of each layer was then calculated by multiplying C content with soil bulk density and the depth increment of the horizon/layer. Aligned with root sampling, the top five mineral layers were summed to have SOC stocks to 50 cm mineral soil depth (Mg C ha^{-1}).

To assess relationships of potential soil controls on NPP components and their relative C allocation, a wide range of plot-specific geochemical properties for the top 30 cm were extracted from an existing database assembled in parallel to this study (TropSOC database v1.0, Doetterl *et al.*, 2021c). Only soil properties for the top 30 cm of mineral soil were used because the assessment of root biomass revealed that the large majority of fine roots (approximately 90 %, relative to 50 cm) were found in organic litter layers and in those top mineral layers for all three investigated geochemical regions (Fig. S3.6). Introducing properties of deeper subsoil (> 30cm) would hence introduce unnecessary bias towards deeper layers with little to no roots.

Included soil variables covered a wide range of predictors such as soil fertility, SOC properties (SOC stocks, C:N ratio) and soil texture (clay, silt and sand content).

3.2.6. Statistical analysis

To assess species composition as well as similarities and dissimilarity of species between the three geochemically regions, a nonmetric multidimensional scaling (NMDS) was performed on the inventory data of the plots, using the 'vegan' package (Oksanen, 2007) and following a rank-based interpretation of the data. NMDS analysis was conducted using the "Bray-Curtis" measure of distance, and number of axes (K=3) and reported the stress value which is a measure of goodness of fit. Further, the coefficient of determination between the ordination distance and the observed dissimilarity in the original data was computed. Since NMDS does not use the absolute abundance of species but rank orders. In this case rather than mafic being X units distant from the felsic region and Y units distant from sedimentary, the NMDS ranks plot/region species similarities as follows: The sedimentary region is the "first" most distant from mafic while the felsic region is the "second" most distant. As such, it is a robust method for multidimensional analysis of tree diversity. Another advantage of NMDS is that it does not rely on normally distributed data. This is specifically important as there are only few abundant species across sites, but many species with site specific appearance, which could result in skewed data (Legendre *et al.*, 2005).

To assess differences in the distribution of C stocks in soil and aboveground biomass, as well as the differences between NPP components (litterfall, wood, fine roots) and the relative C allocation, collected data were analyzed for differences across topographic positions and geochemical regions with data presented as means per plot (± standard deviation, SD). Before the analysis, a residual analysis was conducted to test for the assumptions of ANOVA. For this, the Shapiro-Wilk's test of normality distribution and the Levene's test for homogeneity of variances were used. The tests showed that requirements of normality distribution and homogeneity were not met. Hence, the non-parametric Kruskal-Wallis test was used as an alternative to one-way ANOVA using the R package 'pgirmess'(Giraudoux, 2022). For a post-hoc pairwise comparison of significant differences in C stocks, NPP and C allocation between distinct groups (i.e. topographic positions or geochemical regions), the Dunn's test was used to identify which group levels are significantly different using the 'rstatix' package (Kassambara, 2021).

As multicollinearity and autocorrelation between independent variables was to be expected due to the large number of variables and a relatively small number of aggregated observations, rotated principal component analysis (rPCA) for dimension reduction (Jolliffe, 1995), was conducted before regression analysis. Before conducting the rPCA, due to differences in scales and units among the soil geochemical properties, a transformation method on the input data was applied using the standardization technique to have a mean value of zero and standard deviation of 1 for each variable. All retained rotated components (RCs) were then interpreted based on the loadings of the original variables and using expert knowledge for the likely underlying mechanisms that can affect C dynamics (Table S3.4). A threshold of $r > 0.5$ & < -0.5 was used to decide whether an independent variable that is loaded into an RC is used for the mechanistic interpretation of the RC or not. An eigenvalue >1 and explained the proportion of variance >10% for each RC were used as criteria to include or exclude an RC into the models (Jolliffe, 1995; James *et al.*, 2013).

To assess the effects size and direction (positive or negative) of rotated principal components on different NPP compartments and their relative C allocations, a Bayesian multilevel linear mixed effect models was applied with intercepts set to zero to allow comparison of the effects size of rotated principal components between models for the different NPP components. In the models, the retained RCs were set as fixed effects and plotIDs as random effects using the 'brms' R package (Bürkner, 2017). Compared to traditional statistical models, Bayesian approaches have the advantage of taking all sources of variance into account simultaneously while still allowing for the implementation and assessment of random and fixed factors (random and fixed) into a single model. To assess model uncertainty, a Monte Carlo Markov Chain algorithms (MCMC) was used with a total of 3000 iterations, using 4 separate chains with 1000 warmup iterations. Confidence intervals were subsequently extracted from the posterior parameter distributions, along with the mean effect size, marginal R squared (indicating the proportion of total variance explained by fixed effects) and conditional R squared (indicating the proportion of total variance explained by both fixed and random effects) (Nakagawa *et al.*, 2017), the root mean square error (RMSE) and the ratio of performance to deviation (RPD). A model was interpreted as performing well if RPD > 1.5 along the guidelines given by (Chang *et al.*, 2001). For assessing the relationship between response variables and independent predictors, pairwise Pearson correlation coefficients and least square regression analysis were used. Due to the relatively small number of replicates and therefore limited statistical power, for all the statistical tests p-values <0.05 was designated as significant and p-

values < 0.1 as marginally significant / tendent. All statistical analyses were carried out with R software (R Core Team, 2020).

3.3. Results

3.3.1. Forest structure and species composition

The three regions differ significantly in terms of dominant tree species composition (Fig. S3.2). In the mafic region, the dominant species are Dombeya mukole and Alangium chinense. In the felsic region, Uvariopsis congensis and Chrysophyllum gorungosanum and in the sedimentary region Cleistanthus polystachyus and Syzygium guineense. A complete species list can be found in Doetterl et al. (2021c). NMDS analyses yielded a stress value of 0.04, which indicates an only small error between the actual dissimilarity distances and the ordination distances calculated by NMDS and a good representation of dissimilarity of species composition between plots and regions. Furthermore, NMDS results suggest that all forests are characterized by varying structure and species composition, which is specific for each geochemical region, but similar within each region (Fig. S3.2). Note that an analysis of the Shannon and species richness indices (Table S3.3) did not indicate strong differences between geochemical regions. Forest stands in mafic and sedimentary regions are characterized by a high number of trees per unit area compared to forests in the felsic region (Table S3.3). Forests in the mafic region are characterized by a higher density of small trees of (10 - 20 & 20 - 30 cm diameter at breast height (DBH)) while plots in the sedimentary regions hold a higher density of larger diameter trees (DBH >40 cm; Fig. S3.1). Average tree height and distribution among tree DBH classes are similar in the felsic region compared to the sedimentary region but lower in the mafic region (Table S3.3, Fig. S3.1). Collected living canopy leaves differ between regions with significantly wider C:N ratios in canopy leaves of the sedimentary region compared to those in mafic and felsic regions (Fig. S3.5). Lastly, based on observations during the field campaign, understory vegetation in the mafic and sedimentary regions was usually denser than in the felsic region, which was almost free of any understory vegetation (data not shown).

3.3.2. Patterns of aboveground biomass and soil carbon stocks across geochemical regions and topography

The three regions differ significantly in terms of dominant tree species composition and forest structure (Fig. S3.1; notes S3.1). C stocks of the different biomass and soil components showed distinct patterns across geochemical regions (Fig.3.1a). Wood C stock was significantly higher in the sedimentary (206.4 ± 40.9 Mg C ha^{-1}) compared to the felsic (117.9 ± 29.6 Mg C ha^{-1}) and mafic regions (99.1 ± 17.0 Mg C ha^{-1}) (Fig. 3.1a). The C stock of organic litter layers (sum of L and O horizons) in the sedimentary region (37.3 ± 5.4 Mg C ha^{-1}) was eight times that of the felsic (4.4 ± 0.9 Mg C ha^{-1}) and three times that of the mafic region (12.1 ± 3.0 Mg C ha^{-1}). The living fine roots C stock (to 50 cm mineral soil depth) was higher in the sedimentary (4.4 ± 1.6 Mg C ha^{-1}), compared to the felsic (1.7 ± 0.2 Mg C ha^{-1}), and mafic regions (1.6 ± 0.3 Mg C ha^{-1}), with a significant but small difference between the later. SOC stocks followed a different pattern than root C stocks. SOC was significantly higher in the mafic (208.2 ± 22.6 Mg C ha^{-1}) compared to the felsic (137.9 ± 25.3 Mg C ha^{-1}) or sedimentary regions (125.9 ± 36.7 Mg C ha^{-1}). No significant differences or consistent patterns in biomass C or SOC stocks were detectable related to the topographic position of plots in each geochemical region (Fig. 3.1b), following Kruskal-Wallis tests and pair-wise comparison using Dunn's tests (p-value < 0.05).

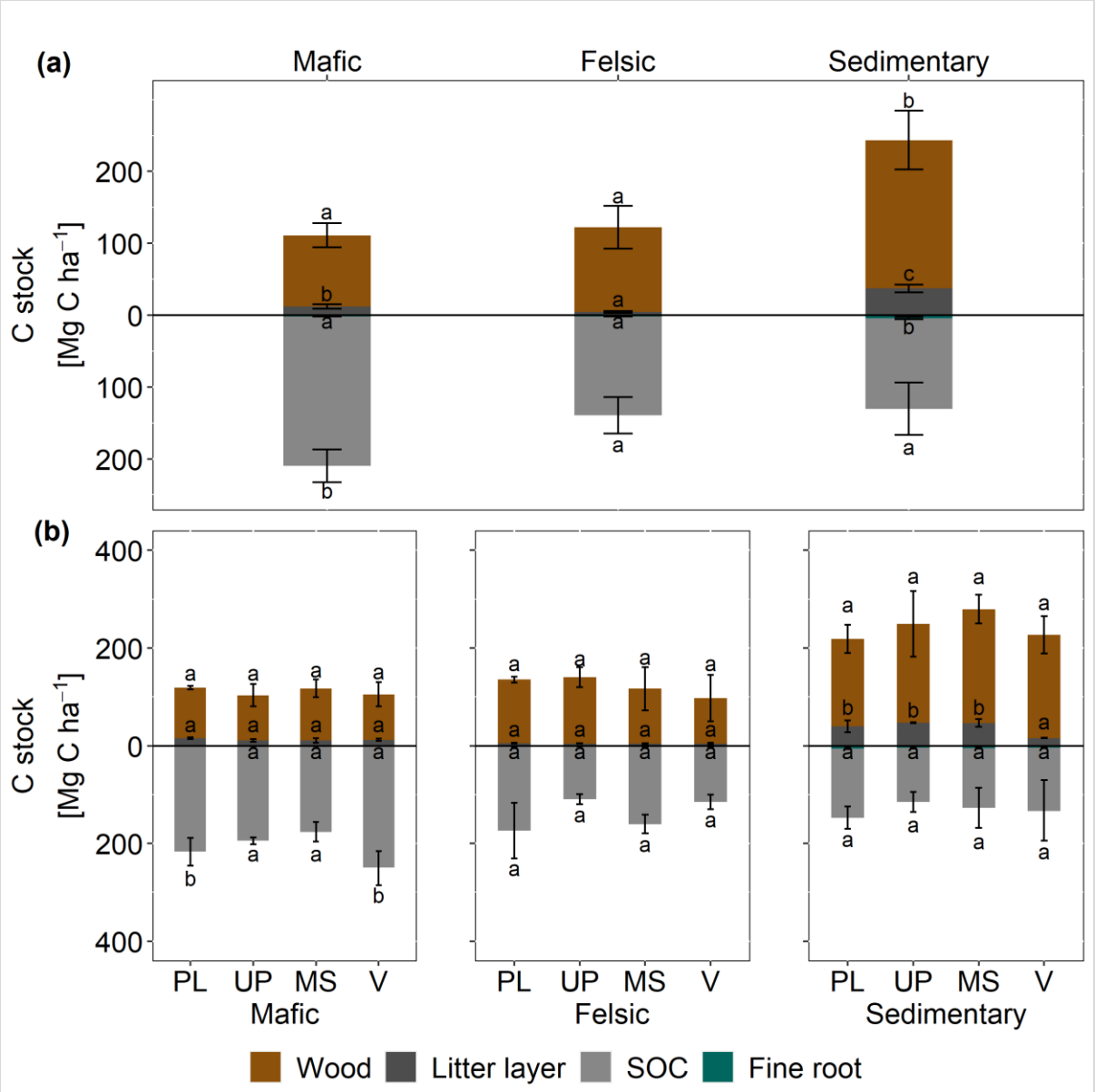

Figure 3.1. (a) Carbon stocks of aboveground woody biomass, organic litter layers (L+O horizon), living fine roots and mineral soil organic carbon (SOC) across geochemical regions (mean ± SD; for wood (n = 12 per region), for litter layer and fine root (n = 8, 12, 12 for mafic, felsic and sedimentary region). SOC stocks were determined for the top 50 cm of the soil profile. (b) C stocks for aboveground coarse woody, litter layers (L and O horizons), living fine roots and SOC across the three geochemical regions and along topographic positions (PL: plateau, UP: upper slope, MS: middle slope, and V: valley) (Mean ± SD). Different letters on top of bars indicate significant differences between geochemical regions or topographic positions separately for each C stock component, following Kruskal-Wallis tests and pair-wise comparison using Dunn's test (p-value < 0.05).

3.3.3. Patterns of C allocation in net primary productivity across geochemical regions and topography

Similar to C stocks, differences in NPP related to the geochemical region of the respective study site were found (Fig. 3.2a). For wood, NPP_{wood} was higher in the mafic (6.2 ± 1.8 Mg C ha^{-1} $year^{-1}$), followed by the felsic (5.01 ± 1.2 Mg C ha^{-1} $year^{-1}$) and lower in the sedimentary region (3.4 ± 1.1 Mg C ha-1 year-1). For leaves, $NPP_{litterfall}$ was higher in the sedimentary region (5.3 ± 0.8 Mg C ha^{-1} $year^{-1}$), followed by the mafic (4.5 ± 0.6 Mg C ha^{-1} $year^{-1}$) and lower in the felsic region (3.3 ± 0.5 Mg C ha^{-1} $year^{-1}$). For fine roots (in O horizon and top 50 cm of mineral soil), NPP_{roots} was more than two-folds higher in the sedimentary region (5.5 ± 2.0 Mg C ha-1 year-1) compared to the felsic region (2.0 ± 0.5 Mg C ha^{-1} $year^{-1}$), and four-folds higher compared to the mafic region (1.1 ± 0.8 Mg C ha^{-1} $year^{-1}$). No significant difference or consistent pattern in NPP were detectable related to the topographic position of plots in each geochemical region (Fig. S4.5). NPP_{sum} was higher in the sedimentary region (14.2 ± 4.0 Mg C ha^{-1} $year^{-1}$) followed by felsic region (11.9 ± 3.0 Mg C ha^{-1} $year^{-1}$) and lower in the mafic region (10.4 ± 2.3 Mg C ha^{-1} $year^{-1}$). Based on Pearson's correlation coefficients (p-value < 0.05), NPP_{sum} was strongly positively correlated with NPP_{roots} and $NPP_{litterfall}$ but there was no relationship between NPP_{sum} and NPP_{wood} (Fig S3.6). Instead, NPP_{wood} was negatively correlated with NPP_{roots} (Fig. S4.6). Relative NPP C allocation into wood was significantly lower in the sedimentary region (24 ± 6 % of total NPP C) compared to the felsic (48 ± 5 %) or mafic (52 ± 6 %) regions, with a non-significant difference between the later (Fig. 3.2b). NPP C allocation into leaves was lower in the felsic (32 ± 2 %), compared to the sedimentary (38 ± 5 %) or mafic (39 ± 3 %) regions. In contrast, relative NPP C allocation to fine roots was significantly different across the geochemical regions and differed by a factor of four with higher values observed in the sedimentary region (38 ± 8 %) followed by the felsic region (20 ± 4 %), and lower in the mafic region (10 ± 4 %). No significant difference or consistent pattern in relative NPP C allocation was detectable in relation to the topographic position of plots in each geochemical region (Fig. S3.5), following Kruskal-Wallis tests and pair-wise comparison using Dunn's test (p-value < 0.05).

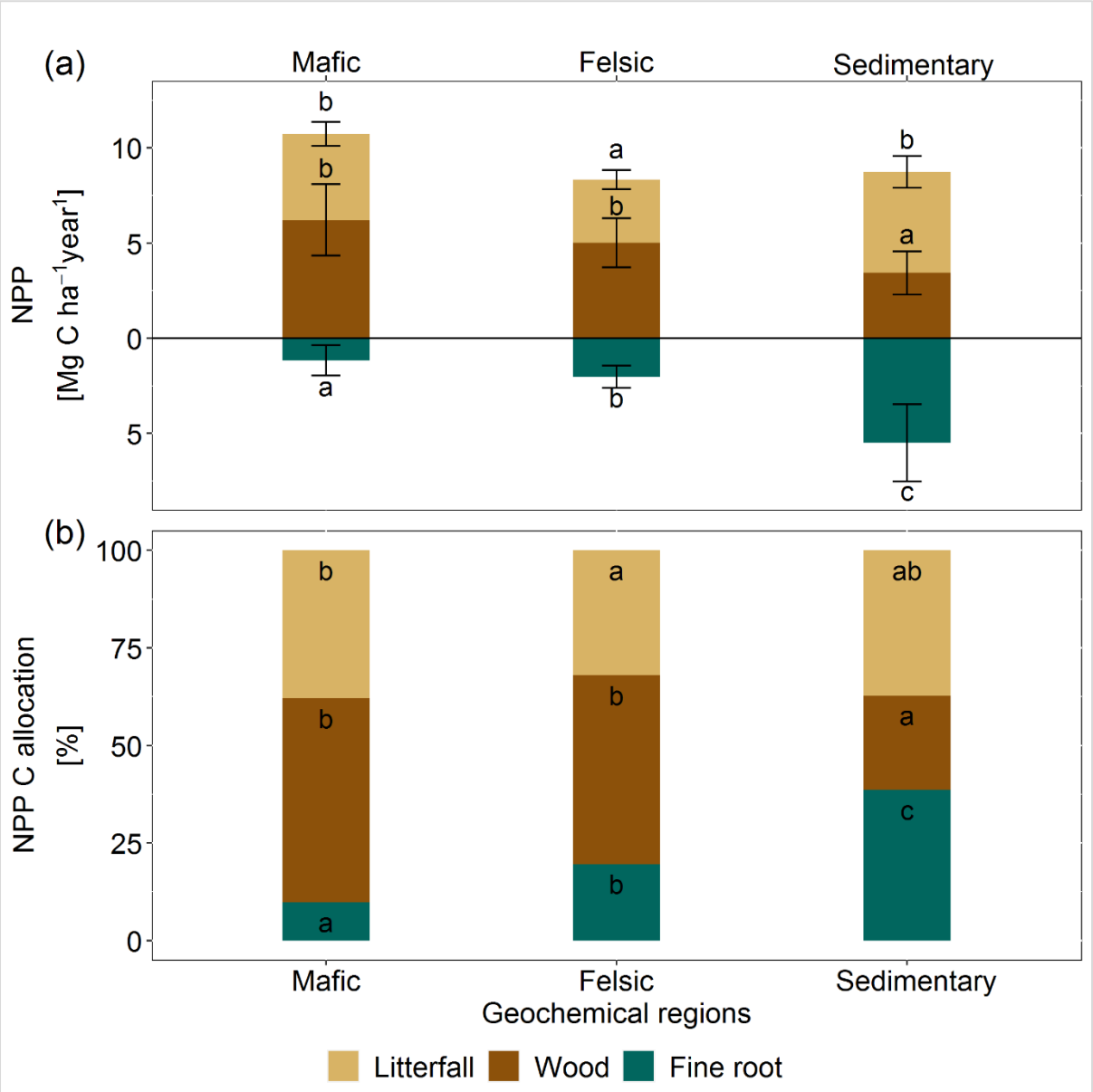

Figure 3.2. (a) Net primary productivity of biomass C for leaf litterfall, wood, and fine roots (≤ 2mm) across the felsic, mafic and sedimentary geochemical regions (Mean ± SD). Y-axis zero value divides aboveground from belowground NPP. (b) Relative NPP C allocation for leaf litterfall, wood and fine roots (as a proportion of NPP_{sum}) tested separately for each NPP component across the three geochemical regions. For both panels, different letters on top of bars indicate significant differences between geochemical regions within each NPP component (NPP_{wood} n = 12 per region, $NPP_{litterfall}$ and NPP_{roots} n = 8, 12, 12 for mafic, felsic and sedimentary region), following Kruskal-Wallis tests and pair-wise comparison using Dunn's test (p-value < 0.05).

3.3.4. Mineral soil controls on NPP and relative C allocation among components

The rPCA yielded 4 significant rotated components (RCs) based on chemical properties of the mineral soil layers in the main rooting zone that all together explained 84.1 % of the cumulative variance of the dataset (Fig. 3.3; Table S3.4). From these components, RC1 and RC2 explained about 54 % of the entire variance in the dataset. RC1 was interpreted as being related to soil exchangeable base cations and predictors for RC2 related to reserve of total base cations in soil. Hence, RCs was interpreted as "Soil exchangeable cations" (RC1) and as "Soil base cation stocks" (RC2). RC3 and RC4 explained about 30.1 % of the variance within the dataset with varying loading of independent predictors that relate to "Soil C:N:P stocks and NP availability" (RC3) and "Soil texture" (RC4).

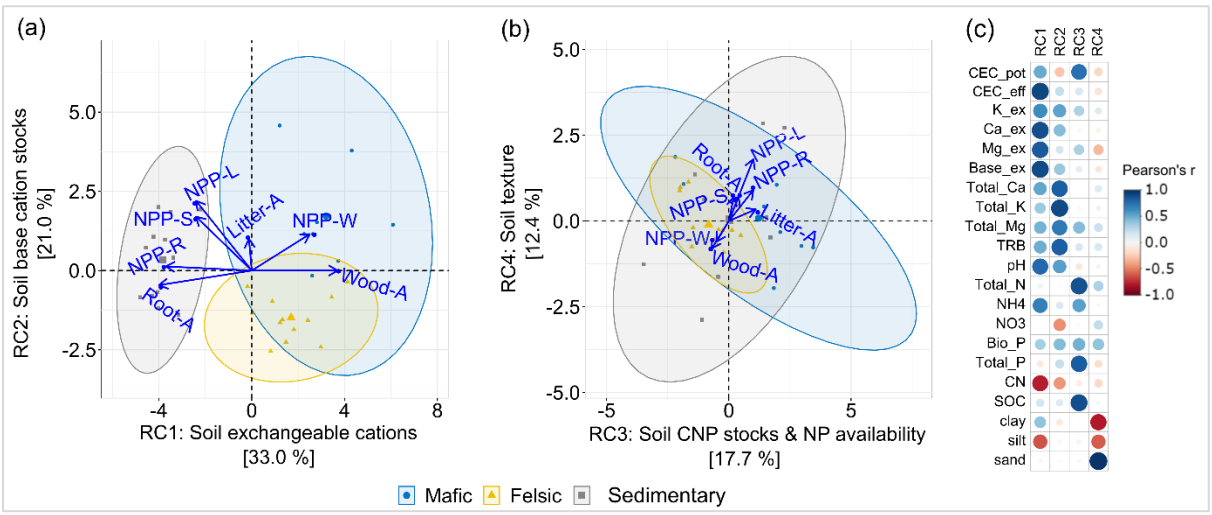

Figure 3.3. Rotated principal component analysis (rPCA) of soil properties and their relation to NPP components. Panels (a) and (b) show the four included rotated components (RCs), their mechanistic interpretation (on axes), and the score vectors that show the coordinate of projection of the NPP compartments and C allocation onto the RCs plane. Note that absolute NPP and relative NPP C allocation vectors (in blue) were not included in the rPCA and are displayed here only for the purpose to visualize their alignment with the RC space. NPP-W: NPP_{wood}, NPP-L: $NPP_{littterfall}$, NPP-R: NPP_{roots}, NPP-S: NPP_{sum}, Wood-A: NPP C allocation to wood, Litter-A: NPP C allocation to leaves, Root-A: NPP C allocation to roots. Points and colored ellipses indicate observations within each geochemical region. Position of the various NPP components within the panels (absolute NPP biomass C and relative NPP C allocation) indicate correlation to RC. The distance between a variable and the center indicates the quality of the variable representation on the RC map, with higher distance indicating stronger-representation of a variable by the RC. Panel (c) shows the loading of the included variables related to soil fertility, SOC properties and texture as soil predictors to the four RCs (details see Table **S**3.4).

When using RCs to predict the various investigated NPP components and their distribution, RC1 - RC2 broadly representing various aspects of soil nutrient status and general soil fertility, together with soil texture (RC4) explained significant amounts of variability and patterns observed in NPP C allocation (Fig. 3.4). Interpreting R^2, RMSE and RPD, all models showed a high to moderate performance in explaining the various components. In general, soil properties explained the patterns of relative C allocation similarly well as they explained the absolute NPP. Additionally, higher explanatory power of the RCs for NPP and relative C allocation to fine roots compared to leaf litterfall or wood components were obsvered. For $NPP_{litterfall}$, the selected RCs explained 52 % of the observed variability and 45 % of the variability in the relative C allocation to litterfall (Fig. 3.4a,d). Predictions of $NPP_{litterfall}$ were mainly driven by a combination of negative correlation to soil exchangeable base cations and soil texture, and a positive correlation to C:N:P stocks and NP availability (Fig. 3.4a). C allocation to litterfall was driven mostly by a negative correlation to soil textural coarseness (Fig. 3.4d). For NPP_{wood}, the selected RCs explained 49 % of the observed variability (Fig. 3b) and 58 % of the variability in the relative C allocation to wood (Fig. 3.4e). Predictions of NPP_{wood} and C allocation to wood were mainly driven by positive correlations to soil exchangeable base cations stocks and availability, C:N:P stocks and NP availability and soil texture (Fig. 3.4b,e). For NPP_{roots} the selected RCs explained 65% of the observed variability (Fig. 3.4c) and 64 % of the variability in the relative C allocation to fine roots (Fig. 3.4f). Predictions of NPP_{roots} and C allocation to fine root were strongly and negatively correlated to soil exchangeable base cations and soil texture (Fig. 3.4c,f).

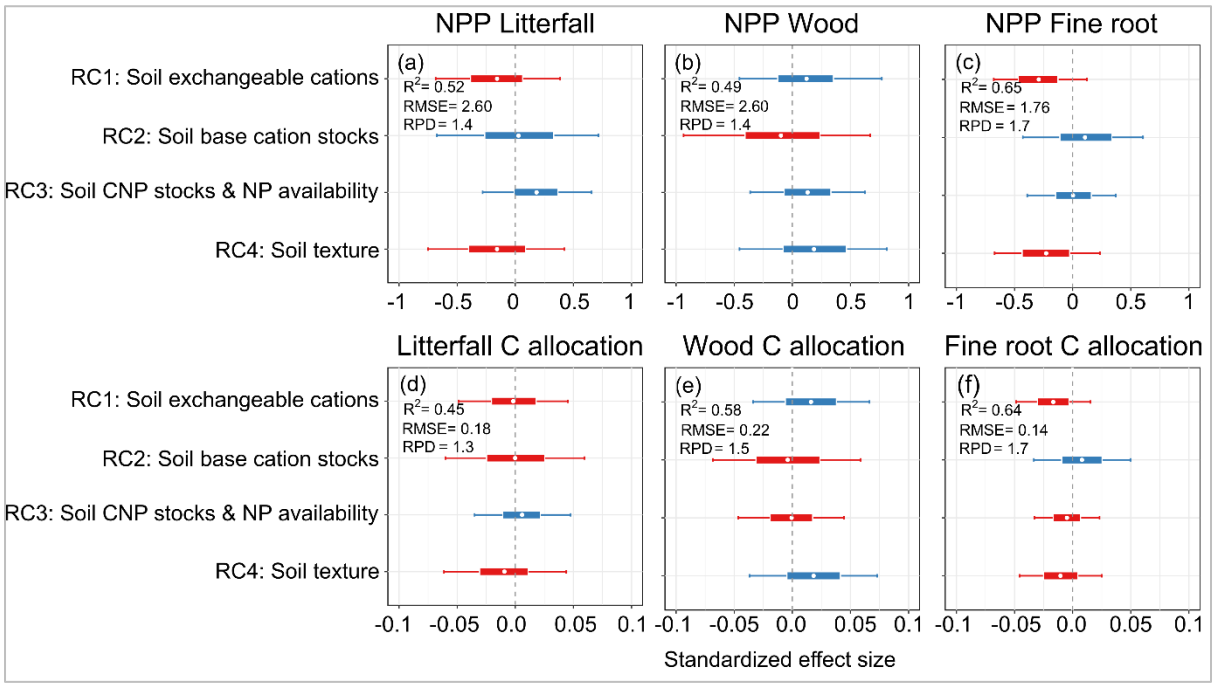

Figure 3.4. Standardized effect size of rotated principal components (RC) as explanatory factors on $NPP_{litterfall}$ (a), NPP_{wood} (b), NPP_{roots} (c), and the relative C allocation into each of these components (as proportion of NPP_{total}) (d-f). Points in the middle of boxplots indicate mean effects size and error bars indicate the 95% confidence intervals. The color codes indicate the direction of the effect with blue indicating a positive effect and red indicating a negative effect on the response variable. Displayed for assessing model performance are marginal R^2 values (i.e., only fixed effects considered), root mean square error (RMSE), and ratio of performance to deviation (RPD). Note that x-axes on panels a-c, and d-f are scaled differently.

3.4. Discussion

3.4.1. Soil parent material drives tropical forest NPP and NPP allocation

Across the three investigated regions of tropical central Africa, forest stands in the mafic and felsic regions (more fertile soils) showed a much higher investment in aboveground biomass (Fig. 3.2a-b, Fig. S3.5a-b) than their counterparts in the sedimentary region (less fertile soil) where soils were characterized by wider C:N ratios, low bioavailable-P and low base cation content (Ca, Mg, and K) as well as low potential and effective CEC. Note that while NPP_{wood} and C allocation in wood was lower in the sedimentary region (Fig. 3.3a), aboveground wood C stocks and NPP_{sum} were higher (Fig. 3.2a). The contrast between NPP_{wood} and wood C stock can be explained largely by how plants respond to changes in nutrient and soil fertility status. Consistent with literature (King *et al.*, 2006; Doughty *et al.*, 2018), trees with high wood C stock tend to grow more slowly resulting in lower wood productivity (Fig. 3.5c; Fig. 3.3a) while still accumulating considerable biomass (Fig. 3.2a). Indeed, data suggest that forests dominated by trees with high wood density and slow growth rates allocate less of their annual C uptake into wood biomass but slowly accumulate and maintain high wood C stocks (Fig. 3.5a-c) in accordance with findings of King et al. (2006). Consistent with these findings, a strong relationship between trees with low wood density and higher wood productivity has also been reported in other tropical regions (Malhi *et al.*, 2004). Note that none of the study sites have been disturbed for at least the last five decades and that the studied forests are considered at their respective climax state with respect to species composition. Therefore, the observed trends (Fig. 4.5) are not resulting from variation in forest age but driven by edaphic factors. Furthermore, this study acknowledges that differences in climatic parameters may influence NPP and C dynamics in tropical montane forest ecosystems. However, the available observational data on mean annual precipitation (MAP) and mean annual temperature (MAT) variability does not show a clear effect on NPP and plant growth across the study sites. This illustrates that local geochemical and edaphic differences between sites are likely more important for explaining the observed patterns of NPP and plant growth than climatic differences. Furthermore, recent work on tropical afromontane forests (Cuni-Sanchez *et al.*, 2021) and sub-saharan African soil systems (von Fromm *et al.*, 2021) have shown a secondary and rather minor influence of climatic over (bio)geochemical controls on biomass C as well as on soil C. Contrastingly, patterns of fine root NPP and root C allocation strongly followed the exact opposite of those trends for wood along the soil fertility gradient (Fig. 3.6; Table 3.S1) with high NPP_{roots} on nutrient-poor soils such as those found in the sedimentary region. Vice

versa, low NPP_{roots} was observed for nutrient-rich soils, whereby soil fertility was strongly related to geochemical regions (Fig. 3.2a-b). This finding is remarkable as the investigated forests grow on soils that developed over millennia under a (at least currently) similar tropical climate and in systems where weathering has strongly altered the chemical composition of soil compared to its parent material (Doetterl *et al.*, 2021b,a).

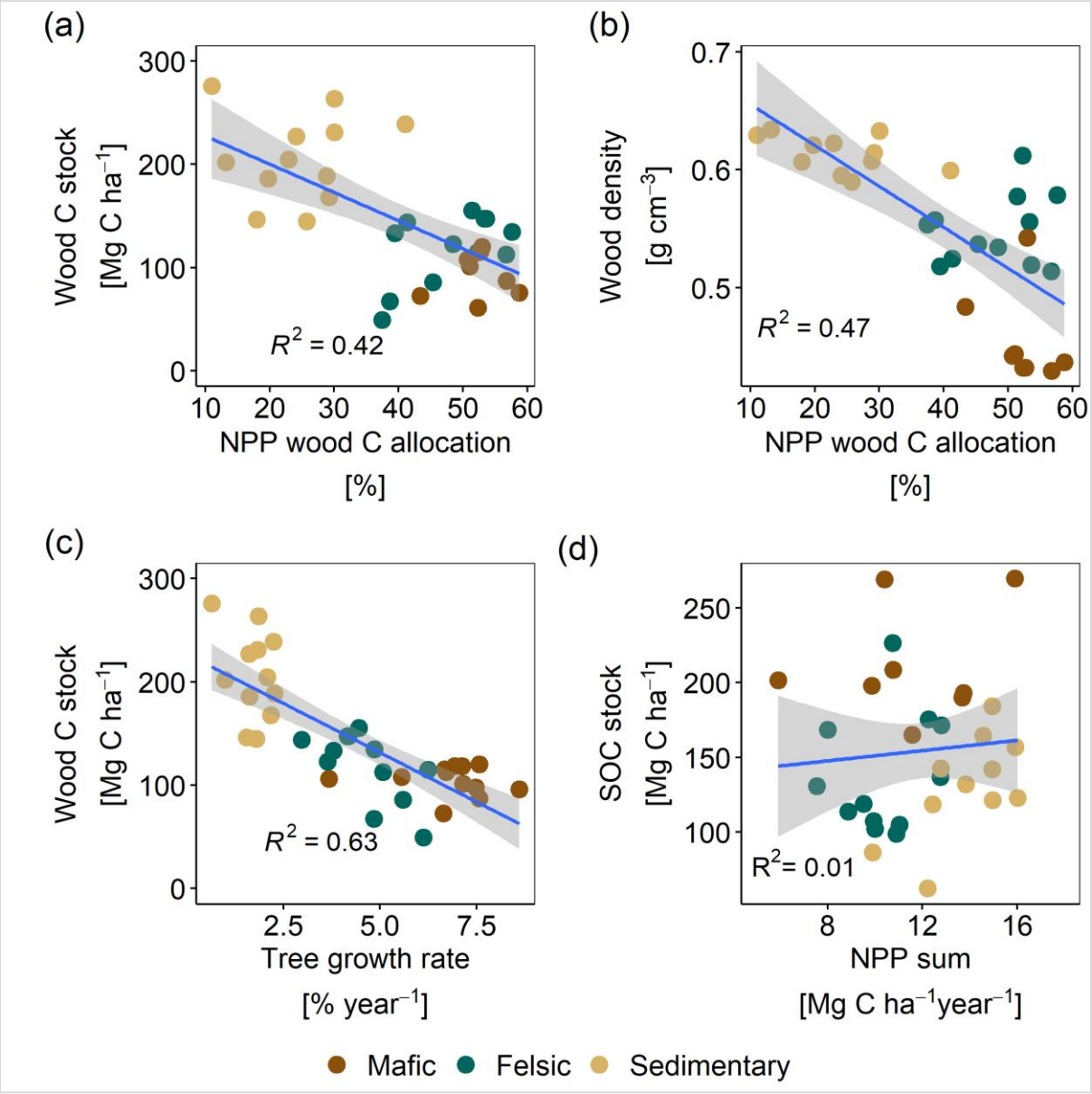

Figure 3.5. (a) Relationship between wood C stock and NPP_{wood} C allocation, (b) relationship between wood density and NPP_{wood} C allocation, (c) relationship between tree growth rate and wood C stock, and (d) relationship between SOC stock and NPP_{total} for the three investigated geochemical regions. The points represent average values per plot (n=8, 12, 12; for mafic, felsic and sedimentary regions respectively). The blue line indicates ordinary least square regression function, and the gray shaded area indicates the 95% confidence interval (p-value < 0.05).

It has been shown that tree species can alter topsoil chemical properties in tropical forest ecosystems (Bauters *et al.*, 2017). However, background information (Doetterl *et al.*, 2021a) on the geologic parent material of these soils reveals that the geochemical differences between soils of the three investigated regions remain consistent with what to expect from soil formation in terms of soil chemical alteration. In addition, in deep subsoil and below the main rooting zone of plants (> 70cm soil depth) a similar range of geochemical variability is found across the study sites as for topsoil layers. Thus, it is most likely that plant communities co-evolved with soil geochemical properties in the area and that these communities are likely to influence top soil chemical properties in agreement with ecological theory. But, the data presented here gives a clear indication that plant community structure and the observed patterns of NPP and their relation to SOC across the sites are the result of soil (geochemical) properties that are distinct across the geologic parent material due to soil formation. First, the negative correlation of C allocation to wood with standing wood biomass stocks (Fig. 3.5a) suggests that in low fertility systems (soils of the sedimentary region) forests establish communities that grow slowly but can result in high (aboveground) biomass (Fig. 3.1, Fig. 3.3). A closer analysis of the relationship of wood components (standing wood biomass, NPP_{wood} and wood C allocation) and soil properties using Kruskal-Wallis tests (p-value < 0.05) is further supportive of this interpretation, showing that wood biomass is higher where soil exchangeable bases and total base cation stocks are lower (Fig. 3.1a; Table S3.1). In contrast, according to Pearson correlation analysis (p-value < 0.05), wood growth and C allocation to wood is higher where soil exchangeable bases and total base cation stocks are higher (Fig. 3.6, Table S3.1). Similarly, data on the chemical composition (C:N ratios) of living canopy leaves (Fig. S3.4) provide further support for the notion that nutrient limited systems tend to develop plant traits that are typically signs of resource conservation strategies (Grau *et al.*, 2017; Urbina *et al.*, 2021) while accumulating comparably thick litter layers (Fig. 3.1a-b) and thick O-horizons (Fig. S3.1). Second, research on plant physiology has shown that nutrient-poor soils force plants to invest more in nutrient acquisition by spending more of their energy and C resources in the nutrient uptake process, by growing more roots, fuel root exudation and C delivered to mycorrhiza to enhance the availability of nutrients and, therefore, reducing resources available for the growth of aboveground plant components (Hartmann *et al.*, 2020; Epihov *et al.*, 2021). This is consistent with evidence highlighting strong shifts in plant C allocation towards more belowground components (Fig.3.1a-b) as soil nutrients become increasingly limiting (Fernández-Martínez *et al.*, 2014; Werner & Homeier, 2015). Additionally, the lower nutrient availability in mineral soil, the more roots grew in the nutrient rich organic litter horizons where

remaining nutrients are recycled back into living biomass. In more nutrient rich mineral soil layers, roots tended to grow more strongly in deeper soil layers (Fig. S3.1). The results of this study suggest that NPP_{roots} and C allocation to roots were primarily driven by exchangeable base cation availability and total cation stocks and only secondary by nitrogen and phosphorus content (Fig. 3.3c; Fig. 3.4c, d). Noteworthy, $NPP_{litterfall}$ remained fairly constant across geochemical regions, relative to the shifts in absolute NPP_{roots} and NPP_{wood} (Fig. 3.2) and showed little to no correlation to the investigated soil and topographic variables (Fig. 3.6). The reasons behind this lack of responsiveness of NPP litterfall are unknown and subject of future investigation.

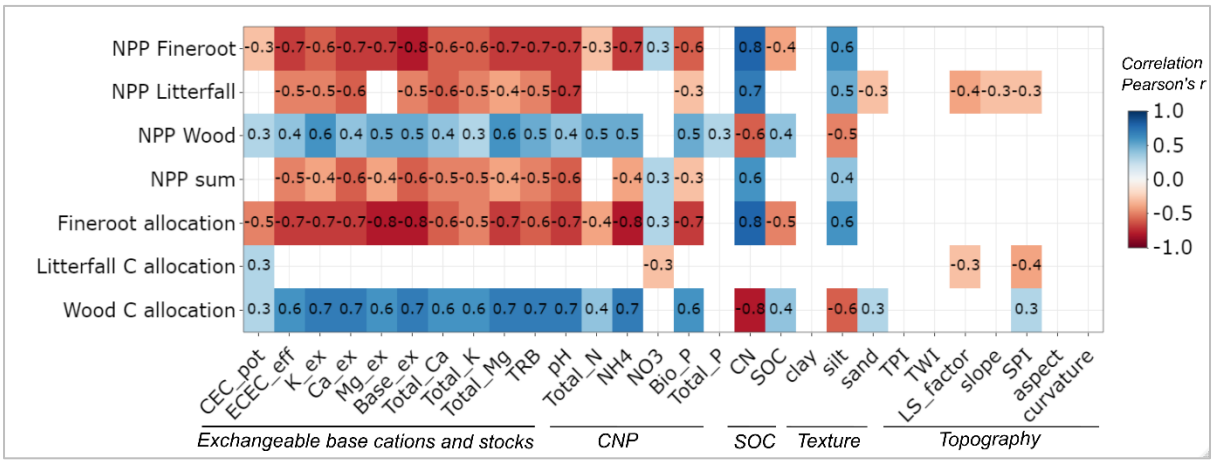

Figure 3.6. Pearson correlations between geochemical soil properties used in our analysis as explanatory variables for NPP (fine roots, litterfall, wood), and the corresponding relative NPP C allocation as response variables. Blank cells indicate non-significant correlations, p-value ≤ 0.05. Note (i) the absence of strong correlations between litterfall C allocation and soil variables, and (ii) the absence of strong correlations between SOC stocks and NPP litterfall or C allocation.

In summary, these results suggest that soil geochemistry impacts tropical montane forest functioning through ecological processes. First, data suggest that fertility constraints have a major effect on shoot:root C allocation strategies in tropical montane forests that relate predominantly to variation in the soil chemical properties, which in turn are inherited from its parent material. Indeed, a recent study conducted at the global scale has shown that rock-derived nutrient limitations are mainly driven by soil parent material (Augusto *et al.*, 2017). But the fact that these patterns hold for deeply weathered tropical soils where nutrients are recycled rather than actively acquired through weathering is unexpected and surprising (Cleveland *et al.*, 2013). When established on nutrient poor soils, tropical forests invest significantly more C in belowground biomass (Fig. 3.3; Fig. 3.6).

Second, consistent with these findings, strong relationships between nutrients and ecosystem properties such as carbon-use efficiency and aboveground wood productivity have been reported at regional to global scales (Malhi *et al.*, 2004; Fernández-Martínez *et al.*, 2014). For example, pan-tropical analyses showed that soil P can explain a significant proportion of the variation observed in NPP_{wood} (Cleveland *et al.*, 2011). However, the results of tis study (estimated effect sizes and pearson correlation coefficients) indicate that the availability of rock-derived cations, in particular total and exchangeable Ca, Mg and K is an overlooked factor governing NPP and biomass allocation (Fig.3.4; Fig. 3.6; Table S3.1).

3.4.2. Local topography does not control patterns of NPP, C allocation or C stocks in tropical forests

Throughout the three investigated geochemical regions of tropical African montane forests, local topographic position along hillslopes did not emerge as a strong driver of NPP, C allocation, or C stocks. While smaller (non-significant) differences in NPP components were observed along topographic positions within each region, these were not consistent across components (Fig. 3.1b; Fig. S3.4a-f). Based on pearson correlation analysis (p-value < 0.05), major topographic indices representing hydrological processes and material fluxes along hillslopes did not correlate with NPP or C allocation for all investigated components (Fig 3.6). However, weak –and not significant- negative correlations were found between soil erosivity indices (LS-factor and SPI) and litterfall NPP and litter C allocation (Fig. 3.6), suggesting a slight decrease in litter productivity with slope length and steepness. Nevertheless, the fact that all NPP and C stock compartments were comparable along topographic positions within each geochemical region (Fig. 3.1; Fig. S3.5), suggests that productivity is likely driven by mechanisms other than topography in these old-growth intact tropical forests. Consistent with these findings, similar results have been reported in other tropical regions. An assessment of the effect of slope gradients (ranging from 0.5 ° to 27 °) on aboveground biomass in Amazonia revealed that slope gradients did not have a detectable effect on aboveground biomass (de Castilho *et al.*, 2006). Similar to NPP, studies on SOC stocks and soil C turnover have shown that the effect of topography in the investigated sites is rather limited to differences related to hydrological conditions between valley and non-valley positions of the local hillslopes (Reichenbach *et al.*, 2021). Although it has been shown that topography can influence tropical forest structure as well as water and nutrient availability (Jucker *et al.*, 2018), the findings of this study provide evidence that topographic features at the hillslope scale, in the absence of severe waterlogging, are not driving plant NPP and C allocation strategies in the investigated

stdy system. Additionally, the results of this study suggest that the lack of strong effects of topography on NPP, C allocation, or C stocks is an indicator that lateral fluxes of soil and water in the investigated study sites do not significantly influence soil nutrient dynamics (Reichenbach *et al.*, 2021; Wilken *et al.*, 2021). While erosional processes have been shown to be significant for tropical montane landscape denudation at geological timescales (Montgomery, 2007; Flores *et al.*, 2020), there is no indication that erosion has altered the soil landscapes in these study systems under intact tropical forest cover (Wilken *et al.*, 2021). For the same area, Doetterl *et al.* (2021a) reported several meters of deeply weathered soils along slope transects. It is therefore astonishing, that in deeply developed soils, (bio)geochemical variables retain a strong explanatory power for NPP and C dynamics. Hence, the explanatory power of soil chemistry, especially for wood and root growth (Fig. 3.2; Fig. 3.4), suggests that NPP patterns are driven by soil properties that relate much more to the regional parent material than topography.

3.4.3. No relationship between NPP C input and SOC stocks in weathered tropical forest soils

Global land-surface models generally simulate an increase of SOC stocks with plant net primary productivity (Todd-Brown *et al.*, 2013; IPCC, 2019). Especially root C input is presumed to be strongly linked and correlated to SOC stocks (Dijkstra *et al.*, 2021), a relationship that is also implemented this way in many assessments of tropical belowground C stocks (Saatchi *et al.*, 2011; Spawn *et al.*, 2020). However, in the three investigated afro-tropical montane forests, SOC stocks did not reflect or relate to neither below- nor aboveground NPP and biomass C stocks (Fig. 3.1a, Fig. 3.2a) or to NPP_{sum} of the investigated systems (Fig. 3.5d). Instead, SOC stocks were higher where root C NPP and stocks were lower (Fig. 3.1a, Fig. 4.2a). These results suggest that, although soil nutrients and fertility emerged as the main drivers of plant NPP and C allocation strategies, C storage and its persistence in soil is likely driven by mechanisms other than C input. Namely, the potential of soils to stabilize SOC through various mineral related stabilization mechanisms that are present or lacking in a given geochemical context (Khomo *et al.*, 2017; Rasmussen *et al.*, 2018; Traoré *et al.*, 2020; von Fromm *et al.*, 2021). Indeed, data for the top 50 cm reported for these study sites shows that the sum of organically complexed, amorphous and crystalline Al and Fe (hydro-) oxides were high in soils developed on mafic compared to their counterparts in the felsic and sedimentary regions (Doetterl *et al.*, 2021a). Recent studies suggest that high amounts of pedogenic Fe and Al (hydro-) oxides in the mafic region are responsible for the efficient stabilization of C inputs

through formation of organo-mineral complexes that represent an additional barrier for microbial decomposers to overcome (von Fromm *et al.*, 2021). In addition, pedogenic, secondary Fe or Al-oxides which are often dominating in highly weathered tropical soils such as the ones investigated in this study, can improve the stability of aggregates and ultimately increase soil C storage potential (Quesada *et al.*, 2020; Kirsten *et al.*, 2021a,b). In line with this assessment, a study (see Chapter 4) on laboratory-based specific heterotrophic soil CO_2 respiration of the investigated soils showed that CO_2 respiration was generally lowest in mafic soils in the study region (Bukombe *et al.*, 2021; Reichenbach *et al.*, 2021). In combination with the results of this study (Fig. 3.1), these findings suggest that soil C input of tropical forests generally exceeds the C stabilization potential of deeply weathered tropical soils given the high annual C input (Lewis *et al.*, 2009a; Sayer *et al.*, 2011) and high turnover rates (Raich & Schlesinger, 1992). This finding has potentially large implications in the way belowground C stocks and dynamics have to be assessed in the future. Data shows that relationships between NPP, biomass and SOC stocks in tropical forests are more soil property driven than what is currently shown in large scale assessments (Del Grosso *et al.*, 2008; Todd-Brown *et al.*, 2014; Sha *et al.*, 2022) or represented in land surface models (Baartman *et al.*, 2018; Thum *et al.*, 2020) (Fig. 3.1; Fig. 3.2).These findings point at the necessity of measuring SOC stocks directly, instead of deriving it from aboveground biomass proxy data.

There are still severe limitations and challenges in conducting field experiments in complex tropical forests which aim to understand soil-plant interaction. For example, the long time (decades) needed to develop mature forest plantations in tropical systems, make it difficult to establish a realistic experimental setup to further disentangle the role of soil geochemistry on forest NPP following long-term manipulations. Likewise, nutrient addition experiments can be greatly informative, but are difficult to implement, and the response time of species composition and forest structure to changes in soil geochemistry are well beyond the time frame of most research funding cycles (Sullivan *et al.*, 2014). Hence, new approaches will be needed to explore the mechanistic linkages between rock-derived nutrients varying with the weathering status of soil and soil parent material as well as their potential control on C dynamics in low fertility systems. These approaches should include a combination of field experiments and detailed long-term observational setups with full NPP monitoring across spatial scales making it possible to integrate soil geochemical changes occurring at longer timescales to short-term responses of the biosphere to environmental change.

3.5. Conclusions

The findings of this study suggest a strong control of local edaphic factors on tropical forest C stocks and dynamics. This adds substantial and previously unknown complexity that needs to be unraveled to better understand plant-soil interactions and its consequences for biogeochemical cycles in the investigated tropical ecosystems. The results of this study show that differences in soil fertility as a result of soils developing from varying parent material - and not topography - have a substantial effect on net primary productivity as well as the root:shoot C allocation in old-growth African tropical montane forest ecosystems. Despite many millennia of weathering under warm humid conditions, soil fertility indicators varied systematically across geochemical regions and were identified as important factors driving NPP and C allocation. Tropical forests growing on more fertile soils allocated less NPP to roots and more to wood than their counterparts in less fertile soils. While the effect of geochemistry on NPP and C allocation across the study sites was clearly distinct, local topography did not influence the variability in NPP and C allocation. Importantly, SOC stocks were not related to vegetation C input and biomass C stocks, with soils seemingly exceeding their maximum potential to stabilize C despite high input.

4. Heterotrophic soil respiration and carbon cycling in African tropical forest soils[2]

4.1. Introduction

Tropical forests and the soils therein are one of the most important and largest global terrestrial carbon (C) pools and serve as important climate regulators (Lewis *et al.*, 2009a; Cleveland *et al.*, 2011; Sayer *et al.*, 2011; Kearsley *et al.*, 2013). They contain about one-third (421 Pg C) of the global soil organic carbon (SOC) stock in the upper 1 m of soil (Köchy *et al.*, 2015) and are characterized by high annual C turnover rates (Raich and Schlesinger, 1992). Generally, climatic parameters (temperature and precipitation) and vegetation input are regarded as the main factors controlling C dynamics in natural tropical systems (Davidson *et al.*, 2000; Rey *et al.*, 2005; Davidson & Janssens, 2006). Vegetation and climate can stimulate or hamper microbial activity and mineralization of C through quality and quantity of organic matter (OM) input to soil (Fontaine *et al.*, 2007) and the availability of water and energy to drive microbial processes. However, recent studies show that SOC dynamics are controlled by a much more complex interplay of geochemistry, topography, climate and biology (Luo *et al.*, 2017, 2019; Doetterl *et al.*, 2018; Haaf *et al.*, 2021), much like pedogenesis in general. For example, on average 72 % of SOC in humid forest biomes is stabilized by interaction with the mineral phase in soil organo-mineral interactions and occlusion by aggregation (Kramer & Chadwick, 2018). Geology can control C dynamics as soils developed from felsic parent material (high SiO2, low Fe and Al and slow chemical weathering rate) provide less potential for C stabilization and a lower capacity to release rock-derived nutrients than soils developed from mafic parent material (low SiO2, high Fe and Al and fast chemical weathering rate), limiting organic matter input. Additionally, topography through its control on water and soil fluxes may influence C dynamics by altering C respiration and input along slope gradients (Berhe *et al.*, 2008). Hydrological features related to topography in tropical forests are likely to influence C cycling and explain spatial patterns of SOC distribution locally by limiting C decomposition in water-saturated valleys (Kwon *et al.*, 2013). Finally, some soils developed from sedimentary parent material can contain a large fraction of geogenic organic carbon (f_{FOC}) of generally poorer quality than fresh organic matter inputs, which can be resistant to decomposition under in situ environmental conditions (Kalks *et al.*, 2021). Hence, in order to explain SOC and its exchange

[2] ***The content of this chapter has been published with minor changes as:*** Bukombe B, Fiener P, Hoyt AM, Kidinda LK, Doetterl S. 2021. Heterotrophic soil respiration and carbon cycling in geochemically distinct African tropical forest soils. *SOIL 7: 639–659.*

between soil and the atmosphere, the interactions of geochemical, geomorphic and climatic drivers are central (Berhe *et al.*, 2012; Luo *et al.*, 2017; Kramer & Chadwick, 2018; Angst *et al.*, 2018; von Fromm *et al.*, 2021).

To date, it is not clear if the relationships between soil geochemistry, topography and climate identified for temperate ecosystems also apply in the tropics. Especially for the African tropics, more work is required to understand how soil geochemical, physical, biological and topographic features interact to influence SOC dynamics. Established observatories in African tropical forests have focused mostly on biodiversity preservation and C storage in the phytosphere (Tyukavina *et al.*, 2013b; Xu *et al.*, 2017), while soils have received much less attention and remain understudied. Generally, data on SOC dynamics from tropical regions are rare compared to the temperate zone, originating mostly from the Amazon basin (Schimel & Braswell, 2005; Schimel *et al.*, 2015; Quesada *et al.*, 2020), and their application to the African tropics may be limited. For example, atmospheric nitrogen deposition is much higher in sub-Saharan Africa than in other tropical regions due to large amounts of recurring biomass burning originating from savanna and dry forests north and south of the humid tropics (Bauters *et al.*, 2018).

Furthermore, long-term chemical weathering in tropical systems has led to the depletion of rock-derived nutrients in soils and has limited the capacity of microorganisms and plants to access these nutrients (Vitousek & Chadwick, 2013; Liu *et al.*, 2015). It is likely that variation in soil weathering stage and nutrient availability in tropical forests affect soil C storage and the exchange of C between plants, soil and the atmosphere. For example, due to their tight coupling driven by the metabolic needs of plants and microorganisms, changes in nutrient availability, such as nitrogen (N) and phosphorus (P), can greatly alter the terrestrial C cycle, partly because CO_2 uptake by terrestrial ecosystems strongly depends on N and P availability (Fernández-Martínez *et al.*, 2014). Furthermore, low N and P availability limits microbial growth and activities and therefore affects the cycling of organic matter (Liu *et al.*, 2015; Jiang *et al.*, 2020). Thus, nutrient limitations in highly weathered tropical soil likely force plant communities to alter belowground and aboveground C allocation (Wright *et al.*, 2011; Fisher *et al.*, 2013). with more roots growing in organic rich topsoil, reducing C input to deeper soil layers (Addo-Danso *et al.*, 2018), thereby affecting SOC stocks.

Additionally, along soil age gradients, SOC stabilization by clay first increases and then decreases, with a reduction in reactive mineral surfaces as weathering advances (Doetterl *et al.*, 2018; Kramer & Chadwick, 2018). As a consequence, clay in old tropical soils has a rather limited potential to protect C against microbial decomposers compared to younger, temperate

soils (Ngongo *et al.*, 2009). In contrast, stable microaggregates rich in iron (Fe) and aluminium (Al) oxyhydroxides found in abundance in tropical soils (Bruun *et al.*, 2010; Torres-Sallan *et al.*, 2017) seem to be of greater importance in stabilizing C in tropical soils, as concentrations of Al and Fe are commonly higher than in many temperate soils (Khomo *et al.*, 2017). This is confirmed by studies conducted across a wide range of tropical ecoregions showing that SOC is mainly regulated by Fe or Al oxyhydroxides – more so than by clay content (Rasmussen *et al.*, 2018; Fang *et al.*, 2019).

Hence, understanding tropical soils C dynamics ultimately depends on mechanistic understanding of these complex interactions and the ability to determine the primary environmental controls on SOC content and respiration. The aim of this study was to answer if C release through heterotrophic respiration from forest soils in the humid tropics follows predictable patterns related to geochemical soil properties and topography. The study postulates that, in the absence of anthropogenic disturbance, soil geochemistry derived from its parent material has a lasting effect on soil C respiration due to its influence on stabilization mechanisms and soil fertility, even in deeply weathered natural tropical soils. In this study soils developed from geochemically distinct parent material along slope gradients were selected under comparable tropical climate and vegetation. This study is centered on the following hypotheses: (1) specific soil respiration and the $\Delta^{14}C$ signature of potential soil respiration in tropical soils are primarily controlled by geochemical properties related to soil fertility derived from and varying with soil parent material. These variations in soil fertility can stimulate or inhibit microbial activity and increase or decrease soil C decomposition rates. (2) The presence or absence of C stabilization mechanisms, in soils, related to mineral geochemistry and soil formation, can increase SOC stocks and decrease heterotrophic C respiration rates by creating an energetic barrier for C decomposers, for example through complexation with organic molecules or by forming stable (micro)aggregates. (3) The topographic origin of a soil sample controls specific soil respiration and its $\Delta^{14}C$ signature indirectly through the environmental conditions under which soil C decomposition takes place in situ, modifying the quality and quantity of the available SOC stock prior to the experiment.

4.2. Materials and methods

4.2.1. Soil samples

For the experiments conducted in this study, 112 soil samples were selected covering three depth categories, including topsoil (0–10 cm), shallow subsoil (30–40 cm) and deep subsoil (60–70 cm). These three depth intervals were selected as they cover a wide range of biogeochemical properties in soil and various levels of organic matter input to soil, both in terms of quantity (more C input near the surface and less at depth) and quality (leaf litter + root-derived C in topsoil; root-derived C in subsoil).

Table 4.1. Chemical composition of unweathered rock samples representing the soil parent material in the investigated three geochemical regions. Values represent mean ± standard errors (n=6, 10 and 3 for mafic, felsic and sedimentary, respectively). Source: Project TropSOC Database Version 1.0 (Doetterl *et al.*, 2021a).

Geochemical region	C[%]	Fe [%]	Al [%]	Si [%]	Ca [%]	K [%]	Mg [%]	P [%]
Mafic	0	8.98 ±0.7	6.26±1.15	14.22±0.8	0.58±0.23	0.08±0.03	1.25±0.13	0.36±0.05
Felic	0	1.08±0.5	0.51±0.38	37.28±1.8	0.01±0.00	0.01±0.01	0.01±0.01	0.01±0.00
sedimentary	4.03	2.32±0.9	0.61±0.23	36.11±4.0	0.01±0.01	0.07±0.03	0.01±0.01	0.02±0.01

4.2.2. Laboratory experiments

4.2.2.1. Potential heterotrophic soil respiration

Heterotrophic respiration per gram SOC (specific potential respiration SPR; $\mu gCO2{-}C.gSOC^{-1}h^{-1}$) was assessed in a lab-based incubation experiment and measured for the three sampling depths across geochemical and topographic gradients. Briefly, 50 g of 12 mm sieved air-dried soil were weighed into a 100 mL beaker. Soil samples were sieved to 12 mm to homogenize the substrate while maintaining aggregate structure at a low level of disturbance. Soil moisture was adjusted to 60 % water holding capacity, selected as the optimum water content level for microbial activity (Rey *et al.*, 2005). Each beaker was placed inside an open 955.5 ± 1.3 mL mason jar covered with Parafilm, allowing for air exchange to avoid oversaturation of CO_2 within the jar that could inhibit microbial activity. Samples were then incubated at 20 °C, similar to the annual mean temperatures of the study sites. Except for keeping soil moisture steady by adding water when necessary, no further amendments were made to the incubated soils. Following a pre-incubation period of 4 days to allow equilibration, all samples were incubated for 120 days and sampled periodically every 1 to 14 days

throughout the experiment, with longer intervals towards the end of the experiment as respiration rates levelled off. The incubation experiment ended when additional CO_2 production was not detectable within measurement error. This was the case when the standard deviation of means of the respiration rate between three consecutive measurement time points was smaller than the standard deviation between three replicates of the same measurement time point. For CO_2 accumulation prior to sampling, mason jars were sealed for several hours per measurement point. The accumulated CO_2 was sampled using a syringe and transferred to pre-evacuated 20 mL vials. To avoid CO_2 saturation effects during measurements, potentially influencing microbial decomposition processes, jars were flushed with background air from the laboratory and checked for moisture content before and after sealing to accumulate CO_2. Generally, CO_2 samples were taken after accumulating between 1000–3000 ppm (parts per million) CO_2. The CO_2 concentration of the extracted gas was subsequently measured using a gas chromatograph (TRACE™ 1300, Thermo Fisher Scientific, Massachusetts, USA) calibrated with five CO_2 standards, covering the range of measured concentrations (0, 500, 1000, 5000 and 10 000 ppm CO_2). Furthermore, the measured CO_2 was corrected for the CO_2 concentration of the ambient air that was used to flush the jars before closing for CO_2 accumulation. After each measurement was completed, each jar was opened and covered with parafilm to allow gas diffusion between CO_2 accumulation periods. In this way, an average of 12 observations of CO_2 production rate per incubated sample were conducted during the course of the experiment. Since the aim was to compare average respiration between samples rather than the absolute values through the entire period of the experiment. Thus, data was analyzed as the weighted average of SPR over the entire length of the experiment after respiration levelled off. The weight was defined by how many days of the incubation experiment each observation represents. Additionally, 20 % of all samples were incubated in triplicate to assess the average difference between samples for the experiment. The resulting average standard error of the mean between the three lab replicates was 9.6 %.

4.2.2.2. $\Delta^{14}C$ of bulk soil and respired CO_2

Soil radiocarbon ($\Delta^{14}C$) content of both bulk soil (SOC) and the corresponding respired CO_2 were measured from the incubated samples. Bulk soil $\Delta^{14}C$ provides an indicator of the persistence of C in the soil and its age (Shi *et al.*, 2020), while the $\Delta^{14}C$ of the respired CO_2 reflects more actively cycling C (Trumbore, 2009). The difference between these measures ($\Delta - \Delta^{14}C$) can provide an indicator of how homogeneous or heterogeneous the system is

(Sierra et al., 2018), depending on whether the $\Delta^{14}C$ signature of the respired CO_2 is similar to, or differs from, the bulk soil $\Delta^{14}C$. Radiocarbon analyses were conducted on composite samples of the bulk soil replicates used for incubation and, correspondingly, on composite samples of the respired CO_2 during incubation. Bulk soil $\Delta^{14}C$ was measured on soil samples before the incubation started. The $\Delta^{14}C$ of respired CO_2 was measured from CO_2 that accumulated over the initial period following the pre-incubation period. The CO_2 accumulation period varied depending on the sample. For top and shallow subsoil with higher CO_2 respiration rates, it took on average 4 –7 d, while for deep soil with low CO_2, it took 10–15 d to accumulate 1 mg C needed for $\Delta^{14}C$ analysis. After accumulation, 120 mL of headspace gas from each field replicate incubation jar was sampled using a syringe. These replicate samples were transferred into a single 400 mL pre-evacuated Restek canister for composite analysis. Radiocarbon concentrations presented in this study are given as fraction modern and $\Delta^{14}C$ following the conventions of (Stuiver & Polach, 1977). All measurements were done with the MICADAS Mini Carbon Data System (Ionplus AG, Switzerland) at the accelerator mass spectrometry (AMS) facility at the Max Planck Institute for Biogeochemistry in Jena, Germany (Steinhof *et al.*, 2017).

4.2.2.3. Assessing geogenic vs. biogenic organic carbon

Radiocarbon measurements were used to assess differences in the age of respired CO_2 versus soil carbon and to estimate the potential contribution of geogenic organic C to the total soil organic C content and to CO_2 respired during incubations. For the latter, the study focused on the sedimentary region, as this is the only geochemical region in study region where soil parent material contains geogenic organic C. For this, two-end member mixing model following Schuur *et al.* (2016) were used to calculate the fraction of the C in the sample originating from biogenic vs. geogenic organic C as follows:

$$F_{FOC} * Geog_{FOC} + F_{bio} * \text{bio-c} = F_{sample} \quad \text{(eq. 4.1)}$$

where F_{FOC}, F_{bio} and F_{sample} represent the fraction modern radiocarbon content (F), geogenic organic C, biogenic C and the measured sample (bulk soil organic C or respired CO_2), respectively, and $Geog_{FOC}$ and bio-c represent the proportion of geogenic organic C and biogenic C contributing to a sample's total C content. For this estimate, the study assumed that geogenic organic C is free of $\Delta^{14}C$ due to the high age of the parent material (Doetterl *et al.*,

2021a; Schlüter, 2006). Furthermore, the study assumed that radiocarbon values of biogenic SOC (F_{bio}) in the sedimentary region follow the same trend with soil depth as the mean measured depth explicit radiocarbon content from plateau soils of the mafic and felsic regions (regions without geogenic organic C), and that these values represent biogenic SOC from active biological cycling in plant–soil systems (Cerri *et al.*, 1985; Kalks *et al.*, 2021). However, because rates of biogenic C cycling likely vary across sites, with potentially slower biogenic cycling in the sedimentary region (see Sect. 4.4), this estimate is likely an upper bound on the geogenic organic C contribution to these samples. Based on these assumptions, Eq. (4.1) was reduced and solved for the proportion of biogenic organic C (bio-c) as follows:

$$\text{bio-c}=F_{sample}/F_{bio} \quad \text{(eq. 4.2)}$$

The fraction of geogenic organic C was then calculated as follows:

$$f_{FOC}=1-\text{bio-c} \quad \text{(eq. 4.3)}$$

4.3. Statistical analysis

4.3.1. Assessing patterns of respiration and $\Delta^{14}C$

To examine differences in mean SPR in relation to the three main factors– topographic position, soil depth and geochemical region, three-way analysis of variance (ANOVA) was conducted. Before ANOVA, residual analysis was conducted to test for the assumptions of ANOVA using Shapiro–Wilk's test of normality distribution and Levene's test for homogeneity of variances (Shapiro & Wilk, 1965). In most cases, the homogeneity and normality tests did not meet the requirement due to the natural variability in the samples and the factorial sampling design. Hence, square root and log transformation methods were used to approximately conform to normality and the ANOVA tests were then conducted on the transformed data set. To compare the means of multiple groups, post hoc pairwise comparison was applied using Bonferroni correction (Day & Quinn, 1989) or Tamhane T2 in the case of unequal variances (Tamhane, 1979).

4.3.2. Predicting SPR and $\Delta^{14}C$

Multiple linear regression was used to assess the explanatory power of soil properties to predict SPR and the difference between the soil and respired CO_2 $\Delta^{14}C$ signature ($\Delta - \Delta^{14}C$). Before running regression models, a wide range of physico-chemical soil properties and an SOC quality indicator (C:N) for the investigated soils were extracted from the TROPSOC database, where, in parallel studies, soil C stabilization mechanisms were assessed by Reichenbach *et al.* (2021) and microbial activity parameters (C, N and P enzymes and microbial biomass) assessed during the incubation experiment (Table S4.1) by Doetterl *et al.* (2021b). Overall, the data set consisted of 37 independent variables and 112 aggregated observations for each of the target variables (for CO_2, results were aggregated from 1350 individual observations of SPR over the course of the experiment). As multicollinearity and autocorrelation between independent variables was to be expected due to this large number of independent variables and a relatively small number of aggregated observations, rotated principal component analysis (rPCA) for dimension reduction (Jolliffe, 1995), was conducted before regression analysis. All retained rotated components (RCs) were then named based on the loadings of the original variables and interpreted them for the likely underlying mechanisms that can affect C dynamics (Table S4.1). A threshold of $r > 0.5$ was used to decide whether an independent variable that was loaded into an RC can be used for the mechanistic interpretation of the RC or not. An eigenvalue > 1 and explained proportion of variance > 5 % for each RC were used as criteria to include or exclude RCs into the regression models (Jolliffe, 1995; James *et al.*, 2013). Furthermore, p-values ($p < 0.1$) and standardized coefficients were used to evaluate the contribution of the explanatory power of individual RCs to the overall model, while the F statistic was used to evaluate the overall relationship between RCs and SPR or $\Delta^{14}C$ for every model. Note that there was no statistical difference in SPR or $\Delta^{14}C$ between the plateau and slope positions within each studied geochemical region (mafic, felsic and sedimentary). Across geochemical regions and soil depths, SPR and $\Delta^{14}C$ differed only between valleys and non-valley positions. Hence, all further analyses were done after splitting the data into two subsets, i.e. (1) non-valley positions (plateau, upper slope and middle slope) versus (2) valley positions (valleys and foot slope). When predicting the target variables, each regression analysis was done for three subsets of data, i.e. one model containing all data, one with only topsoil data and one with only subsoil data. Samples from valley positions were excluded from this part of the analysis due to the sample size of the valley subset being too small (nine sites; 27 soil samples) for reliable

regression analyses. Hence, the analysis to identify controls via regression and RCs to predict SPR and $\Delta^{14}C$ is focused on non-valley positions (27 sites; 85 soil samples).

4.3.3. Assessing relative importance of explanatory variables

Lastly, the relative importance of each individual RC in predicting the target variables was assessed by interpreting the standardized coefficients (−1 to 1) and p-values associated with each regression model. When predicting target variables with all data, soil depth was included as an additional explanatory variable in addition to the rotated components (RCs). This was done in order to avoid interpreting variables as being important for the model when they were instead just auto-correlated with soil depth. In a final step, partial correlation analysis was conducted following Doetterl *et al.* (2015b), to interpret the explanatory power of independent variables in the model, while controlling for soil depth. The findings were contextualize with respect to microbial (extracellular enzyme activity; Doetterl *et al.,* 2021b), mineralogical (pedogenic oxides; Reichenbach *et al.,* 2021) and soil fertility parameters (available nutrients and exchangeable base cations; Doetterl *et al.,* 2021a). For all statistical tests, due to the relatively small sample size and to avoid type II statistical errors, a threshold of $p < 0.1$ was used to indicate significant difference. R^2 and root mean squared error (RMSE) were used as evaluation metrics for model performance. All statistics were performed using R statistical software and the packages "psych" and "ppcor" (R Core Team, 2020).

4.4. Results

4.4.1. Patterns of respiration and $\Delta^{14}C$

4.4.1.1. Topography and soil depth

For all three geochemical regions in non-valley topographic positions, SPR and Δ14C decreased with soil depth (Fig. 4.1a-b and Fig. 4.2a-b, respectively). For SPR, differences with soil depth were smallest for sites in the sedimentary and largest for sites in the mafic region. For $\Delta^{14}C$, relative changes with depth were similar for mafic and felsic geochemical regions in both soil and respired CO_2, but samples from the sedimentary region were consistently more depleted in $\Delta^{14}C$ than their counterparts from mafic and felsic regions (Fig. 4.2a-b). In valley positions, SPR did not follow a clear trend with soil depth. In the mafic region, SPR decreased with depth, while in the felsic region it increased with depth (Fig. 4.1b). No statistically

significant differences in SPR with depth were observed for the sedimentary region (Fig. 4.1b). All regions show a strong trend of depletion of $\Delta^{14}C$ with depth in valleys (Fig. 4.2a-b).

4.4.1.2. Geochemistry and soil depth

Consistently, for non-valley profiles, SPR was higher in felsic and mafic regions than in the sedimentary region (Fig. 4.1a). Additionally, while topsoil samples between mafic and felsic did not show differences in SPR, subsoil samples in the felsic region showed higher SPR than their mafic counterparts and SPR in the sedimentary region was generally lowest. The $\Delta^{14}C$ values of both soil and respired CO_2 in mafic and felsic regions were not significantly different from each other for either top- or subsoil. Bulk soil samples from the sedimentary region were consistently depleted compared to their mafic and felsic counterparts. At valley positions, SPR in topsoil was not significantly different for mafic and felsic samples. Sedimentary samples were slightly lower in SPR in topsoil than their mafic and felsic counterparts, but not nearly as low as at non-valley positions (Fig. 4.1b). In subsoils, SPR was highest in the felsic and lowest in the mafic region, while the sedimentary region was not significantly different from the mafic samples (Fig. 4.1b). As in non-valley counterparts, $\Delta^{14}C$ activity in valley positions was lowest in samples from the sedimentary region and differences between the mafic and felsic regions were generally small (statistical tests were not possible due to the small sample size; Fig. 4.2a-b).

4.4.2. Patterns of SOC stock and available nutrient across geochemical region

SOC stocks in the topsoil were similar across all geochemical regions. However, SOC stock significantly decreased with depth for the felsic but not for the mafic or sedimentary region (Fig. 4.1c). Available phosphorus (bio-P) was not significantly different between the mafic and felsic regions, except in the topsoil where samples from the mafic region show the highest values (Fig. 4.1d). Bioavailable P decreased with soil depth for the mafic and felsic regions but not for the sedimentary region where it was consistently lower than in soils of the mafic and felsic regions across all sampled depths.

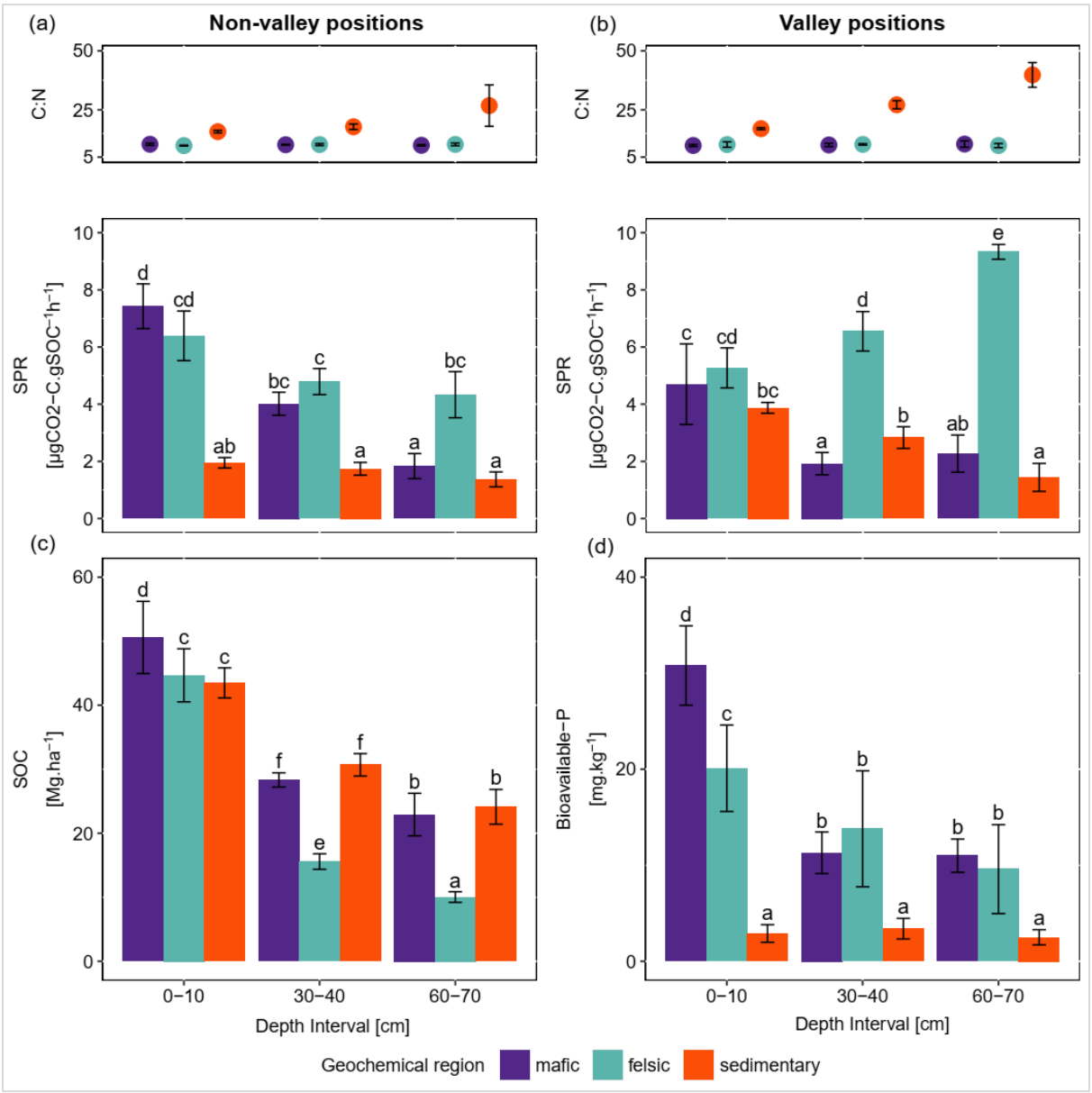

Figure 4.1. Average and standard errors based on field replicates. (a) C:N ratio as points (top) and specific potential respiration (SPR) as bars (bottom) for non-valley positions (n=9). (b) C:N ratio as points (top) and specific potential respiration (SPR) as bars (bottom) for valley positions (n=3). (c) SOC stocks and (d) bioavailable phosphorus for non-valley positions (n=9). The same letters on top of the bars indicate no significant difference following ANOVA tested for differences between depth intervals across geochemical regions. ANOVA tests were performed separately for non-valley and valley positions.

4.4.3. Patterns and differences in $\Delta^{14}C$ of bulk soils vs. $\Delta^{14}C$ of respired CO_2

Across all study regions a strong relationship ($R^2 = 0.81$; $p < 0.1$) was found between $\Delta^{14}C$ of the bulk soil and $\Delta^{14}C$ of the respired CO_2. In non-valley positions, soil C was consistently more depleted than its respired C counterparts, and depth trends in the $\Delta^{14}C$ of respired CO_2 were much less pronounced (Fig. 4.2a). Notably, the differences in $\Delta^{14}C$ between soil and CO_2 were consistently smaller in the felsic and mafic regions than in the sedimentary region. In valley positions, differences in $\Delta^{14}C$ between soils and respired CO_2 generally followed the same trends as for non-valley positions, with the exception of the $\Delta^{14}C$ of respired CO_2 in the sedimentary region being similarly depleted to the soil (Fig. 4.2a-b).

A significant contribution of geogenic organic C to both SOC and respired CO_2 was found in the sedimentary region (Table 4.2). There, the calculated contribution of geogenic organic C to total SOC in bulk soil and respired CO_2 increased with soil depth with similar trends for valley and non-valley positions. However, the calculated contribution of geogenic organic C to respired CO_2 was much higher in valley subsoil (19 %–39 % geogenic organic C in respired CO2) than in non-valley subsoil (7 %–9 % geogenic organic C in respired CO_2). Generally, the contribution of biogenic C to total C was consistently higher (61 %–97 %) in respired CO_2 than in SOC of the corresponding bulk soil (48 %–98 %) in both valley and non-valley positions. Microbial respiration discriminated against geogenic organic C in non-valley positions by a factor of 3–7 ($Geog_{FOC}$ bulk soil/respired CO_2) but did not discriminate against geogenic organic C in valley positions (0.7–1.5 $Geog_{FOC}$ bulk soil/respired CO_2).

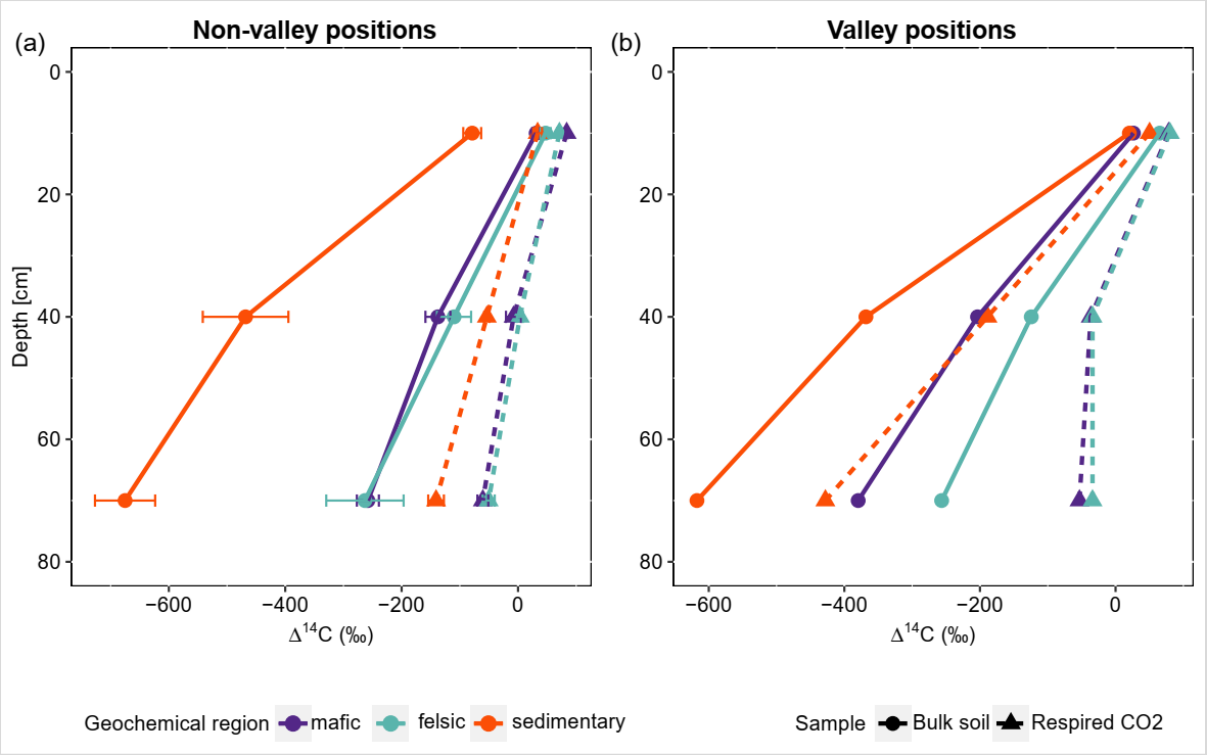

Figure 4.2. Average and standard errors based on all composite samples for non-valley positions only. (a) Radiocarbon content ($\Delta^{14}C$) of the bulk soil and respired CO_2 for non-valley positions. (b) $\Delta^{14}C$ of the bulk soil and respired CO_2 for valley positions (n=27 for non-valleys and n=9 valleys for each depth interval). Note that at non-valley positions, each point in panel (a) represents three observations from composite samples. At valley positions, each point in panel (b) represents one observation from composite samples.

Table 4.2. Biogenic and geogenic organic carbon contribution in the sedimentary region to SOC and respired CO_2 as a percent of total C and ratio bulk soil/respired C for both parameters. Values are displayed separately for non-valley and valley positions per soil depth (n=1 per soil depth and position due to merging of replicates into composites prior to analysis). Note that these values are an upper bound on the contribution of geogenic organic C, as these estimates may be affected by variable rates of biogenic C cycling.

		Biogenic [%]			Geogenic [%]		
Position	Depth [cm]	Bulk soil	Respired gas	Bulk/Respired	Bulk soil	Respired gas	Bulk/Respired
Non-valley	0-10	89	96	0.9	11	4	2.8
	30-40	61	93	0.6	39	7	6.0
	60-70	48	91	0.5	52	9	5.8
Valley	0-10	98	97	1.0	2	3	0.7
	30-40	72	81	0.9	28	19	1.5
	60-70	57	61	0.9	43	39	1.1

4.4.4. Predicting SPR and $\Delta - \Delta^{14}C$

4.4.4.1. Explanatory variables and mechanistic interpretation

For the non-valley subset of the data, rotated principal component analyses yielded five significant rotated components (RCs) that together explained 74.5 % of the cumulative variance of the data set (Table S 4.1). From these components, RC1 and RC2 explained about 49 % of the entire variance in the data set, and were loaded with 13 (RC1) and 10 (RC2) independent but highly auto-correlated predictors within each RC. Predictors for RC1 related to soil organic matter characteristics and microbial activity. Predictors for RC2 related to the chemistry of the soil solution. RC3–RC5 explained about 5 %–11 % of the variance within the data set, with varying loading of two to three independent predictors that relate mechanistically to soil texture (RC3), aggregation (RC4) and C:N ratio + O horizon C stock (RC5).

4.4.4.2. Regressions and relative importance of RCs for predicting SPR and $\Delta - \Delta^{14}C$

Using the rotated components identified above and soil depth as an additional variable, SPR was predicted for the non-valley subset of data with $R^2 = 0.47$ (RMSE = 1.9 $\mu gCO_2{-}CgSOC{-}1$; n=85). When predicting only topsoils, R2 increased to 0.62 (RMSE = 1.7 $\mu gCO_2{-}CgSOC{-}1$; n=28). When predicting only subsoils, R2 decreased to 0.32 (RMSE = 1.6 $\mu gCO_2{-}CgSOC{-}1$; n=57). Δ-$\Delta^{14}C$ was predicted similarly in all three submodels ($R^2 = 0.75$–0.94; RMSE = 18.1 ‰–88.4 ‰; Table 4.3). Besides soil depth, RC2 (soil solution chemistry) and RC3 (soil texture) were the most important predictors for SPR. Note that, in subsoil, RC3 (soil texture) was no longer selected as a predictor for SPR although it was a highly important predictor in topsoil. $\Delta - \Delta^{14}C$, in general, was predicted by a wider range of variables than SPR. Topsoil $\Delta - \Delta^{14}C$ was predicted by the RCs “soil solution chemistry”, “C:N ratio” and “soil texture”. In subsoil, $\Delta - \Delta^{14}C$ was predicted by the RCs' “SOM and microbial activity”, “soil solution chemistry” and “aggregation”, as well as “C:N ratio and O horizon C stock”. Note that RC4 aggregation, related to the amount of C associated with microaggregates, played only a minor role as predictor in all data and subsoil predictions of $\Delta - \Delta^{14}C$. Aggregation did not contribute to the predictive power of topsoil $\Delta - \Delta^{14}C$ and was not included in any model for predicting SPR.

Table 4.3. Results of three regression models (topsoil only, subsoil only and all data) using RC scores to predict SPR and $\Delta - \Delta^{14}C$, including standardized coefficients and model performance indicators. For models using all data, soil depth was included as an additional explanatory variable. Blank cells indicate non-significant predictors (p value < 0.1) that were not selected by the model. Note: SOM is soil organic matter.

	Standardized Coefficients					
	Topsoil		Subsoil		All data	
Explanatory variables	SPR	Δ-$\Delta^{14}C$	SPR	Δ-$\Delta^{14}C$	SPR	Δ-$\Delta^{14}C$
Soil depth					-0.3	-0.4
SOM and microbial activity (RC1)				0.4		0.2
Soil solution chemistry (RC2)	0.5	0.4	0.4	0.5	0.5	
Soil Texture (RC3)	-0.7	-0.4			-0.3	-0.1
Aggregation (RC4)				-0.3		-0.2
C:N ratio and O horizon (RC5)		-0.6		-0.5		-0.6
R^2	0.62	0.94	0.32	0.75	0.47	0.79
RMSE	1.7	18.1	1.6	87.4	1.9	88.4
F-stat	7.46	75.1	4.8	31.3	11.2	49.3
p-value	0.0001	<0.05	0.0056	<0.05	<0.05	<0.05

4.4.4.3. Controlling for soil depth: partial correlations

Partial correlation analysis revealed little to no statistically significant changes in correlation between most RCs and the target variables when comparing zero-order and depth-controlled correlations (Fig. 5.3). However, a marked and significant reduction in correlation was observed between SPR and RC1 (SOM and microbial activity), as well as between $\Delta - \Delta^{14}C$ and RC1 when controlling for soil depth. A smaller but significant reduction in correlation after introducing soil depth as a control was observed for SPR and RC4 (aggregation). Thus, the reduction in correlation after controlling for soil depth indicates that the relationship of those RC1 and RC4 to target variables is, in part, dependent on soil depth and cannot be interpreted as being fully independent.

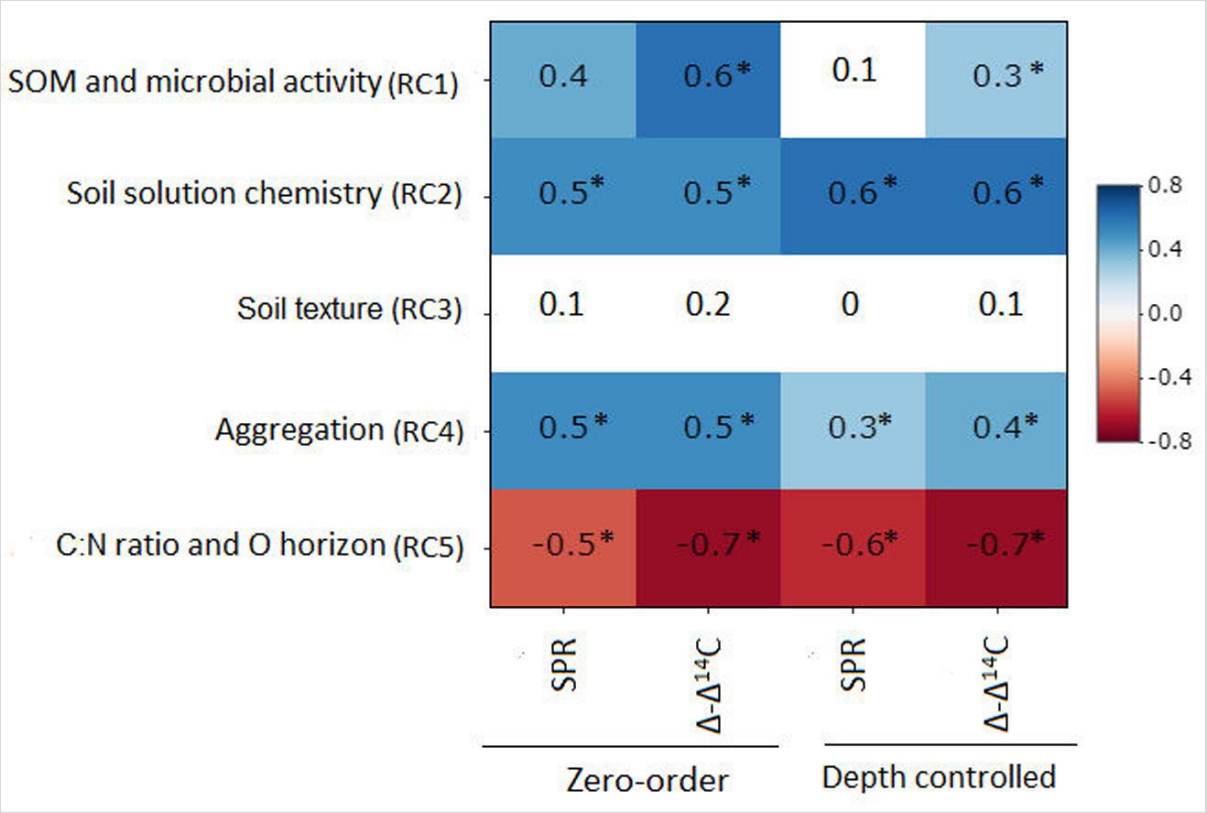

Figure 4.3. Zero-order and partial correlations displayed as Pearson's r between target variables (SPR and $\Delta - \Delta^{14}C$) and explanatory variables, controlling for soil depth. Colour indicates the relationship (red is a negative correlation, blue is a positive correlation and white is a weak correlation). The intensity of the colour indicates the strength of the correlation. Asterisks indicate that correlations are significant at p value< 0.1.

4.5. Discussion

4.5.1. Fertility and microbial activity

Across soil depth, the chemistry of the soil solution (RC2 composed of pH, base saturation, potential cation exchange capacity, exchangeable acidity, etc.; Table S4.1) played an important role in predicting SPR and $\Delta^{14}C$ in the lab incubation experiment (Fig. 4.3; Table 4.3). Additionally, available nutrients (dissolved N and bioavailable P) reported by Doetterl *et al.* (2021b) for the same soils as investigated, were positively correlated to SPR and $\Delta^{14}C$ of respired CO_2 (Fig. S4.1) in the mafic and felsic regions. Note that $\Delta^{14}C$ signatures of the bulk soil and respired CO_2 were nearly identical along depth intervals and between the two contrasting (mafic and felsic) parent materials (Fig. 4.2a). This suggests that the cycling of biogenic C, particularly in the topsoil, can occur at a similar rate between soils developed from contrasting parent material (Fig. 4.3) if soil fertility constraints are satisfied. In contrast, in the

sedimentary region, poor soil fertility is likely one of the main causes of lower rates of C cycling in soil. Soils in this region had the lowest available nutrients, with substantially lower concentrations of bioavailable P (Fig. 4.1d) and NH^{+}_{4} (data not presented) than soils in the mafic and felsic regions. This adds to the existing literature suggesting that nutrient limitation, especially N and P, can significantly inhibit microbial growth and activity, hence lowering soil C turnover rates (Kunito *et al.*, 2009; Fang *et al.*, 2014). In addition, the depletion of N and high C:N values (153.9 ± 68.5) of geogenic organic C, which encompasses a substantial part of total C in subsoils of the sedimentary region (Table 5.2), was likely an additional factor reducing soil respiration rates (Whitaker *et al.*, 2014). However, respiration rates in the topsoil of the sedimentary were also lower compared to the mafic or felsic region (Fig. 4.1), but geogenic organic C content in the topsoil was low compared to the subsoil (Table 4.2). Thus, the study concludes that, for the investigated tropical forest systems, soil fertility constraints such as the composition of the soil solution (Table S4.2) are likely more important contributors to explain respiration rates than the presence of geogenic organic C content or other C quality constraints.

4.5.2. The role of tropical weathering and mineral related C stabilization mechanisms in explaining soil respiration

In contrast to studies on soils in temperate climate zones (Franzluebbers & Arshad, 1997; Hassink, 1997; Schleuß *et al.*, 2014), in this study, aggregation and soil texture played only a secondary role in explaining variability in SPR and $\Delta^{14}C$ and their influence decreased with soil depth (Table 4.3). This observation is explained with the fact that clay minerals at advanced weathering stages, such as kaolinite, dominating in tropical soils, generally show lower activity and reactive surfaces than clay minerals dominating earlier weathering stages (e.g. smectite and vermiculite; Doetterl *et al.*, 2018). Lower reactivity of these clays and reduced ability to complex with organic compounds reduce the capacity of the clay fraction to stabilize C in tropical soils compared to temperate soils (Six *et al.*, 2002). In contrast, high amounts of Fe and Al oxyhydroxides as a result of long-term soil weathering have been shown to have a greater influence on C stabilization mechanisms and soil C content (von Fromm *et al.*, 2021; Khomo *et al.*, 2017; Reichenbach *et al.*, 2021). For example, amorphous, oxalate extractable Fe or Al oxides improve the stability of aggregates and can ultimately limit microbial activity (Nagy *et al.*, 2018; Kirsten *et al.*, 2021a). Comparing the findings of SPR to the abundance of oxalate or DCB-extractable Fe or Al amorphous and crystalline pedogenic oxides reported by

Reichenbach *et al.* (2021), the results show a weak to no correlation (Fig. S4.3b-c). This result is interpreted as an indication that C stabilized by such minerals does not contribute to soil respiration in a significant way in a short-term respiration experiment such as the one conducted in this study. Its effects on the long-term SOC stability are more likely related to the formation of stable aggregates (Kleber *et al.*, 2005; (Kleber *et al.*, 2005; Rasmussen *et al.*, 2018; Traoré *et al.*, 2020). Stable metal–organic complexes then represent energetic barriers in soil that are hard to overcome for microorganisms to access potential C resources (Bruun *et al.*, 2010). The importance of these mechanisms is illustrated by the fact that although mafic soils were generally more fertile than soils in the felsic or sedimentary region, SPR was lower and decreased more strongly with depth in mafic soils (75 % decrease in deep subsoil compared to topsoil) than in felsic soils (33 % decrease; Fig. 4.1a). These findings suggest that SOC stocks in the mafic region are higher and SPR lower due to the presence of mineral-related stabilization mechanisms that are lacking in other regions, consistent with the findings of Reichenbach *et al.* (2021). Interestingly, the data suggest that C associated with pyrophosphate extractable oxides (organo–metallic complexes) is readily available to microbial decomposers and can contribute to respiration in a short-term experiment such as this one (Fig. S4.3a).

In summary, the contrasting relationship of pedogenic oxides of different origin and formation to SPR and $\Delta^{14}C$ illustrates the need to improve the understanding of metal–organic interactions and their role in C stabilization in tropical soils, as the results seemingly confirm (the role of metal oxides) and also contradict (the role of clay) findings from younger soils in the temperate zone (Khomo *et al.*, 2017). These results, linked to those of Reichenbach *et al.* (2021), show that the presence or absence of mineral stabilization mechanisms is particularly important for long-term soil C stocks in tropical soils, varying largely with soil parent material, while short-term respiration relies on readily available C sources. However, given that annual plant C inputs are high in tropical forest systems (Lewis *et al.*, 2009; Sayer *et al.*, 2011), exceeding what deeply weathered soils can stabilize (see also chapter 3), the soil and environmental conditions under which C can be decomposed or stabilized seem to be more important for short-term respiration.

4.5.3. Accessibility of old C sources to microbial decomposers and its contribution to SOC

The presence of geogenic organic C in the sedimentary region (up to 52 % of SOC stock in deeper subsoil) (Table 4.2), had a marked effect on SOC stocks in subsoils that would otherwise be similarly low to those of the felsic region (Fig. 4.1c). Consistent with this finding, a recent study shows that geogenic organic C can make a large contribution to SOC in subsoils (Kalks et al., 2021). While geogenic organic C in the study region is of poor quality as indicated by depleted N and high C:N values (153.9 ± 68.5), this study shows that geogenic organic C was microbially available (Fig. 4.2), leading to the respiration of CO_2 with comparably old $\Delta^{14}C$ signatures. However, the study was unable to quantitatively disentangle the slower biogenic C cycling from the contribution of geogenic organic C using $\Delta^{14}C$ of CO_2. Thus, whether the presence of geogenic organic C and/or other unfavourable chemical soil characteristics in the sedimentary region contributed to a general slowing of C cycling remains unknown.

Nevertheless, under the ideal conditions for microbial activity evoked by this experimental setup, similar to in situ topsoil conditions, microbial organisms can decompose these older, less accessible C sources, thereby decreasing the residence time of the geogenic organic C (Hemingway *et al.,* 2018). The fact that $\Delta^{14}C$ signatures in respired CO_2 do not mirror the signature of their C sources in soil indicates that microorganisms do continue to discriminate against these older, poorer C sources if alternatives are available (Fig. 4.2; Feng *et al.*, 2017).

Being a non-renewable source of organic matter, the fact that geogenic organic C can still be found in topsoil is likely related, on the one hand, to the underlying erosion rates that continuously degrade the mountainous landscapes of the East African Rift system and, on the other hand, to the discrimination against geogenic organic C by microbial decomposers in the presence of other, more available C sources. While erosion rates at annual or decadal timescales are negligible for the investigated tropical forests (Drake *et al.*, 2019; Wilken *et al.*, 2021) underlying geological erosion rates estimated for tropical mountain forests globally (Morgan, 2005) range between 0.03–0.2 t $ha^{-1}y^{-1}$. Assuming an average bulk density in the study area's topsoil of roughly 1.3 g cm^{-3} (Doetterl *et al.,* 2021a), 6.8–45.3 thousand years are required to erode the top 10 cm of soil. Thus, slow erosion of soil at millennial timescales may explain the residual content of geogenic organic C in topsoil. The loss of soil material as a result of slow processes of landscape denudation do not directly affect the biological processes investigated in this study. However, erosion at geological timescales cannot be ignored as a mechanism for

the long-term rejuvenation of soil surfaces (Montgomery, 2007; Flores *et al.*, 2020) in pristine tropical catchments, and in this study, lead to the exposure of geogenic C sources to surface conditions.

4.5.4. Respiration in tropical forests is unaffected by lateral fluxes and is only controlled by in situ forest hydrological conditions

While the results did not show differences in respiration and $\Delta^{14}C$ along slope gradients within any of the geochemical regions, significant differences in SPR were observed between valley and non-valley positions (Fig. 4.1a-b). The absence of differences along slopes is a strong indicator that lateral fluxes of matter and water do not significantly influence SOC dynamics at timescales relevant to create topography-dependent differences in C cycling. This finding is supported by work conducted at the global scale which found that erosion in pristine tropical forests was negligible (Vågen & Winowiecki, 2019). Furthermore, at the regional scale in the same study region, Drake *et al.* (2019) found that riverine particulate matter draining from pristine tropical forest catchments are generally dominated by soluble and particulate organic matter fluxes, with little to no mineral sediment being transported. Their result is a strong indicator for little to no erosion of mineral soil in pristine catchments, in agreement with the findings of this study.

In this study, the effect of topography was limited to differences in hydrological conditions between valleys and non-valley positions. In valley positions, decomposition of C in subsoil was generally reduced due to the nearly continuous water saturation, limiting the supply of oxygen (Linn & Doran, 1984; Skopp *et al.*, 1990). These conditions are likely present at the investigated study sites, as supported by the findings of extensive gleyic features in all studied subsoils in valley positions. However, under the ideal conditions for microbial decomposition of C during the laboratory experiment, decomposition of C from valley subsoil was often higher than that of their non-valley counterparts (Fig. 4.1). This observation is explained with the presence of C sources that, although they sometimes have old $\Delta^{14}C$ signatures (Fig. 4.2), become readily available to decomposers once environmental constraints, such as water saturation, are removed (Fig. 4.1b).

4.6. Conclusions

This study shows that geochemical differences in soils that are the result of soil formation from varying parent material (mafic, felsic and sedimentaryary) continue to influence the microbial activity, SOC stocks and C turnover in tropical soils even after many millennia of weathering and almost complete pedogenic alteration of the parent material. The chemistry of the soil solution, namely soil fertility, and the availability of P and N for microbial decomposers were identified as being the most important variables explaining patterns of heterotrophic respiration under idealized well-aerated topsoil conditions. C stabilization mechanisms, including the presence or absence of pedogenic oxides between geochemical regions, were identified as indirect controls to explain variation in soil respiration through their effect on soil aggregation and as potential energetic barriers that decomposers are forced to overcome. Patterns of $\Delta^{14}C$ with soil depth were largely driven by the presence or absence of geogenic organic carbon of low quality, which is inherited from parent material. Under idealized, well-aerated topsoil conditions, these geogenic C sources became available to microbial decomposers, especially in the absence of better alternative energy and nutrient sources.

Furthermore, the analyses revealed that soil respiration was driven in parallel by contrasting processes, limiting microbial activity and slowing down C cycling. C in soil of the studied sedimentary region was low in quality, resulting in low specific respiration, slower C cycling and high SOC stocks. C in the soil of the mafic region was lower in accessibility due to its stabilization with minerals, also resulting in low specific respiration and high SOC stocks in the subsoil. Thus, while geochemistry differed drastically between soils in those two systems, particularly in subsoils, both show low specific respiration for entirely different reasons. In contrast, soils in the felsic region showed high specific soil respiration, as no strong mineral driven stabilization mechanisms were present and as soil C of favourable quality was readily available for microorganisms to decompose.

While the impact of geochemistry on C dynamics was clearly distinct between the studied soils, topography only played a secondary role in these densely vegetated tropical forest systems. Hydrological features, such as water saturation in valleys, partially inhibited microbial activity in situ, leaving labile C sources available for decomposition under the idealized laboratory conditions. Erosional processes rejuvenating soils and landscapes at geological timescales did account for significant differences in C cycling across geochemical regions due to the surfacing of geogenic organic carbon, but did not act at timescales to create topography dependent differences in C cycling. The study concludes that geochemistry, parent material and its lasting

role on pedogenesis are key factors to consider to improve the understanding of C release from tropical forest soils. Improving the spatial representation of C dynamics at larger spatial scales using the variables and controls identified in this study could potentially be an important improvement for predicting and modelling future C turnover in tropical forest

5. Synthesis and general conclusions

The aim of this thesis was to develop a mechanistic understanding of the effects that change in soil geochemical and geomorphic features has on: (1) rock-derived element content of the forest canopy (canopy chemistry) as this is central to understand nutrient recycling and limitation in tropical forest ecosystems; (2) plant biomass productivity, soil and vegetation C stocks, and plant C allocation strategies between different compartments. This question is scientifically elemental as it has an implication in understanding of how plants respond to changes in soil properties and how biomass productivity relates to soil C socks; (3) specific potential soil heterotrophic respiration rate and C turnover in African tropical forest systems. Understanding SOC respiration and turnover rate can help to identify a set of primary environmental factors that drive SOC dynamics across diverse landscapes and to better understand the soil-plant-atmosphere continuum. To achieve this, the thesis used a combination of forest inventories, field vegetation monitoring, laboratory-based incubation experiments, and radiocarbon measurements.

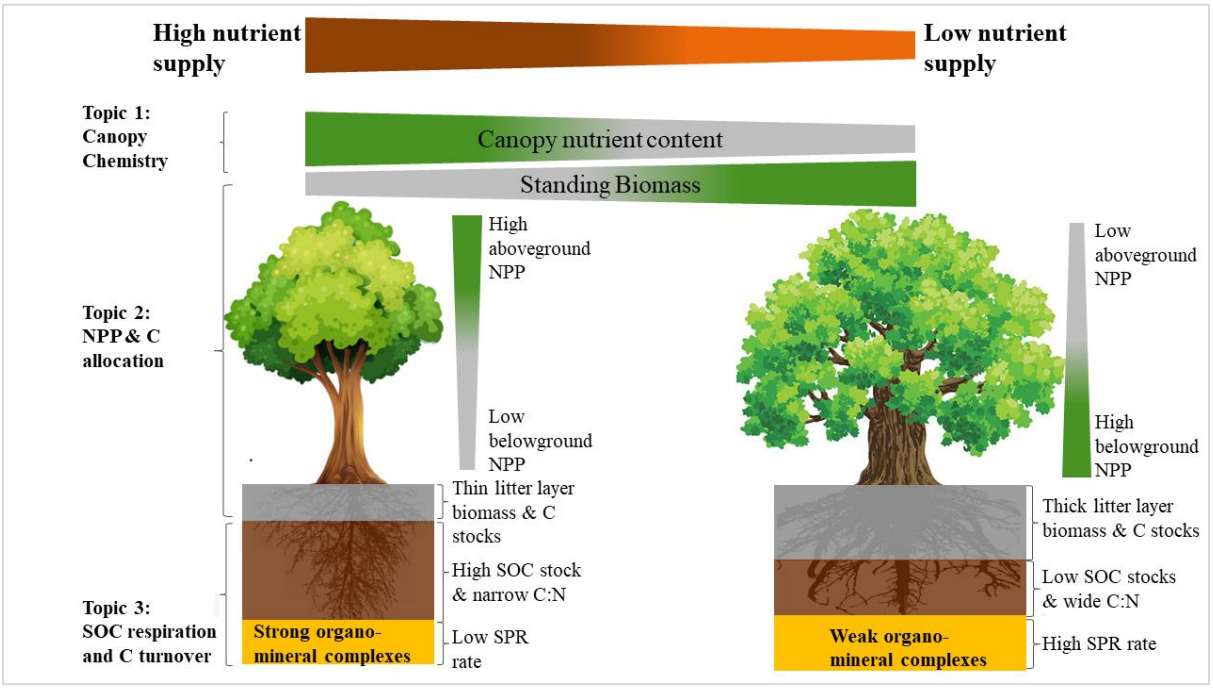

Figure 5.1. Synthesis of the thesis with highlights of main topics covered and key findings. From top to bottom: the first topic assessed major nutrient uptake and concentrations in the canopy, the second topic assessed plant NPP and C allocation in different compartments and the third chapter assessed potential specific soil heterotrophic respiration and ^{14}C signature of SOC and respired CO_2.

5.1. Main findings and synthesis

To address the first objective and the associated research question, the thesis began with an assessment of essential and rock derived-canopy elements (leaf N, P, Ca, K, Mg, Na, C:N, C:P, and N:P) in old-growth tropical forests. Overall, the thesis found significant differences in canopy chemistry between the three geochemical (i.e. Mafic, felsic and sedimentary) regions (Figure 5.1; for details see Chapter 2). Primary and rocked-derived canopy nutrients were higher in fertile soils developed in mafic and felsic regions, and lower in nutrient-poor soils developed in sedimentary region. In contrast, the ratios of carbon to rock-derived nutrients, were higher in sedimentary region and lower in felsic and mafic regions. When assessing the major controls on canopy nutrients and chemistry, the results revealed that canopy chemistry followed consistent patterns related to soil fertility as a result of differences in soil geochemical properties between regions. Soil base cation stocks and pH emerged as the major drivers of canopy chemistry (Fig. 2.3). Furthermore, the results revealed minor differences in canopy chemistry between topographic positions within geochemical regions. However, these differences were not significant and consistent across all regions (Fig. S2.1). As such, topographic positions along catena in these old-growth forests did not emerge as a strong driver of canopy chemistry. Altogether these results revealed significant effects of soil geochemical properties derived from the parent material on canopy chemistry. These results have implications in the understanding the way tropical forests function. The role of canopy chemistry on forest functioning is not a new topic among biogechemists and ecologsgist comunities. For example, canopy chemistry has been shown to influence forest ecosystem function including: NPP and nutrient cycling through organic litter layer decomposition (Jobbágy & Jackson, 2004; Hättenschwiler *et al.*, 2008; Reich *et al.*, 2009). However, the link among parent material geochemistry, canopy chemistry and tropical forests functioning remains understudied and is not fully understood. This is because current understanding of canopy chemistry is often limited to N and P concentrations, with little to no attention on rock-derived nutrients—one of the weak points of forest ecological studies as reported by (Dietze, 2014). This thesis adds to the body of existing knowledge by linking canopy rock-derived nutrients to the associated soil geochemistry reflecting the local parent material (Fig. 2.1; Fig. 2.3). In line with this results, a recent study conducted in the same region in secondary tropical forests along succession gradients showed that Ca is the most limiting nutrient more than N and P (Bauters *et al.*, 2022). Furthermore, while N and P are well documented for tropical biogeochemistry, often the drivers are not clear. Such understanding can be improved by

considering local edaphic parameters (Norby *et al.*, 2017). Chapter two revealed also a strong effect of soil geochemical properties more than topographic features, suggesting that change in soil geochemical properties as a result of diverse parent material is likely the main source of variation in canopy chemistry in old-growth African tropical forests. In summary, these results suggest that canopy chemistry exhibits greater variation across- than within geochemical regions (Han *et al.*, 2011), indicating that nutrient supply through weathering of the parent material across geochemical regions has resulted in soils with diverse properties that can influence plant growth and shape canopy chemistry. However, responses of different tree communities as a mechanism to cope with nutrient limitations remain unanswered, but this study provides foundation knowledge and an opportunity for future research in the region. Specifically, understanding the resorption rate for each major nutrient in these tropical montane forests and between species should be followed up to understand the whole nutrient cycle in African tropical montane forests.

Chapter three assessed the effect that changes in soil geochemical properties and topography have on plant standing biomass, C stocks, NPP and C allocation between compartments (leaf, wood, and fine roots). Furthermore, chapter three investigated how C inputs relates to SOC stocks in old-growth tropical forests systems across geochemical regions. The results showed distinct patterns of standing biomass C stocks, NPP, C allocation and SOC stocks across geochemical regions (Fig. 3.1, Fig. 3.2, Fig. 5.1). In general, chapter three revealed that biomass C stocks, NPP and C allocation into plant compartments (Litter, wood and roots) are constrained by soil fertility inherited from the parent material. Litter, wood and roots biomass C stocks were higher in nutrient-poor sites (sedimentary region) and lower in nutrient-rich sites (Mafic and felsic regions) (Fig. 3.1). Furthermore, NPP and C allocation to fine roots were higher in nutrient-poor sites and lower in nutrient-rich sites. In contrast, NPP and C allocation to aboveground wood were higher in nutrient-rich sites (mafic and felsic) and lower in nutrient-poor sites (sedimentary). NPP and C allocation to litter did not differ between geochemical regions (Fig. 3.2). Finally, SOC stocks followed different patterns vis-à-vis to the roots productivity and roots C stocks. Topographic positions and the associated indices derived from the DEM did not significantly affect or correlate with biomass C stocks, NPP, C allocation, or SOC stocks in all investigated forest stands and geochemical regions. In contrast, a set variables representing rock derived nutrient and base cation stocks showed strong effects on biomass C stocks, NPP, and C allocation into litter, wood and fine roots (Fig. 3.4, Fig. 3.6). Altogether, these results suggest that the current process understanding of shoot to root ratio and how they relate to SOC stocks in tropical forests ecosystems is not fully understood and may have

substantial impacts on the way C fluxes are estimated in biogeochemical models. For example, the paucity of belowground data for tropical systems especially old-growth African tropical forests (Norby et. al, 2016) often leads to the use fixed ratios of shoot:root biomass/C allocation and application of allometric models to estimate ecosystem C budgets (Mokany *et al.*, 2006; Cleveland *et al.*, 2013; Gherardi & Sala, 2020). However, the results of chapter three revealed surprising patterns in NPP and C allocation among plant compartments (Fig. 3.2). Data shows that forest stands growing in nutrient-rich sites invest most of their resources in aboveground NPP. The reason for this is not completely clear, but it is likely associated with the competion for resources essential for photosynthetic processes. In contrast, as a result of fertility constraints, forest stands growing in nutrient-limited sites allocate most of their biomass into fine roots likely to mine essential plant nutrients. Furthermore, as strategies to cope with nutrient limitation, forest stands in nutrient-limited sites build up their standing biomass and C stocks while minimizing their aboveground NPP and turnover rate. While NPP is often correlated with SOC stocks in biogeochemical models, results in these results shows that NPP did not relate to SOC stocks. Despite higher NPP fine root and root C stocks in the sedimentary region, SOC stocks remained lower compared to its counterparts the mafic and felsic regions. The interplay between geochemistry and SOC might explain differences in SOC stocks between regions and suggest that SOC in these regions is likely driven by mechanisms other than input as recently shown by (Reichenbach *et al.*, 2021) for the same study sites.

In summary, the shift in C allocation and lack of correlation between C input and SOC stocks have two major implications in the understanding tropical forest biogechemistry: First, the current approache of deriving roots biomas C from aboveground biomass may under- or overestimate C stocks and budget in these tropical biomes. Second, the correlation of below- and aboveground biomass to SOC stocks or the use of belowground biomass as a proxy for SOC stocks may lead to further uncertainties in SOC stocks and overall C fluxes estimates in tropical forest systems. Nevertheless, the response of plants to changes in soil geochemistry in African tropical systems need further research. Specifically, research that takes into account soil geochemistry, canopy, wood and litter nutrient content at the same time are need to explore the process of resource conservation and the impact this has on C and nutrient cycles in old-growth African tropical forests.

Chapter four assessed depth explicit drivers of specific potential heterotrophic soil respiration (SPR) and C turnover via radiocarbon signatures ($\Delta^{14}C$) of bulk and respired C across geochemical and geomorphic gradients. Overall, differences in SPR and $\Delta^{14}C$ signature of respired CO_2 and SOC were observed between topographic positions and geochemical regions.

However, along topographic positions, differences were mainly observed between non-valley (Plateau, Upperslope, and Midslope) and valley positions, but there were no consistent and significant differences between non-valley positions. Data for all regions show that differences between non-valley and valley positions were mainly driven by hydrological features due to gleyic properties that dominated valley positions. For non-valley profiles, SPR was higher in the felsic and mafic regions than in the sedimentary region. While topsoil samples between mafic and felsic did not show differences in SPR, SPR in subsoil samples from the felsic and mafic regions decreased by 35% and 75 % for felsic and mafic regions respectively. Overall, SPR in the sedimentary region did not change with depth and was consistently lower compared to their counterparts in felsic and mafic regions. For both top and subsoils, there were no differences in $\Delta^{14}C$ signatures of both SOC and respired CO_2 between mafic and felsic. However, samples from the sedimentary region were consistently and significantly depleted in $\Delta^{14}C$ for either SOC or respired CO_2. Radiocarbon data revealed that soils in sedimentary region were dominated by geogenic carbon. This is because, organic carbon in these sediments was mainly depleted $\Delta^{14}C$ and characterized by high C:N values compared to their counterparts in felsic and mafic regions. A closer analysis revealed that soil solution chemistry and soil texture were the most important factors explaining variability in SPR, and the effects of these predictors increased with depth. $\Delta^{14}C$ was mainly driven by a larger set of variables than SPR, including C:N of organic substrate, and soil solution chemistry. Specifically, the results revealed that SPR and $\Delta^{14}C$ were driven by soil geochemical properties representing soil weathering stage and local parent material, strengthning the importance of soil geochemical properties in explaining SOC availability to microbial decomposers and C cycling. In addition, the results revealed the role C availabitlity (labile VS recalcitrant) can play in C cycling. Data shows that the presence of metal cations (Fe and Al)-hydroxides had a strong influence on SOC stabilization mechanisms. These mechanisms are likely a result of metal-SOC complexes that create energetic barriers strong for microbial decomposers to break. Altogether, these results suggest that in the absence of strong mineral-associated stabilization mechanisms or poor accessible organic carbon such as organic substrate with high C:N values, SOC stock in African tropical forest systems is susceptible to microbial decomposers and is likely to affect the way SOC turnover is modelled in these tropical systems.

5.2. General conclusions

This thesis assessed the role of soil geochemistry and topography as drivers of the C cycle via soil-plant interactions in African old-growth tropical forests. There are parts of the C fluxes which are not covered in this thesis and potential focus for future research has been highlighted in the respective chapters and in section 5.1 of the thesis. However, the major fluxes that are known to influence C estimates were fully covered throughout this thesis. First, thesis revealed how soil geochemical properties derived from the parent material drive canopy chemistry mainly major nutrient and rock derived nutrients. Second, the thesis revealed that change in soil geochemical properties alter plant NPP and C allocation as forest stands shift from nutrient–rich towards nutrient-limited soils and the implication this has on shoot:root ratios in African tropical forests. Finally, the results of the thesis show that soil geochemistry is the main driver of SOC and C turnover in deeply weathered tropical forest soils. This thesis adds insight to the existing body of knowledge in the following ways: (1) Major nutrients uptake in relation to the geological parent material, (2) plant C allocation strategies in relation to soil geochemical origin, (3) the relationship of NPP to SOC stocks in tropical forest, and (4) SOC respiration rate and turnover in relation to deeply weathered soils that originated from distinct parent material. There are two major reasons to believe that these insights will make a significant improvement in the understanding of the plant-soil relationship and C cycling in African tropical systems. First, while large scale variation in C fluxes is often attributed to climate, this finding is remarkable as the investigated forests grow on soils that developed over millennia under a similar tropical climate and in systems where weathering has strongly altered the chemical composition of soil compared to its parent material. Second, the results demonstrate that, even in deeply weathered tropical soils, parent material still has a long-lasting effect on soil chemistry that can influence and control C input, microbial activities, the amount of subsoil C stocks and the turnover rate of SOC stock. Therefore, geochemistry of local parent material is an overlooked factor that drive C fluxes in African tropical montane forests. Soil parent material and its control on soil chemistry need to be taken into account to understand and predict C stabilization and rates of C cycling in soils and old-growth forests of African tropical ecosystems.

References

Abdi H, Williams LJ. **2010**. Principal component analysis. *WIREs Computational Statistics* **2**: 433–459.

Addo-Danso SD, Prescott CE, Adu-Bredu S, Duah-Gyamfi A, Moore S, Guy RD, Forrester DI, Owusu-Afriyie K, Marshall PL, Malhi Y. **2018**. Fine-root exploitation strategies differ in tropical old growth and logged-over forests in Ghana. *Biotropica* **50**: 606–615.

Aiba S, Takyu M, Kitayama K. **2005**. Dynamics, productivity and species richness of tropical rainforests along elevational and edaphic gradients on Mount Kinabalu, Borneo In: Forest Ecosystems and Environments: Scaling Up from Shoot Module to Watershed. Kohyama T, Canadell J, Ojima DS, Pitelka LF, eds. Tokyo: Springer Tokyo, 41–48.

Andersen KM, Turner BL, Dalling JW. **2014**. Seedling performance trade-offs influencing habitat filtering along a soil nutrient gradient in a tropical forest. *Ecology* **95**: 3399–3413.

Angst G, Messinger J, Greiner M, Häusler W, Hertel D, Kirfel K, Kögel-Knabner I, Leuschner C, Rethemeyer J, Mueller CW. **2018**. Soil organic carbon stocks in topsoil and subsoil controlled by parent material, carbon input in the rhizosphere, and microbial-derived compounds. *Soil Biology and Biochemistry* **122**: 19–30.

Aoki M, Fujii K, Kitayama K. **2012**. Environmental control of root exudation of low-molecular weight organic acids in tropical rainforests. *Ecosystems* **15**: 1194–1203.

Asner GP, Anderson CB, Martin RE, Tupayachi R, Knapp DE, Sinca F. **2015**. Landscape biogeochemistry reflected in shifting distributions of chemical traits in the Amazon forest canopy. *Nature Geoscience* **8**: 567–573.

Asner GP, Mascaro J. **2014**. Mapping tropical forest carbon: Calibrating plot estimates to a simple LiDAR metric. *Remote Sensing of Environment* **140**: 614–624.

Assefa D, Rewald B, Sandén H, Godbold DL. **2017**. Fine root dynamics in Afromontane forest and adjacent land uses in the Northwest Ethiopian highlands. *Forests* **8**.

Augusto L, Achat DL, Jonard M, Vidal D, Ringeval B. **2017a**. Soil parent material-A major driver of plant nutrient limitations in terrestrial ecosystems. *Global change biology* **23**: 3808–3824.

Baartman JEM, Temme AJAM, Saco PM. **2018**. The effect of landform variation on vegetation patterning and related sediment dynamics. *Earth Surface Processes and Landforms* **43**: 2121–2135.

Baltzer JL, Thomas SC, Nilus R, Burslem DFRP. **2005**. Edaphic specialization in tropical trees: physiological correlates and responses to reciprocal transplantation. *Ecology* **86**: 3063–3077.

Banin L, Feldpausch TR, Phillips OL, Baker TR, Lloyd J, Affum-Baffoe K, Arets EJMM, Berry NJ, Bradford M, Brienen RJW. **2012**. What controls tropical forest architecture? Testing environmental, structural and floristic drivers. *Global Ecology and Biogeography* **21**: 1179–1190.

Bates D, Mächler M, Bolker B, Walker S. 2015. Fitting Linear Mixed-Effects Models Using lme4. *Journal of Statistical Software* 67: 1–48.

Bauters M, Drake TW, Verbeeck H, Bodé S, Hervé-Fernández P, Zito P, Podgorski DC, Boyemba F, Makelele I, Ntaboba LC, *et al.* 2018. High fire-derived nitrogen deposition on central African forests. *Proceedings of the National Academy of Sciences of the United States of America* **115**: 549–554.

Bauters M, Drake TW, Wagner S, Baumgartner S, Makelele IA, Bodé S, Verheyen K, Verbeeck H, Ewango C, Cizungu L, *et al.* 2021. Fire-derived phosphorus fertilization of African tropical forests. *Nature Communications* **12**: 5129.

Bauters M, Janssens IA, Wasner D, Doetterl S, Vermeir P, Griepentrog M, Drake TW, Six J, Barthel M, Baumgartner S, *et al.* 2022. Increasing calcium scarcity along Afrotropical forest succession. *Nature Ecology & Evolution* **6**: 1122–1131.

Bauters M, Verbeeck H, Doetterl S, Ampoorter E, Baert G, Vermeir P, Verheyen K, Boeckx P. **2017**. Functional composition of tree communities changed topsoil properties in an old experimental tropical plantation. *Ecosystems* **20**: 861–871.

Beer C, Reichstein M, Tomelleri E, Ciais P, Jung M, Carvalhais N, Rödenbeck C, Arain MA, Baldocchi D, Bonan GB, *et al.* 2010. Terrestrial gross carbon dioxide uptake: global distribution and covariation with climate. *Science* **329**: 834–838.

Berhe AA, Harden JW, Torn MS, Harte J. **2008**. Linking soil organic matter dynamics and erosion-induced terrestrial carbon sequestration at different landform positions. *Journal of Geophysical Research: Biogeosciences* **113**.

Berhe AA, Harden JW, Torn MS, Kleber M, Burton SD, Harte J. **2012**. Persistence of soil organic matter in eroding versus depositional landform positions. *Journal of Geophysical Research: Biogeosciences* **117**: 1–16.

Besnard S, Koirala S, Santoro M, Weber U, Nelson J, Gütter J, Herault B, Kassi J, N'Guessan A, Neigh C, *et al.* 2021. Mapping global forest age from forest inventories, biomass and climate data. *Earth System Science Data* **13**: 4881–4896.

Brunner I, Bakker MR, Björk RG, Hirano Y, Lukac M, Aranda X, Børja I, Eldhuset TD, Helmisaari HS, Jourdan C, *et al.* 2013. Fine-root turnover rates of European forests revisited: an analysis of data from sequential coring and ingrowth cores. *Plant and Soil* **362**: 357–372.

Bruun T, Elberling B, Christensen BT. **2010**. Soil Biology & Biochemistry lability of soil organic carbon in tropical soils with different clay minerals. *Soil Biology and Biochemistry* **42**: 888–895.

Buendia C, Arens S, Hickler T, Higgins SI, Porada P, Kleidon A. **2014**. On the potential vegetation feedbacks that enhance phosphorus availability – insights from a process-based model linking geological and ecological timescales. *Biogeosciences* **11**: 3661–3683.

Bürkner P-C. **2017**. brms: An R Package for Bayesian Multilevel Models Using Stan. *Journal of Statistical Software* **80**: 1–28.

Canham CD. **1988**. Growth and canopy architecture of shade-tolerant trees: Response to canopy gaps. *Ecology* **69**: 786–795.

Cardelús CL, MacK MC, Woods C, Demarco J, Treseder KK. **2009**. The influence of tree species on canopy soil nutrient status in a tropical lowland wet forest in Costa Rica. *Plant and Soil* **318**: 47–61.

de Castilho C V, Magnusson WE, de Araújo RNO, Luizão RCC, Luizão FJ, Lima AP, Higuchi N. **2006**. Variation in aboveground tree live biomass in a central Amazonian Forest: Effects of soil and topography. *Forest Ecology and Management* **234**: 85–96.

Cerri C, Feller C, Balesdent J, Victoria R, Plenecassagne A. **1985**. Application du traçage isotopique en 13C, à l'étude de la dynamique de la matière organique dans les sols. *Comptes Rendus de l'Académie des Sciences, Paris, t.300, série II* **300**: 423–428.

Chadwick KD, Asner GP. **2016**. Tropical soil nutrient distributions determined by biotic and hillslope processes. *Biogeochemistry* **127**: 273–289.

Chang C-W, Laird DA, Mausbach MJ, Hurburgh CR. **2001**. Near-infrared reflectance spectroscopy–principal components regression analyses of soil properties. *Soil Science Society of America Journal* **65**: 480–490.

Chapin FS, Vitousek PM, Van Cleve K. **1986**. The nature of nutrient limitation in plant communities. *The American Naturalist* **127**: 48–58.

Chave J, Réjou-Méchain M, Búrquez A, Chidumayo E, Colgan MS, Delitti WBC, Duque A, Eid T, Fearnside PM, Goodman RC, *et al.* 2014. Improved allometric models to estimate the aboveground biomass of tropical trees. *Global Change Biology* **20**: 3177–3190.

Cleveland CC, Houlton BZ, Smith WK, Marklein AR, Reed SC, Parton W, Del Grosso SJ, Running SW. **2013**. Patterns of new versus recycled primary production in the terrestrial biosphere. *Proceedings of the National Academy of Sciences* **110**: 12733 LP – 12737.

Cleveland CC, Townsend AR, Taylor P, Alvarez-Clare S, Bustamante MMC, Chuyong G, Dobrowski SZ, Grierson P, Harms KE, Houlton BZ, *et al.* 2011. Relationships among net primary productivity, nutrients and climate in tropical rain forest: a pan-tropical analysis. *Ecology Letters* **14**: 939–947.

Cordeiro AL, Norby RJ, Andersen KM, Valverde-Barrantes O, Fuchslueger L, Oblitas E, Hartley IP, Iversen CM, Gonçalves NB, Takeshi B, *et al.* 2020. Fine-root dynamics vary with soil depth and precipitation in a low-nutrient tropical forest in the Central Amazonia. *Plant-Environment Interactions* **1**: 3–16.

Cuni-Sanchez A, Sullivan MJP, Platts PJ, Lewis SL, Marchant R, Imani G, Hubau W, Abiem I, Adhikari H, Albrecht T, *et al.* 2021. High aboveground carbon stock of African tropical montane forests. *Nature* **596**: 536–542.

Dargie GC, Lewis SL, Lawson IT, Mitchard ETA, Page SE, Bocko YE, Ifo SA. **2017**. Age, extent and carbon storage of the central Congo Basin peatland complex. *Nature* **542**: 86–90.

Davidson EA, Janssens IA. **2006**. Temperature sensitivity of soil carbon decomposition and feedbacks to climate change. *Nature* **440**: 165–173.

Davidson EA, Trumbore SE, Amundson R. **2000**. Soil warming and organic carbon content. *Nature* **408**: 789–790.

Day RW, Quinn GP. **1989**. Comparisons of treatments after an analysis of variance in ecology. *Ecological Monographs* **59**: 433–463.

Dietze MC. **2014**. Gaps in knowledge and data driving uncertainty in models of photosynthesis. *Photosynthesis Research* **119**: 3–14.

Dijkstra FA, Zhu B, Cheng W. **2021**. Root effects on soil organic carbon: a double-edged sword. *New Phytologist* **230**: 60–65.

Doetterl S, Asifiwe RK, Baert G, Bamba F, Bauters M, Boeckx P, Bukombe B, Cadisch G, Cooper M, Cizungu LN, Hoyt, A., Kabaseke, C., Kalbitz, K., Kidinda, L., Maier, A., Mainka, M., Mayrock, J., Muhindo, D., Mujinya, B.B., Mukotanyi, S.M., Nabahungu, L., Reichenbach, M., Rewald, B., Six, J., Stegmann, A., Summerauer, L., Unseld, R., Vanlauwe, B., Van Oost, K., Verheyen, K., Vogel, C., Wilken, F., Fiener, P. 2021a. Organic matter cycling along geochemical, geomorphic, and disturbance gradients in forest and cropland of the African Tropics -- project TropSOC database version 1.0. *Earth System Science Data* **13**: 4133–4153.

Doetterl S, Bauters M, Berhe AA, Chivenge P, Finke P. **2021b**. Preface: Tropical biogeochemistry of soils in the Congo Basin and the African Great Lakes region.

Doetterl S, Berhe AA, Arnold C, Bodé S, Fiener P, Finke P, Fuchslueger L, Griepentrog M, Harden JW, Nadeu E, Schnecker, J., Six, J., Trumbore, S., Van Oost, K., Vogel, C., Boeckx, P.2018. Links among warming, carbon and microbial dynamics mediated by soil mineral weathering. *Nature Geoscience* **11**: 589–593.

Doetterl S, Berhe AA, Nadeu E, Wang Z, Sommer M, Fiener P. **2016**. Erosion, deposition and soil carbon: A review of process-level controls, experimental tools and models to address C cycling in dynamic landscapes. *Earth-Science Reviews* **154**: 102–122.

Doetterl S, Bukombe B, Cooper M, Kidinda L, Muhindo D, Reichenbach M, Stegmann A, Summerauer L, Wilken F, Fiener P. **2021c**. TropSOC Database. V. 1.0. *GFZ Data Services*.

Doetterl S, Stevens A, Six J, Merckx R, Van Oost K, Casanova Pinto M, Casanova-Katny A, Muñoz C, Boudin M, Zagal Venegas E, Boeckx, P., 2015. Soil carbon storage controlled by interactions between geochemistry and climate. *Nature Geoscience* **8**: 780–783.

Doughty CE, Goldsmith GR, Raab N, Girardin CAJ, Farfan-Amezquita F, Huaraca-Huasco W, Silva-Espejo JE, Araujo-Murakami A, da Costa ACL, Rocha W, Galbraith, D., Meir, P., Metcalfe, D.B., Malhi, Y. 2018. What controls variation in carbon use efficiency among Amazonian tropical forests? *Biotropica* **50**: 16–25.

Drake TW, Van Oost K, Barthel M, Bauters M, Hoyt AM, Podgorski DC, Six J, Boeckx P, Trumbore SE, Cizungu Ntaboba L, Spencer, R.G.M. 2019. Mobilization of aged and biolabile soil carbon by tropical deforestation. *Nature Geoscience* **12**: 541–546.

Eger A, Yoo K, Almond PC, Boitt G, Larsen IJ, Condron LM, Wang X, Mudd SM. **2018**. Does soil erosion rejuvenate the soil phosphorus inventory? *Geoderma* **332**: 45–59.

Epihov DZ, Saltonstall K, Batterman SA, Hedin LO, Hall JS, van Breugel M, Leake JR, Beerling DJ. **2021**. Legume–microbiome interactions unlock mineral nutrients in regrowing tropical forests. *Proceedings of the National Academy of Sciences* **118**: e2022241118.

Fairley RI, Alexander IJ. **1985**. Methods of calculating fine root production in forests. In: Fitter AH, ed. Ecological interactions in soil. Special Publication Number 4 of The British Ecological Society. 37–47.

Fang K, Qin S, Chen L, Zhang Q, Yang Y. **2019**. Al/Fe Mineral Controls on Soil Organic Carbon Stock Across Tibetan Alpine Grasslands. *Journal of Geophysical Research: Biogeosciences* **124**: 247–259.

Fang H, Wang Y, Yu G, Minjie X. **2014**. Changes in soil heterotrophic respiration, carbon availability , and microbial function in seven forests along a climate gradient. *ECOLOGICAL RESEARCH* **29**: 1077–1086.

FAO. **2006**. *Guidelines for soil description, 4th edition*. Rome: FAO.

Fernández-Martínez M, Vicca S, Janssens IA, Sardans J, Luyssaert S, Campioli M, Chapin III FS, Ciais P, Malhi Y, Obersteiner M, *et al.* 2014. Nutrient availability as the key regulator of global forest carbon balance. *Nature Climate Change* **4**: 471–476.

Fick SE, Hijmans RJ. **2017**. WorldClim 2: new 1-km spatial resolution climate surfaces for global land areas. *International Journal of Climatology* **37**: 12.

Fisher JB, Malhi Y, Torres IC, Metcalfe DB, van de Weg MJ, Meir P, Silva-Espejo JE, Huasco WH. **2013**. Nutrient limitation in rainforests and cloud forests along a 3,000-m elevation gradient in the Peruvian Andes. *Oecologia* **172**: 889–902.

Flores BM, Staal A, Jakovac CC, Hirota M, Holmgren M, Oliveira RS. **2020**. Soil erosion as a resilience drain in disturbed tropical forests. *Plant and Soil* **450**: 11–25.

Fontaine S, Barot S, Barré P, Bdioui N, Mary B, Rumpel C. **2007**. Stability of organic carbon in deep soil layers controlled by fresh carbon supply. *Nature* **450**: 277–280.

Franzluebbers AJ, Arshad MA. **1997**. Particulate organic carbon content and potential mineralization as affected by tillage and texture. *Soil Science Society of America Journal* **61**: 1382–1386.

Freschet GT, Pagès L, Iversen CM, Comas LH, Rewald B, Roumet C, Klimešová J, Zadworny M, Poorter H, Postma JA, *et al.* 2021. A starting guide to root ecology: strengthening ecological concepts and standardising root classification, sampling, processing and trait measurements. *New Phytologist* **232**: 973–1122.

Friedlingstein P, Meinshausen M, Arora VK, Jones CD, Anav A, Liddicoat SK, Knutti R. **2014**. Uncertainties in CMIP5 Climate Projections due to Carbon Cycle Feedbacks. *Journal of Climate* **27**: 511–526.

von Fromm SF, Hoyt AM, Lange M, Acquah GE, Aynekulu E, Berhe AA, Haefele SM, McGrath SP, Shepherd KD, Sila AM, Six, J., Towett, E.K., Trumbore, S.E., Vågen, T.-G., Weullow, E., Winowiecki, L.A., Doetterl, S. 2021. Continental-scale controls on soil organic carbon across sub-Saharan Africa. *SOIL* **7**: 305–332.

Fyllas NM, Patiño S, Baker TR, Bielefeld Nardoto G, Martinelli LA, Quesada CA, Paiva R, Schwarz M, Horna V, Mercado LM, antos, A., Arroyo, L., Jiménez, E.M., Luizão, F.J., Neill, D.A., Silva, N., Prieto, A., Rudas, A., Silviera, M., Vieira, I.C.G., Lopez-Gonzalez, G., Malhi, Y., Phillips, O.L., Lloyd, J. 2009. Basin-wide variations in foliar properties of Amazonian forest: phylogeny, soils and climate. *Biogeosciences* **6**: 2677–2708.

Gherardi LA, Sala OE. **2020**. Global patterns and climatic controls of belowground net carbon fixation. *Proceedings of the National Academy of Sciences* **117**: 20038 LP – 20043.

Gill RA, Jackson RB. **2000**. Global patterns of root turnover for terrestrial ecosystems. *New Phytologist* **147**: 13–31.

Giraudoux P. **2022**. pgirmess: Spatial Analysis and Data Mining for Field Ecologists. https://cran.r-project.org/web/packages/pgirmess/index.html.

Giweta M. **2020**. Role of litter production and its decomposition, and factors affecting the processes in a tropical forest ecosystem: a review. *Journal of Ecology and Environment* **44**: 11.

Grau O, Peñuelas J, Ferry B, Freycon V, Blanc L, Desprez M, Baraloto C, Chave J, Descroix L, Dourdain A, Guitet, S., Janssens, I.A., Sardans, J., Hérault, B. 2017. Nutrient-cycling mechanisms other than the direct absorption from soil may control forest structure and dynamics in poor Amazonian soils. *Scientific Reports* **7**: 45017.

Del Grosso S, Parton W, Stohlgren T, Zheng D, Bachelet D, Prince S, Hibbard K, Olson R. **2008**. Global potential net primary production predicted from vegetation class, precipitation, and temperature. *Ecology* **89**: 2117–2126.

Guns M, Vanacker V. **2014**. Shifts in landslide frequency–area distribution after forest conversion in the tropical Andes. *Anthropocene* **6**: 75–85.

Haaf D, Six J, Doetterl S. **2021**. Global patterns of geo-ecological controls on the response of soil respiration to warming. *Nature Climate Change* **11**: 623–627.

Han W, Fang J, Guo D, Zhang Y. **2005**. Leaf nitrogen and phosphorus stoichiometry across 753 terrestrial plant species in China. *New Phytologist* **168**: 377–385.

Han WX, Fang JY, Reich PB, Ian Woodward F, Wang ZH. **2011**. Biogeography and variability of eleven mineral elements in plant leaves across gradients of climate, soil and plant functional type in China. *Ecology Letters* **14**: 788–796.

Hartmann H, Bahn M, Carbone M, Richardson AD. **2020**. Plant carbon allocation in a changing world – challenges and progress: introduction to a Virtual Issue on carbon allocation. *New Phytologist* **227**: 981–988.

Hassink J. **1997**. The capacity of soils to preserve organic C and N by their association with clay and silt particles. *Plant and Soil* **191**: 77–87.

Hättenschwiler S, Aeschlimann B, Coûteaux M-M, Roy J, Bonal D. **2008**. High variation in foliage and leaf litter chemistry among 45 tree species of a neotropical rainforest community. *New Phytologist* **179**: 165–175.

Heineman KD, Jensen E, Shapland A, Bogenrief B, Tan S, Rebarber R, Russo SE. **2011**. The effects of belowground resources on aboveground allometric growth in Bornean tree species. *Forest Ecology and Management* **261**: 1820–1832.

Hemingway JD, Hilton RG, Hovius N, Eglinton TI, Haghipour N, Wacker L, Chen M-C, Galy VV. **2018**. Microbial oxidation of lithospheric organic carbon in rapidly eroding tropical mountain soils. *Science* **360**: 209–212.

Hobbie EA. **2006**. Carbon allocation to ectomycorrhizal fungi correlates with belowground allocation in culture studies. *Ecology* **87**: 563–569.

Hobley EU, Wilson B. **2016**. The depth distribution of organic carbon in the soils of eastern Australia. *Ecosphere* **7**: e01214.

Hofhansl F, Chacón-Madrigal E, Fuchslueger L, Jenking D, Morera-Beita A, Plutzar C, Silla F, Andersen KM, Buchs DM, Dullinger S, Fiedler, K., Franklin, O., Hietz, P., Huber, W., Quesada, C.A., Rammig, A., Schrodt, F., Vincent, A.G., Weissenhofer, A., Wanek, W. 2020. Climatic and edaphic controls over tropical forest diversity and vegetation carbon storage. *Scientific Reports* **10**: 5066.

Holdaway RJ, Richardson SJ, Dickie IA, Peltzer DA, Coomes DA. **2011**. Species-and community-level patterns in fine root traits along a 120 000-year soil chronosequence in temperate rain forest. *Journal of Ecology* **99**: 954–963.

Huang Y, Ciais P, Santoro M, Makowski D, Chave J, Schepaschenko D, Abramoff RZ, Goll DS, Yang H, Chen Y, Wei, W., Piao, S. 2021. A global map of root biomass across the world's forests. *Earth System Science Data* **13**: 4263–4274.

Huang C, Wu C, Gong H, You G, Sha L, Lu H. **2020**. Decomposition of roots of different diameters in response to different drought periods in a subtropical evergreen broad-leaf forest in Ailao Mountain. *Global Ecology and Conservation* **24**: e01236.

Hubau W, Lewis SL, Phillips OL, Affum-Baffoe K, Beeckman H, Cuní-Sanchez A, Daniels AK, Ewango CEN, Fauset S, Mukinzi JM, Sheil, D., Sonké, B., Sullivan, M.J.P., Sunderland, T.C.H., Taedoumg, H., Thomas, S.C., White, L.J.T., Abernethy, K.A., Adu-Bredu, S., Amani, C.A., Baker, T.R., Banin, L.F., Baya, F., Begne, S.K., Bennett, A.C., Benedet, F., Bitariho, R., Bocko, Y.E., Boeckx, P., Boundja, P., Brienen, R.J.W., Brncic, T., Chezeaux, E., Chuyong, G.B., Clark, C.J., Collins, M., Comiskey, J.A., Coomes, D.A., Dargie, G.C., de Haulleville, T., Kamdem, M.N.D., Doucet, J.-L., Esquivel-Muelbert, A., Feldpausch, T.R., Fofanah, A., Foli, E.G., Gilpin, M., Gloor, E., Gonmadje, C., Gourlet-Fleury, S., Hall, J.S., Hamilton, A.C., Harris, D.J., Hart, T.B., Hockemba, M.B.N., Hladik, A., Ifo, S.A., Jeffery, K.J., Jucker, T., Yakusu, E.K., Kearsley, E., Kenfack, D., Koch, A., Leal, M.E., Levesley, A., Lindsell, J.A., Lisingo, J., Lopez-Gonzalez, G., Lovett, J.C., Makana, J.-R., Malhi, Y., Marshall, A.R., Martin, J., Martin, E.H., Mbayu, F.M., Medjibe, V.P., Mihindou, V., Mitchard, E.T.A., Moore, S., Munishi, P.K.T., Bengone, N.N., Ojo, L., Ondo, F.E., Peh, K.S.-H., Pickavance, G.C., Poulsen, A.D., Poulsen, J.R., Qie, L., Reitsma, J., Rovero, F., Swaine, M.D., Talbot, J., Taplin, J., Taylor, D.M., Thomas, D.W., Toirambe, B., Mukendi, J.T., Tuagben, D., Umunay, P.M., van der Heijden, G.M.F., Verbeeck, H., Vleminckx, J., Willcock, S., Wöll, H., Woods, J.T., Zemagho, L. 2020. Asynchronous carbon sink saturation in African and Amazonian tropical forests. *Nature* **579**: 80–87.

Imani G, Boyemba F, Lewis S, Nabahungu NL, Calders K, Zapfack L, Riera B, Balegamire C, Cuni-Sanchez A. **2017**. Height-diameter allometry and above ground biomass in tropical montane forests: Insights from the Albertine Rift in Africa. *PLOS ONE* **12**: e0179653.

IPCC. **2019**. *Climate Change and Land: an IPCC special report* ((eds.) P.R. Shukla, J. Skea, E. Calvo Buendia, V. Masson-Delmotte, H.-O. Pörtner, D. C. Roberts, P. Zhai, R. Slade, S. Connors, R. van Diemen, M. Ferrat, E. Haughey, S. Luz, S. Neogi, M. Pathak, J. Petzold, J. Portugal Pereira, P. Vyas, E. Huntley, K. Kissick, M, Ed.).

IUSS Working Group WRB. **2015**. World Reference Base for Soil Resources 2014, update 2015 International soil classification system for naming soils and creating legends for soil maps. World Soil Resources Reports No. 106.

Jackson, R B, Mooney H A, Schulze, E D. **1997**. A global budget for fine root biomass, surface area, and nutrient contents. *Proceedings of the National Academy of Sciences* **94**: 7362–7366.

James G, Witten D, Hastie T, Tibishirani R. **2013**. *An Introduction to Statistical Learning with Applications in R*. New York, USA: Springer New York.

Jiang Z, Liu H, Wang H, Peng J, Meersmans J, Green SM, Quine TA, Wu X, Song Z. **2020**. Bedrock geochemistry influences vegetation growth by regulating the regolith water holding capacity. *Nature Communications* **11**: 2392.

Jobbágy EG, Jackson RB. **2004**. The uplift of soil nutrients by plants: biogeochemical consequences across scales. *Ecology* **85**: 2380–2389.

Jolliffe IT. **1995**. Rotation of principal components: choice of normalization constraints Rotation of principal components: choice of normalization constraints. *Journal of Applied statistics* **22**: 29–35.

Jucker T, Bongalov B, Burslem DFRP, Nilus R, Dalponte M, Lewis SL, Phillips OL, Qie L, Coomes DA. **2018**. Topography shapes the structure, composition and function of tropical forest landscapes. *Ecology Letters* **21**: 989–1000.

Kaiser HF. **1958**. The varimax criterion for analytic rotation in factor analysis. *Psychometrika* **23**: 187–200.

Kalks F, Noren G, Mueller CW, Helfrich M, Rethemeyer J, Don A. **2021**. Geogenic organic carbon in terrestrial sediments and its contribution to total soil carbon. *SOIL* **7**: 347–362.

Kaspari M, Garcia MN, Harms KE, Santana M, Wright SJ, Yavitt JB. **2008**. Multiple nutrients limit litterfall and decomposition in a tropical forest. *Ecology Letters* **11**: 35–43.

Kassambara A. **2021**. rstatix: Pipe-friendly framework for basic statistical tests. https://cran.r-project.org/web/packages/rstatix/index.html.

Kearsley E, De Haulleville T, Hufkens K, Kidimbu A, Toirambe B, Baert G, Huygens D, Kebede Y, Defourny P, Bogaert J, Beeckman, H., Steppe, K., Boeckx, P., Verbeeck, H. 2013. Conventional tree height-diameter relationships significantly overestimate aboveground carbon stocks in the Central Congo Basin. *Nature Communications* **4**: 8.

Khomo L, Trumbore SE, Bern CR, Chadwick OA. **2017**. Timescales of carbon turnover in soils with mixed crystalline mineralogies. *SOIL* **3**: 17–30.

Kidinda LK, Olagoke FK, Vogel C, Bukombe B, Kalbitz K, Doetterl S. **2022**. Microbial properties in tropical montane forest soils developed from contrasting parent material—An incubation experiment. *Journal of Plant Nutrition and Soil Science* **n/a**.

King DA, Davies SJ, Tan S, Noor NSMd. **2006**. The role of wood density and stem support costs in the growth and mortality of tropical trees. *Journal of Ecology* **94**: 670–680.

Kirsten M, Mikutta R, Kimaro DN, Feger K-H, Kalbitz K. **2021a**. Aluminous clay and pedogenic Fe oxides modulate aggregation and related carbon contents in soils of the humid tropics. *SOIL* **7**: 363–375.

Kirsten M, Mikutta R, Vogel C, Thompson A, Mueller CW, Kimaro DN, Bergsma HLT, Feger K-H, Kalbitz K. **2021b**. Iron oxides and aluminous clays selectively control soil carbon storage and stability in the humid tropics. *Scientific Reports* **11**: 5076.

Kleber M, Bourg IC, Coward EK, Hansel CM, Myneni SCB, Nunan N. **2021**. Dynamic interactions at the mineral–organic matter interface. *Nature Reviews Earth & Environment* **2**: 402–421.

Kleber M, Mikutta R, Torn MS, Jahn R. **2005**. Poorly crystalline mineral phases protect organic matter in acid subsoil horizons. *European Journal of Soil Science* **56**: 717–725.

Knapp AK, Smith MD. **2001**. Variation among biomes in temporal dynamics of aboveground primary production. *Science* **291**: 481–484.

Köchy M, Hiederer R, Freibauer A. **2015**. Global distribution of soil organic carbon – Part 1: Masses and frequency distributions of SOC stocks for the tropics, permafrost regions, wetlands, and the world. *Soil* **1**: 351–365.

Kramer MG, Chadwick OA. **2018**. Climate-driven thresholds in reactive mineral retention of soil carbon at the global scale. *Nature Climate Change* **8**: 1104–1108.

Krishna MP, Mohan M. **2017**. Litter decomposition in forest ecosystems: a review. *Energy, Ecology and Environment* **2**: 236–249.

Kunito T, Akagi Y, Park HD, Toda H. **2009**. Influences of nitrogen and phosphorus addition on polyphenol oxidase activity in a forested Andisol. *European Journal of Forest Research* **128**: 361–366.

Kwon H-Y, Mueller S, Dunn JB, Wander MM. **2013**. Modeling state-level soil carbon emission factors under various scenarios for direct land use change associated with United States biofuel feedstock production. *Biomass and Bioenergy* **55**: 299–310.

Legendre P, Borcard D, Peres-Neto PR. **2005**. Analyzing beta diversity: Partitioning the spatial variation of community composition data. *Ecological Monographs* **75**: 435–450.

Lewis SL, Edwards DP, Galbraith D. **2015**. Increasing human dominance of tropical forests. *Science*. **349**: 827–832.

Lewis SL, Lopez-Gonzalez G, Sonké B, Affum-Baffoe K, Baker TR, Ojo LO, Phillips OL, Reitsma JM, White L, Comiskey JA, Ewango, C.E.N., Feldpausch, T.R., Hamilton, A.C., Gloor, M., Hart, T., Hladik, A., Lloyd, J., Lovett, J.C., Makana, J.-R., Malhi, Y., Mbago, F.M., Ndangalasi, H.J., Peacock, J., Peh, K.S.-H., Sheil, D., Sunderland, T., Swaine, M.D., Taplin, J., Taylor, D., Thomas, S.C., Votere, R., Wöll, H. 2009. Increasing carbon storage in intact African tropical forests. *Nature* **457**: 1003–1006.

Lewis SL, Sonké B, Sunderland T, Begne SK, Lopez-Gonzalez G, van der Heijden GMF, Phillips OL, Affum-Baffoe K, Baker TR, Banin L, Bastin, J.-F., Beeckman, H., Boeckx, P., Bogaert, J., De Cannière, C., Chezeaux, E., Clark, C.J., Collins, M., Djagbletey, G., Djuikouo, M.N.K., Droissart, V., Doucet, J.-L., Ewango, C.E.N., Fauset, S., Feldpausch, T.R., Foli, E.G., Gillet, J.-F., Hamilton, A.C., Harris, D.J., Hart, T.B., de Haulleville, T., Hladik, A., Hufkens, K., Huygens, D., Jeanmart, P., Jeffery, K.J., Kearsley, E., Leal, M.E., Lloyd, J., Lovett, J.C., Makana, J.-R., Malhi, Y., Marshall, A.R., Ojo, L., Peh, K.S.-H., Pickavance, G., Poulsen, J.R., Reitsma, J.M., Sheil, D., Simo, M., Steppe, K., Taedoumg, H.E., Talbot, J., Taplin, J.R.D., Taylor, D., Thomas, S.C., Toirambe, B., Verbeeck, H., Vleminckx, J., White, L.J.T., Willcock, S., Woell, H., Zemagho, L. 2013. Above-ground biomass and structure of 260 African tropical forests. *Philosophical Transactions of the Royal Society B: Biological Sciences* **368**: 20120295.

Linn DM, Doran JW. **1984**. Effect of water-filled pore space on carbon dioxide and nitrous oxide production in tilled and nontilled soils. *Soil Science Society of America Journal* **48**: 1267–1272.

Liu L, Gundersen P, Zhang W, Zhang T, Chen H, Mo J. **2015**. Effects of nitrogen and phosphorus additions on soil microbial biomass and community structure in two reforested tropical forests. *Scientific Reports* **5**.

Lobo E, Dalling JW. **2013**. Effects of topography, soil type and forest age on the frequency and size distribution of canopy gap disturbances in a tropical forest. *Biogeosciences* **10**: 6769–6781.

van Loon MP, Schieving F, Rietkerk M, Dekker SC, Sterck F, Anten NPR. **2014**. How light competition between plants affects their response to climate change. *New Phytologist* **203**: 1253–1265.

Lowatschek P. **2021**. Decay rates of fine roots in tropical forest soils and temperature dependency of the tea bag decomposition method.

Lukac M. **2012**. Fine root turnover- measuring roots: an updated approach. In: Mancuso S, ed. Berlin, Heidelberg: Springer Berlin Heidelberg, 363–373.

Luo Z, Feng W, Luo Y, Baldock J, Wang E. **2017**. Soil organic carbon dynamics jointly controlled by climate, carbon inputs, soil properties and soil carbon fractions. *Global Change Biology* **23**: 4430–4439.

Luo Z, Wang G, Wang E. **2019**. Global subsoil organic carbon turnover times dominantly controlled by soil properties rather than climate. *Nature Communications* **10**: 1–10.

Ma H, Mo L, Crowther TW, Maynard DS, van den Hoogen J, Stocker BD, Terrer C, Zohner CM. **2021**. The global distribution and environmental drivers of aboveground versus belowground plant biomass. *Nature Ecology & Evolution* **5**: 1110–1122.

Malhi Y, Adu-Bredu S, Asare RA, Lewis SL, Mayaux P. **2013**. African rainforests: past, present and future. *Philosophical Transactions of the Royal Society B: Biological Sciences* **368**.

Malhi Y, Baker TR, Phillips OL, Almeida S, Alvarez E, Arroyo L, Chave J, Czimczik CI, Fiore AD, Higuchi N, Killeen, T.J., Laurance, S.G., Laurance, W.F., Lewis, S.L., Montoya, L.M.M., Monteagudo, A., Neill, D.A., Vargas, P.N., Patiño, S., Pitman, N.C.A., Quesada, C.A., Salomão, R., Silva, J.N.M., Lezama, A.T., Martínez, R.V., Terborgh, J., Vinceti, B., Lloyd, J. 2004. The above-ground coarse wood productivity of 104 Neotropical forest plots. *Global Change Biology* **10**: 563–591.

Malhi Y, Girardin CAJ, Goldsmith GR, Doughty CE, Salinas N, Metcalfe DB, Huaraca Huasco W, Silva-Espejo JE, del Aguilla-Pasquell J, Farfán Amézquita F, Aragão, L.E.O.C., Guerrieri, R., Ishida, F.Y., Bahar, N.H.A., Farfan-Rios, W., Phillips, O.L., Meir, P., Silman, M. 2017. The variation of productivity and its allocation along a tropical elevation gradient: a whole carbon budget perspective. *New Phytologist* **214**: 1019–1032.

Martin AR, Thomas SC. **2011**. A reassessment of carbon content in tropical trees. *PLOS ONE* **6**.

Massmann A, Cavaleri MA, Oberbauer SF, Olivas PC, Porder S. **2022**. Foliar stoichiometry is marginally sensitive to soil phosphorus across a lowland tropical rainforest. *Ecosystems* **25**: 61–74.

McCormack ML, Dickie IA, Eissenstat DM, Fahey TJ, Fernandez CW, Guo D, Helmisaari H-S, Hobbie EA, Iversen CM, Jackson RB, *et al.* 2015. Redefining fine roots improves understanding of below-ground contributions to terrestrial biosphere processes. *New Phytologist* **207**: 505–518.

Mokany K, Raison RJ, Prokushkin AS. **2006**. Critical analysis of root: shoot ratios in terrestrial biomes. *Global Change Biology* **12**: 84–96.

Montgomery DR. **2007**. Soil erosion and agricultural sustainability. *Proceedings of the National Academy of Sciences* **104**: 13268–13272.

Moore S, Adu-Bredu S, Duah-Gyamfi A, Addo-Danso SD, Ibrahim F, Mbou AT, de Grandcourt A, Valentini R, Nicolini G, Djagbletey G, Owusu-Afriyie, K., Gvozdevaite, A., Oliveras, I., Ruiz-Jaen, M.C., Malhi, Y. 2017. Forest biomass, productivity and carbon cycling along a rainfall gradient in West Africa. *Global Change Biology* **24**: 496–510.

Morris EK, Caruso T, Buscot F, Fischer M, Hancock C, Maier TS, Meiners T, Müller C, Obermaier E, Prati D, Socher, S.A., Sonnemann, I., Wäschke, N., Wubet, T., Wurst, S., Rillig, M.C. 2014. Choosing and using diversity indices: insights for ecological applications from the German Biodiversity Exploratories. *Ecology and Evolution* **4**: 3514–3524.

Moser G, Leuschner C, Hertel D, Graefe S, Soethe N, Iost S. **2011**. Elevation effects on the carbon budget of tropical mountain forests (S Ecuador): the role of the belowground compartment. *Global Change Biology* **17**: 2211–2226.

Nadeu E, Quiñonero-Rubio JM, de Vente J, Boix-Fayos C. **2015**. The influence of catchment morphology, lithology and land use on soil organic carbon export in a Mediterranean mountain region. *CATENA* **126**: 117–125.

Nagy RC, Porder S, Brando P, Davidson EA, Figueira AM e S, Neill C, Riskin S, Trumbore S. **2018**. Soil carbon dynamics in soybean cropland and forests in mato grosso, brazil. *Journal of Geophysical Research: Biogeosciences* **123**: 18–31.

Nakagawa S, Johnson PCD, Schielzeth H. **2017**. The coefficient of determination R^2 and intra-class correlation coefficient from generalized linear mixed-effects models revisited and expanded. *Journal of The Royal Society Interface* **14**.

Nakagawa S, Schielzeth H. **2013**. A general and simple method for obtaining R^2 from generalized linear mixed-effects models. *Methods in Ecology and Evolution* **4**: 133–142.

Ngongo ML, Van Ranst E, Baert G, Kasongo EL, Verdoodt A, Mujinya BB, Mukalay JM. **2009**. *Guide des Sols en R.D. Congo. Tome 1: Etude et Gestion*. Ecole Technique Salama-Don Bosco.

Norby RJ, Gu L, Haworth IC, Jensen AM, Turner BL, Walker AP, Warren JM, Weston DJ, Xu C, Winter K. **2017**. Informing models through empirical relationships between foliar phosphorus, nitrogen and photosynthesis across diverse woody species in tropical forests of Panama. *New Phytologist* **215**: 1425–1437.

Nyirambangutse B, Zibera E, Uwizeye FK, Nsabimana D, Bizuru E, Pleijel H, Uddling J, Wallin G. **2017**. Carbon stocks and dynamics at different successional stages in an Afromontane tropical forest. *Biogeosciences* **14**: 1285–1303.

Oksanen J. **2007**. vegan: Community ecology package. R package version 1.8-5. *https://cran.r-project.org/web/packages/vegan/index.html*.

Ollinger S V. **2011**. Sources of variability in canopy reflectance and the convergent properties of plants. *New Phytologist* **189**: 375–394.

Ostonen I, Lõhmus K, Pajuste K. **2005**. Fine root biomass, production and its proportion of NPP in a fertile middle-aged Norway spruce forest: Comparison of soil core and ingrowth core methods. *Forest Ecology and Management* **212**: 264–277.

Paoli GD. **2006**. Divergent leaf traits among congeneric tropical trees with contrasting habitat associations on Borneo. *Journal of Tropical Ecology* **22**: 397–408.

Paoli GD, Curran LM, Slik JWF. **2008**. Soil nutrients affect spatial patterns of aboveground biomass and emergent tree density in southwestern Borneo. *Oecologia* **155**: 287–299.

Pérez-Harguindeguy N, Díaz S, Garnier E, Lavorel S, Poorter H, Jaureguiberry P, Bret-Harte MS, Cornwell WK, Craine JM, Gurvich DE, Urcelay, C., Veneklaas, E.J., Reich, P.B., Poorter, L., Wright, I.J., Ray, P., Enrico, L., Pausas, J.G., Vos, A.C. de, Buchmann, N., Funes, G., Quétier, F., Hodgson, J.G., Thompson, K., Morgan, H.D., Steege, H. ter, Sack, L., Blonder, B., Poschlod, P., Vaieretti, M.V., Conti, G., Staver, A.C., Aquino, S., Cornelissen, J.H.C. 2013. New handbook for standardised measurement of plant functional traits worldwide. *Australian Journal of Botany* **61**: 167–234.

Poorter L, Bongers F. **2006**. Leaf traits are good predictors of plant performance across 53 rain forest species. *Ecology* **87**: 1733–1743.

Porder S, Vitousek PM, Chadwick OA, Chamberlain CP, Hilley GE. **2007**. Uplift, Erosion, and Phosphorus Limitation in Terrestrial Ecosystems. *Ecosystems* **10**: 159–171.

Quesada CA, Paz C, Oblitas Mendoza E, Phillips OL, Saiz G, Lloyd J. 2020. Variations in soil chemical and physical properties explain basin-wide Amazon forest soil carbon concentrations. *SOIL* **6**: 53–88.

Quesada CA, Phillips OL, Schwarz M, Czimczik CI, Baker TR, Patiño S, Fyllas NM, Hodnett MG, Herrera R, Almeida S. **2012**. Basin-wide variations in Amazon forest structure and function are mediated by both soils and climate. *Biogeosciences* **9**: 2203–2246.

R Core Team. **2020**. R: A language and environment for statistical computing. *R Foundation for Statistical Computing*. *https://www.r-project.org/*.

Raich JW, Schlesinger WH. **1992**. The global carbon dioxide flux in soil respiration and its relationship to vegetation and climate. *Tellus B* **44**: 81–99.

Rammig A, Lapola DM. **2021**. The declining tropical carbon sink. *Nature Climate Change* **11**: 727–728.

Rasmussen C, Heckman K, Wieder WR, Keiluweit M, Lawrence CR, Berhe AA, Blankinship JC, Crow SE, Druhan JL, Hicks Pries CE, Marin-Spiotta, E., Plante, A.F., Schädel, C., Schimel, J.P., Sierra, C.A., Thompson, A., Wagai, R. 2018. Beyond clay: towards an improved set of variables for predicting soil organic matter content. *Biogeochemistry* **137**: 297–306.

Reich PB, Oleksyn J, Wright IJ. **2009**. Leaf phosphorus influences the photosynthesis-nitrogen relation: a cross-biome analysis of 314 species. *Oecologia* **160**: 207–212.

Reichenbach M, Fiener P, Garland G, Griepentrog M, Six J, Doetterl S. **2021**. The role of geochemistry in organic carbon stabilization against microbial decomposition in tropical rainforest soils. *SOIL* **7**: 453–475.

Réjou-Méchain M, Tanguy A, Piponiot C, Chave J, Hérault B. **2017**. Biomass: an R Package for Estimating Above-Ground Biomass and Its Uncertainty in Tropical Forests. *Methods in Ecology and Evolution* **8**: 1163–1167.

Rey A, Petsikos C, Jarvis PG, Grace J. **2005**. Effect of temperature and moisture on rates of carbon mineralization in a Mediterranean oak forest soil under controlled and field conditions. *European Journal of Soil Science* **56**: 589–599.

Riutta T, Malhi Y, Kho LK, Marthews TR, Huaraca Huasco W, Khoo M, Tan S, Turner E, Reynolds G, Both S, Burslem, D.F.R.P., Teh, Y.A., Vairappan, C.S., Majalap, N., Ewers, R.M. 2018. Logging disturbance shifts net primary productivity and its allocation in Bornean tropical forests. *Global Change Biology* **24**: 2913–2928.

Ross CW, Hanan NP, Prihodko L, Anchang J, Ji W, Yu Q. **2021**. Woody-biomass projections and drivers of change in sub-Saharan Africa. *Nature Climate Change* **11**: 449–455.

Russo SE, Brown P, Tan S, Davies SJ. **2008**. Interspecific demographic trade-offs and soil-related habitat associations of tree species along resource gradients. *Journal of Ecology* **96**: 192–203.

Saatchi SS, Harris NL, Brown S, Lefsky M, Mitchard ETA, Salas W, Zutta BR, Buermann W, Lewis SL, Hagen S, Petrova, S., White, L., Silman, M., Morel, A. 2011. Benchmark map of forest carbon stocks in tropical regions across three continents. *Proceedings of the National Academy of Sciences of the United States of America* **108**: 9899–9904.

Salinas N, Cosio EG, Silman M, Meir P, Nottingham AT, Roman-Cuesta RM, Malhi Y. **2021**. Editorial: Tropical montane forests in a changing environment. *Frontiers in Plant Science* **12**.

Sayer EJ, Heard MS, Grant HK, Marthews TR, Tanner EVJ. **2011**. Soil carbon release enhanced by increased tropical forest litterfall. *Nature Climate Change* **1**: 304–307.

Schimel D, Braswell BH. **2005**. The role of mid-latitude mountains in the carbon cycle: global perspective and a Western US case study. In: Global perspective and a Western US case study. 449–456.

Schimel D, Stephens BB, Fisher JB. **2015**. Effect of increasing CO_2 on the terrestrial carbon cycle. *Proceedings of the National Academy of Sciences of the United States of America*.

Schleuß PM, Heitkamp F, Leuschner C, Fender AC, Jungkunst HF. **2014**. Higher subsoil carbon storage in species-rich than species-poor temperate forests. *Environmental Research Letters* **9**: 11.

Schlüter T. **2006**. *Geological Atlas of Africa: with Notes on Stratigraphy, Tectonics, Economic Geology, Geohazard and Geosites of Each Country*. Berlin: Springer.

Schmidt MWI, Torn MS, Abiven S, Dittmar T, Guggenberger G, Janssens IA, Kleber M, Kögel-Knabner I, Lehmann J, Manning DAC, Nannipieri, P., Rasse, D.P., Weiner, S., Trumbore, S.E. 2011. Persistence of soil organic matter as an ecosystem property. *Nature* **478**: 49–56.

Schuur EAG, Druffel E, Trumbore SE (Eds.). 2016. *Radiocarbon and Climate Change*. Switzerland. Springer International Publishing.

Sha Z, Bai Y, Li R, Lan H, Zhang X, Li J, Liu X, Chang S, Xie Y. **2022**. The global carbon sink potential of terrestrial vegetation can be increased substantially by optimal land management. *Communications Earth & Environment* **3**: 8.

Shapiro SS, Wilk MB. **1965**. An analysis of variance test for normality (complete samples). *Biometrika* **52**: 591–611.

Shi Z, Allison SD, He Y, Levine PA, Hoyt AM, Beem-Miller J, Zhu Q, Wieder WR, Trumbore S, Randerson JT. **2020**. The age distribution of global soil carbon inferred from radiocarbon measurements. *Nature Geoscience* **13**: 555–559.

Six J, Conant RT, Paul EA, Paustian K. **2002**. Stabilization mechanisms of soil organic matter: Implications for C-saturation of soils. *Plant and Soil* **241**: 155–176.

Skopp J, Jawson MD, Doran JW. **1990**. Steady-state aerobic microbial activity as a function of soil water content. *Soil Science Society of America Journal* **54**: 1619–1625.

Spawn SA, Sullivan CC, Lark TJ, Gibbs HK. **2020**. Harmonized global maps of above and belowground biomass carbon density in the year 2010. *Scientific Data* **7**: 112.

ter Steege H, Pitman NCA, Phillips OL, Chave J, Sabatier D, Duque A, Molino J-F, Prévost M-F, Spichiger R, Castellanos H, von Hildebrand, P., Vásquez, R., 2006. Continental-scale patterns of canopy tree composition and function across Amazonia. *Nature* **443**: 444–447.

Steinhof A, Altenburg M, Machts H. **2017**. Sample preparation at the Jena 14C laboratory. *radiocarbon* **59**: 3.

Stephenson NL, van Mantgem PJ. **2005**. Forest turnover rates follow global and regional patterns of productivity. *Ecology letters* **8**: 524–531.

Stuiver M, Polach HA. **1977**. Reporting of 14C data. *Radiocarbon* **19**: 355–363.

Sullivan BW, Alvarez-Clare S, Castle SC, Porder S, Reed SC, Schreeg L, Townsend AR, Cleveland CC. **2014**. Assessing nutrient limitation in complex forested ecosystems: alternatives to large-scale fertilization experiments. *Ecology* **95**: 668–681.

Tamhane AC. **1979**. A comparison of procedures for multiple comparisons of means with unequal variances. *Journal of the American Statistical Association* **74**: 471–480.

Tang J, Riley WJ. **2015**. Weaker soil carbon–climate feedbacks resulting from microbial and abiotic interactions. *Nature Climate Change* **5**: 56–60.

Tchatchou B, Sonwa DJ, Ifo S, Tiani AM. **2015**. Deforestation and forest degradation in the Congo Basin: State of knowledge, current causes and perspectives. Center for International Forestry Research (CIFOR). *https://www.cifor.org/knowledge/publication/5894/*.

Thum T, Nabel JEMS, Tsuruta A, Aalto T, Dlugokencky EJ, Liski J, Luijkx IT, Markkanen T, Pongratz J, Yoshida Y, Zaehle, S. 2020. Evaluating two soil carbon models within the global land surface model JSBACH using surface and spaceborne observations of atmospheric CO_2. *Biogeosciences* **17**: 5721–5743.

Tian D, Reich PB, Chen HYH, Xiang Y, Luo Y, Shen Y, Meng C, Han W, Niu S. **2019**. Global changes alter plant multi-element stoichiometric coupling. *New Phytologist* **221**: 807–817.

Tiessen H, Chacon P, Cuevas E. **1994**. Phosphorus and nitrogen status in soils and vegetation along a toposequence of dystrophic rainforests on the upper Rio Negro. *Oecologia* **99**: 145–150.

Todd-Brown KEO, Randerson JT, Hopkins F, Arora V, Hajima T, Jones C, Shevliakova E, Tjiputra J, Volodin E, Wu T, Zhang, Q., Allison, S.D. 2014. Changes in soil organic carbon storage predicted by Earth system models during the 21st century. *Biogeosciences* **11**: 2341–2356.

Todd-Brown KEO, Randerson JT, Post WM, Hoffman FM, Tarnocai C, Schuur EAG, Allison SD. **2013**. Causes of variation in soil carbon simulations from CMIP5 Earth system models and comparison with observations. *Biogeosciences* **10**: 1717–1736.

Tonin AM, Gonçalves JF, Bambi P, Couceiro SRM, Feitoza LAM, Fontana LE, Hamada N, Hepp LU, Lezan-Kowalczuk VG, Leite GFM, Lemes-Silva, A.L., Lisboa, L.K., Loureiro, R.C., Martins, R.T., Medeiros, A.O., Morais, P.B., Moretto, Y., Oliveria, P.C.A., Pereira, E.B., Ferreira, L.P., Pérez, J., Petrucio, M.M., Reis, D.F., S. Rezende, R., Roque, N., Santos, L.E.P., Siegloch, A.E., Tonello, G., Boyero, L. 2017. Plant litter dynamics in the forest-stream interface: precipitation is a major control across tropical biomes. *Scientific Reports* **7**: 10799.

Torres-Sallan G, Schulte RPO, Lanigan GJ, Byrne KA, Reidy B, Simó I, Six J, Creamer RE. **2017**. Clay illuviation provides a long-term sink for C sequestration in subsoils. *Scientific Reports* **7**: 45635.

Traoré S, Thiombiano L, Bationo BA, Kögel-Knabner I, Wiesmeier M. **2020**. Organic carbon fractional distribution and saturation in tropical soils of West African savannas with contrasting mineral composition. *CATENA* **190**: 104550.

Treseder KK. **2004**. A meta-analysis of mycorrhizal responses to nitrogen, phosphorus, and atmospheric CO_2 in field studies. *New Phytologist* **164**: 347–355.

Trumbore S. **2009**. Radiocarbon and soil carbon dynamics. *Annual Review of Earth and Planetary Sciences* **37**: 47–66.

Tyukavina A, Hansen MC, Potapov P, Parker D, Okpa C, Stehman SV, Kommareddy I, Turubanova S. **2018**. Congo Basin forest loss dominated by increasing smallholder clearing. *Science Advances* **4**: eaat2993.

Tyukavina A, Stehman S V., Potapov P V., Turubanova SA, Baccini A, Goetz SJ, Laporte NT, Houghton RA, Hansen MC. **2013**. National-scale estimation of gross forest aboveground carbon loss: A case study of the Democratic Republic of the Congo. *Environmental Research Letters* **8**: 14.

Urbina I, Grau O, Sardans J, Margalef O, Peguero G, Asensio D, LLusià J, Ogaya R, Gargallo-Garriga A, Van Langenhove L, Verryckt, L.T., Courtois, E.A., Stahl, C., Soong, J.L., Chave, J., Hérault, B., Janssens, I.A., Sayer, E., Peñuelas, J. 2021. High foliar K and P resorption efficiencies in old-growth tropical forests growing on nutrient-poor soils. *Ecology and Evolution* **11**: 8969–8982.

Vågen TG, Winowiecki LA. **2019**. Predicting the spatial distribution and severity of soil erosion in the global tropics using satellite remote sensing. *Remote Sensing* **11**: 1–18.

Vallicrosa H, Sardans J, Maspons J, Peñuelas J. **2022a**. Global distribution and drivers of forest biome foliar nitrogen to phosphorus ratios (N:P). *Global Ecology and Biogeography* **31**: 861–871.

Vallicrosa H, Sardans J, Maspons J, Zuccarini P, Fernández-Martínez M, Bauters M, Goll DS, Ciais P, Obersteiner M, Janssens IA, Peñuelas, J. 2022b. Global maps and factors driving forest foliar elemental composition: the importance of evolutionary history. *New Phytologist* **233**: 169–181.

Vieira SA, Alves LF, Duarte-Neto PJ, Martins SC, Veiga LG, Scaranello MA, Picollo MC, Camargo PB, do Carmo JB, Neto ES, Santos, F.A.M., Joly, C.A., Martinelli, L.A. 2011. Stocks of carbon and nitrogen and partitioning between above- and belowground pools in the Brazilian coastal Atlantic Forest elevation range. *Ecology and evolution* **1**: 421–434.

Vitousek PM. **1984**. Litterfall, nutrient cycling, and nutrient limitation in tropical forests. *Ecology* **65**: 285–298.

Vitousek PM, Chadwick OA. **2013**. Pedogenic thresholds and soil process domains in basalt-derived soils. *Ecosystems* **16**: 1379–1395.

Werner FA, Homeier J. **2015**. Is tropical montane forest heterogeneity promoted by a resource-driven feedback cycle? Evidence from nutrient relations, herbivory and litter decomposition along a topographical gradient. *Functional Ecology* **29**: 430–440.

Whitaker J, Ostle N, McNamara NP, Nottingham AT, Stott AW, Bardgett RD, Salinas N, Ccahuana AJQ, Meir P. **2014**. Microbial carbon mineralization in tropical lowland and montane forest soils of Peru. *Frontiers in Microbiology* **5**: 720.

White LJT, Masudi EB, Ndongo JD, Matondo R, Soudan-Nonault A, Ngomanda A, Averti IS, Ewango CEN, Sonké B, Lewis SL. **2021**. Congo Basin rainforest — invest US$150 million in science. *Nature* **598**: 411–414.

Wieder WR, Cleveland CC, Smith WK, Todd-Brown K. **2015**. Future productivity and carbon storage limited by terrestrial nutrient availability. *Nature Geoscience* **8**: 441–444.

Wilken F, Fiener P, Ketterer M, Meusburger K, Muhindo DI, van Oost K, Doetterl S. **2021**. Assessing soil redistribution of forest and cropland sites in wet tropical Africa using 239+240Pu fallout radionuclides. *SOIL* **7**: 399–414.

Wright SJ, Yavitt JB, Wurzburger N, Turner BI, Tanner EVJ, Sayer EJ, Santiago LS, Kaspari M, Hedin LO, Harms KE, Garcia, M.N., Corre, M.D. 2011. Potassium, phosphorus, or nitrogen limit root allocation, tree growth, or litter production in a lowland tropical forest. *Ecology* **92**: 1616–1625.

Xia S-W, Chen J, Schaefer D, Goodale UM. **2016**. Effect of topography and litterfall input on fine-scale patch consistency of soil chemical properties in a tropical rainforest. *Plant and Soil* **404**: 385–398.

Xu L, Saatchi SS, Shapiro A, Meyer V, Ferraz A, Yang Y, Bastin JF, Banks N, Boeckx P, Verbeeck H, Lewis, S.L., Muanza, E.T., Bongwele, E., Kayembe, F., Mbenza, D., Kalau, L., Mukendi, F., Ilunga, F., Ebuta, D. 2017. Spatial distribution of carbon stored in forests of the Democratic Republic of Congo. *Scientific Reports* **7**: 1–12.

Yoo K, Mudd SM. **2008**. Discrepancy between mineral residence time and soil age: Implications for the interpretation of chemical weathering rates. *GEOLOGY* **36**: 35–38.

Yuan ZY, Chen HYH. **2013**. Simplifying the decision matrix for estimating fine root production by the sequential soil coring approach. *Acta Oecologica* **48**: 54–61.

Yude P, A. BR, Jingyun F, Richard H, E. KP, A. KW, L. PO, Anatoly S, L. LS, G. CJ, *et al.* 2011. A Large and Persistent Carbon Sink in the World's Forests. *Science* **333**: 988–993.

Zanne AE, Coomes D, Jansen S, Lewis SL, Swenson NG, Chave J. **2009**. Towards a worldwide wood economics spectrum. *Ecology Letters* **12**: 351–366.

Zhu J, Hu H, Tao S, Chi X, Li P, Jiang L, Ji C, Zhu J, Tang Z, Pan Y, *et al.* 2017. Carbon stocks and changes of dead organic matter in China's forests. *Nature Communications* **8**: 151.

Appendices

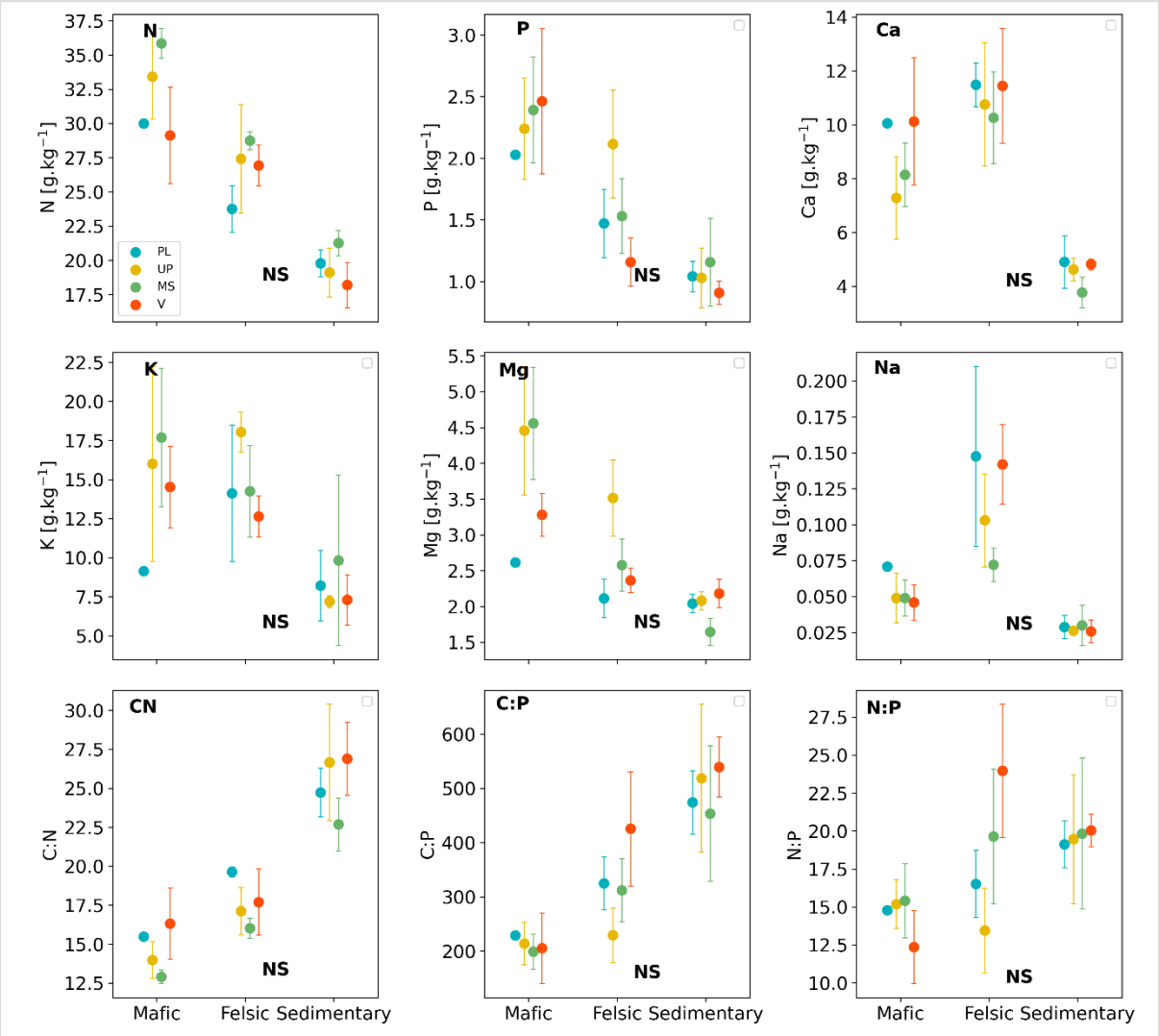

Figure S2.1: Distribution of the investigated canopy chemistry along topographic positions for the three geochemical regions.

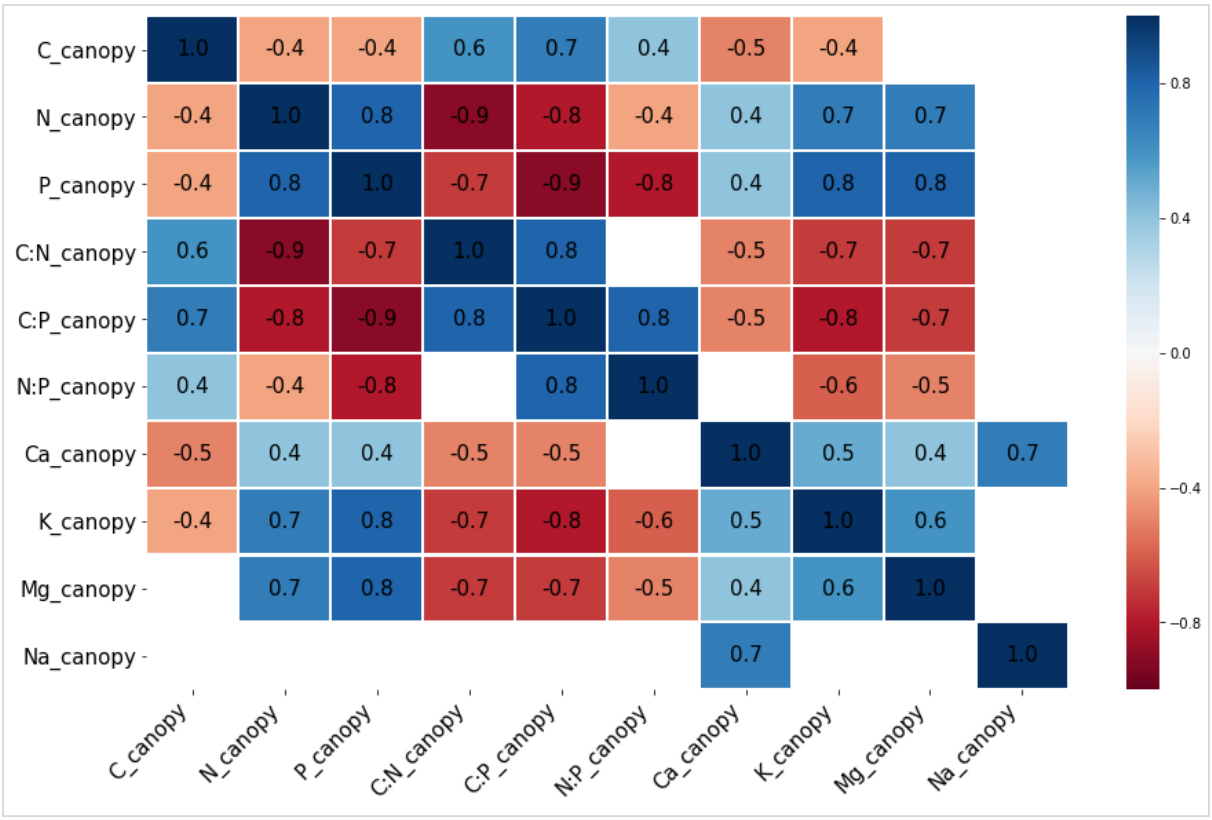

Figure S2.2. Pearson correlations between canopy chemistry (leaf carbon, leaf nitrogen content, leaf phosphorus content, leaf C:N ratio, leaf NP ratio, leaf CP ratio, leaf calcium content, leaf potassium, leaf magnesium content, and leaf sodium content). Blank cells indicate non-significant correlations, p-value ≤ 0.05.

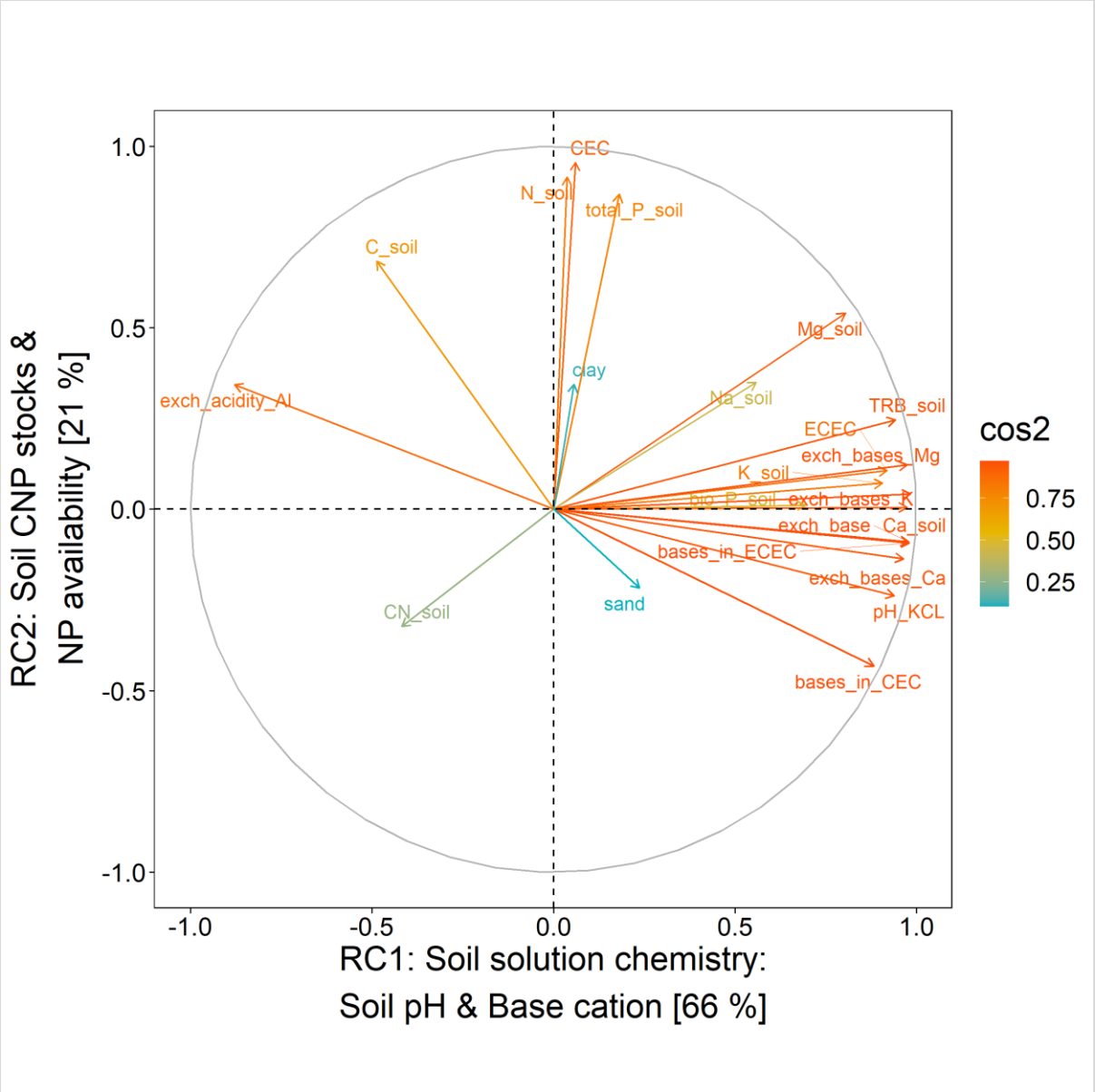

Figure S2.3: Biplot showing correlation between independent variables. Positively correlated variables are grouped together. Negatively correlated variables are positioned in the opposite quadrants. The distance between a variable and the center indicates the representation of that variable on the factor map. Variables that are far from the center are well represented on the factor map.

Table S2.1. Community weighted (mean± sd, n=10,12,12 for mafic, felsic, and sedimentary region respectively) concentrations of major nutrients in the canopy along topographic positions (PL: Plateau, UP: Upper slope, MS: Midslope, V: Valley) for the three investigated geochemical regions. From left to right: Leaf carbon content, leaf nitrogen content, leaf phosphorus content, leaf carbon to nitrogen ratio, leaf carbon to phosphorus ratio, leaf nitrogen to phosphorus ratio, leaf calcium content, leaf potassium content, leaf magnesium content, and leaf sodium content. The weighting factor is the proportion of community basal area to the total basal area of the plot.

Region	Slope	C[g.kg^{-1}]	N[g.kg^{-1}]	P[g.kg^{-1}]	C:N	C:P	N:P	Ca[g.kg^{-1}]	K[g.kg^{-1}]	Mg[g.kg^{-1}]	Na[g.kg^{-1}]
Mafic	PL	464.32±0 (a)	30±0 (a)	2.03±0 (a)	15.48±0 (a)	228.88±0 (a)	14.8±0 (a)	10.06±0 (a)	9.15±0 (a)	2.62±0 (a)	0.07±0 (a)
	UP	464.01±6.57 (a)	33.43±3.79 (a)	2.24±0.51 (a)	13.99±1.45 (a)	214.11±47.76 (a)	15.2±2 (a)	7.28±1.88 (a)	16±7.64 (a)	4.46±1.1 (a)	0.05±0.02 (a)
	MS	462.48±2.5 (a)	35.86±1.33 (a)	2.39±0.53 (a)	12.91±0.54 (a)	199.12±39.62 (a)	15.4±3 (a)	8.15±1.45 (a)	17.7±5.41 (a)	4.56±0.96 (a)	0.05±0.02 (a)
	V	467.56±15.5 (a)	29.13±4.3 (a)	2.46±0.72 (a)	16.32±2.8 (a)	205.41±79.8 (a)	12.4±2.9 (a)	10.13±2.89 (a)	14.53±3.19 (a)	3.28±0.37 (a)	0.05±0.02 (a)
Felsic	PL	466.51±40.87 (a)	23.76±2.09 (a)	1.47±0.34 (a)	19.64±0.39 (a)	325.11±59.49 (a)	16.5±2.7 (a)	11.49±1 (a)	14.12±5.34 (a)	2.12±0.33 (a)	0.15±0.08 (a)
	UP	463.42±27.12 (a)	27.43±4.87 (a)	2.12±0.54 (a)	17.12±1.86 (a)	229.34±61.67 (a)	13.5±3.4 (a)	10.76±2.8 (a)	18.04±1.58 (a)	3.52±0.65 (a)	0.1±0.04 (a)
	MS	460.21±9.5 (a)	28.75±0.79 (a)	1.53±0.37 (a)	16.02±0.77 (a)	312.13±71.5 (a)	19.7±5.4 (a)	10.27±2.09 (a)	14.25±3.59 (a)	2.58±0.45 (a)	0.07±0.01 (a)
	V	474.5±52 (a)	26.94±1.84 (a)	1.16±0.24 (a)	17.7±2.6 (a)	425.68±129.04 (a)	24±5.4 (a)	11.45±2.61 (a)	12.63±1.61 (a)	2.37±0.21 (a)	0.14±0.03 (a)
Mixed	PL	487.68±8.32 (a)	19.78±1.22 (a)	1.04±0.15 (a)	24.73±1.9 (a)	474.52±71.23 (a)	19.1±1.9 (a)	4.91±1.2 (a)	8.22±2.76 (a)	2.04±0.16 (a)	0.03±0.01 (a)
	UP	503.48±36.35 (a)	19.12±2.2 (a)	1.03±0.3 (a)	26.66±4.57 (a)	518.83±166.9 (a)	19.5±5.2 (a)	4.63±0.51 (a)	7.2±0.48 (a)	2.08±0.16 (a)	0.03±0 (a)
	MS	480.95±18.16 (a)	21.27±1.13 (a)	1.16±0.44 (a)	22.68±2.09 (a)	453.76±153.01 (a)	19.8±6.1 (a)	3.78±0.7 (a)	9.84±6.68 (a)	1.64±0.23 (a)	0.03±0.02 (a)
	V	485.79±9.08 (a)	18.2±2.03 (a)	0.91±0.12 (a)	26.9±2.87 (a)	539.51±67.58 (a)	20.1±1.3 (a)	4.82±0.25 (a)	7.3±1.96 (a)	2.18±0.24 (a)	0.03±0.01 (a)

Table S2.2. Mixed effect model results showing standardized effects size of geochemical regions (reference: felsic region) and topographic positions (reference: midslope position) as explanatory factors on leaf nitrogen, phosphorus, leaf C:N, leaf CP, leaf NP, leaf calcium, leaf potassium, leaf magnesium, and leaf sodium. The estimated values indicate the mean effects sizes, the 95% confidence intervals (CI) of the estimates, p-values, the marginal $R^{2,}$ and conditional R^2 values as results of mixed-effects models. In the models, geochemical regions and topography positions were set as fixed effects and species as random effects (PL: Plateau, UP: Upper slope, MS: Midslope, V: Valley).

	Independent variables	Estimates	CI	p-value	R^2.adj.m	R^2.adj.c
N_canopy	(Intercept)	2.65	2.42 – 2.89	**<0.001**	0.30	0.70
	region [Mafic]	0.62	0.25 – 0.98	**0.001**		
	region [Mixed]	-0.39	-0.72 – -0.05	0.025		
	slope [PL]	-0.16	-0.33 – 0.01	0.066		
	slope [UP]	-0.12	-0.26 – 0.01	0.076		
	slope [V]	-0.26	-0.41 – -0.11	**0.001**		
P_canopy	(Intercept)	1562.32	1304.71 – 1819.94	**<0.001**	0.30	0.69
	region [Mafic]	552.84	160.94 – 944.73	**0.006**		
	region [Mixed]	-611.47	-978.85 – -244.10	**0.001**		
	slope [PL]	78.37	-115.01 – 271.75	0.427		
	slope [UP]	129.81	-27.40 – 287.02	0.106		
	slope [V]	12.62	-161.66 – 186.91	0.887		
C:N_canopy	(Intercept)	18.89	16.99 – 20.78	**<0.001**	0.32	0.61
	region [Mafic]	-4.1	-6.83 – -1.37	**0.003**		
	region [Mixed]	4.92	2.29 – 7.55	**<0.001**		
	slope [PL]	-0.24	-1.84 – 1.37	0.773		
	slope [UP]	1.2	-0.11 – 2.50	0.073		
	slope [V]	1.47	0.03 – 2.91	0.045		
C:P_canopy	(Intercept)	354.48	304.41 – 404.56	**<0.001**	0.38	0.53
	region [Mafic]	-121.41	-186.77 – -56.05	**<0.001**		
	region [Mixed]	163.02	98.08 – 227.95	**<0.001**		
	slope [PL]	-6.51	-56.15 – 43.13	0.797		
	slope [UP]	2.72	-37.76 – 43.20	0.895		
	slope [V]	27.06	-16.99 – 71.11	0.229		
N:P_canopy	(Intercept)	20.01	17.88 – 22.13	**<0.001**	0.14	0.36
	region [Mafic]	-3.59	-6.37 – -0.80	**0.012**		
	region [Mixed]	2.71	-0.06 – 5.47	0.055		
	slope [PL]	-1.5	-3.59 – 0.58	0.158		
	slope [UP]	-1.54	-3.24 – 0.16	0.076		
	slope [V]	-1.08	-2.93 – 0.77	0.254		

Table S2.2. Mixed effect model results showing standardized effects size of geochemical regions (reference: felsic region) and topographic positions (reference: midslope position) as explanatory factors on leaf nitrogen, phosphorus, leaf C:N, leaf CP, leaf NP, leaf calcium, leaf potassium, leaf magnesium, and leaf sodium. The estimated values indicate the mean effects sizes, the 95% confidence intervals (CI) of the estimates, p-values, the marginal $R^{2,}$ and conditional R^2 values as results of mixed-effects models. In the models, geochemical regions and topography positions were set as fixed effects and species as random effects (PL: Plateau, UP: Upper slope, MS: Midslope, V: Valley).

	Independent variables	Estimates	CI	p-value	R^2.adj.m	R^2.adj.c
Ca_canopy	(Intercept)	10969.84	9416.71 – 12522.98	**<0.001**	0.23	0.35
	region [Mafic]	-3021.18	-4907.23 – -1135.14	**0.002**		
	region [Mixed]	-6481.72	-8380.50 – -4582.94	**<0.001**		
	slope [PL]	-42.94	-1721.78 – 1635.90	0.96		
	slope [UP]	308.29	-1062.79 – 1679.37	0.659		
	slope [V]	1029.83	-445.59 – 2505.26	0.171		
K_canopy	(Intercept)	15613.55	13262.56 – 17964.55	**<0.001**	0.21	0.5
	region [Mafic]	-622.25	-3891.76 – 2647.25	0.709		
	region [Mixed]	-7705.46	-10895.75 – -4515.18	**<0.001**		
	slope [PL]	245.45	-1872.23 – 2363.13	0.82		
	slope [UP]	479	-1245.70 – 2203.70	0.586		
	slope [V]	-849.18	-2742.32 – 1043.96	0.379		
Mg_canopy	(Intercept)	2997.27	2548.51 – 3446.03	**<0.001**	0.25	0.38
	region [Mafic]	1068.8	515.24 – 1622.36	**<0.001**		
	region [Mixed]	-759.17	-1315.17 – -203.16	**0.007**		
	slope [PL]	-328.81	-805.67 – 148.06	0.177		
	slope [UP]	132.37	-256.96 – 521.69	0.505		
	slope [V]	-281.72	-701.73 – 138.29	0.189		
Na_canopy	(Intercept)	105	83.72 – 126.28	**<0.001**	0.23	0.3
	region [Mafic]	-66.31	-90.42 – -42.21	**<0.001**		
	region [Mixed]	-88.19	-112.62 – -63.75	**<0.001**		
	slope [PL]	11.88	-12.69 – 36.45	0.343		
	slope [UP]	12	-8.10 – 32.09	0.242		
	slope [V]	16.37	-5.01 – 37.75	0.133		

Table S2.3. Rotated principal component analysis for four principal components (RC) that were retained with Eigenvalues >1 and proportion variance ≥10 %. The upper part of the table shows eigenvalues, proportional, cumulative variance, and mechanistic interpretation of specific RCs. The bottom part represents loadings. Blank cells indicate that variables are not represented by the corresponding RCs and the loadings of those variables onto the RC are near or equal to zero.

Rotated components	RC1	RC2	RC3
Eigenvalue	12.6	4.0	2.3
Proportion variance (%)	0.6	0.2	0.1
Cumulative variance (%)	0.6	0.8	0.9

Mechanistic interpretation		Soil exchangeable bases & base cation stocks	Soil NP & nutrient exchange	Soil texture
Independent variables	Units			
clay	%			0.8
silt	%			-1.0
sand	%	-0.4		0.4
CEC_pot	0.01 me g-1		0.9	
ECEC_pot	0.01 me g-1	0.9		
pH_KCL		0.9		
exch_Mg	0.01 me g-1	1.0		
exch_Ca	0.01 me g-1	1.0		
exch_K	0.01 me g-1	1.0		
exch_base	0.01 me g-1	1.0		
exch_Al	0.01 me g-1	-0.9		
base_CEC_pot	%	0.9	-0.4	
base_CEC_eff	%	1.0		
total_N	%		1.0	
Bio-P	0.01 me g-1	0.7		
total_Ca	%	1.0		
total_K	%	0.9		
total_Mg	%	0.8	0.6	
total_Na	%	0.6		0.6
TRB	%	0.9		
total_P	%		0.8	

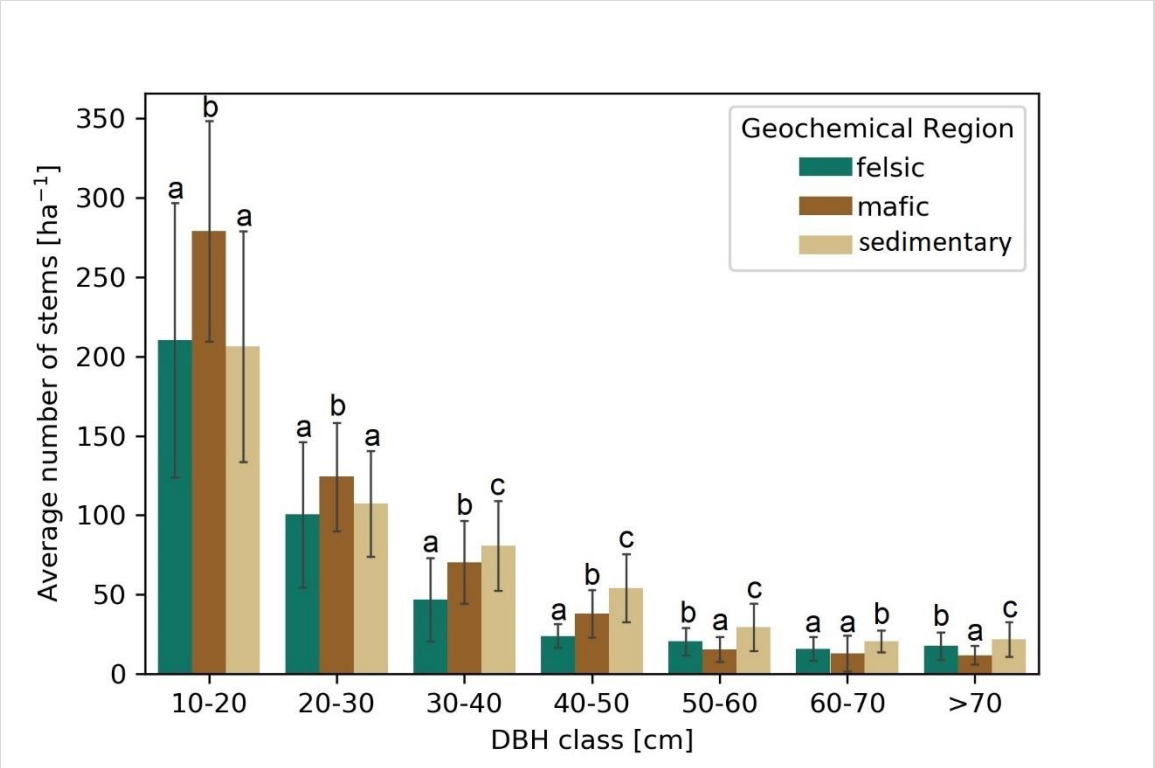

Figure S3.1. Contribution of each diameter class to the total number of trees per unit area. The contribution to the average number of trees per hectare by diameter at breast height for the felsic, mafic and sedimentary geochemical regions. Differences between regions (Mean ± SD; n= 12 per DBH class per region) were assessed separately for each DBH class with letters above bars indicating statistically significant differences, following Kruskal-Wallis tests and pair-wise comparison using Dunn's test (p-value < 0.05). Data taken from Doetterl et al. (2021c).

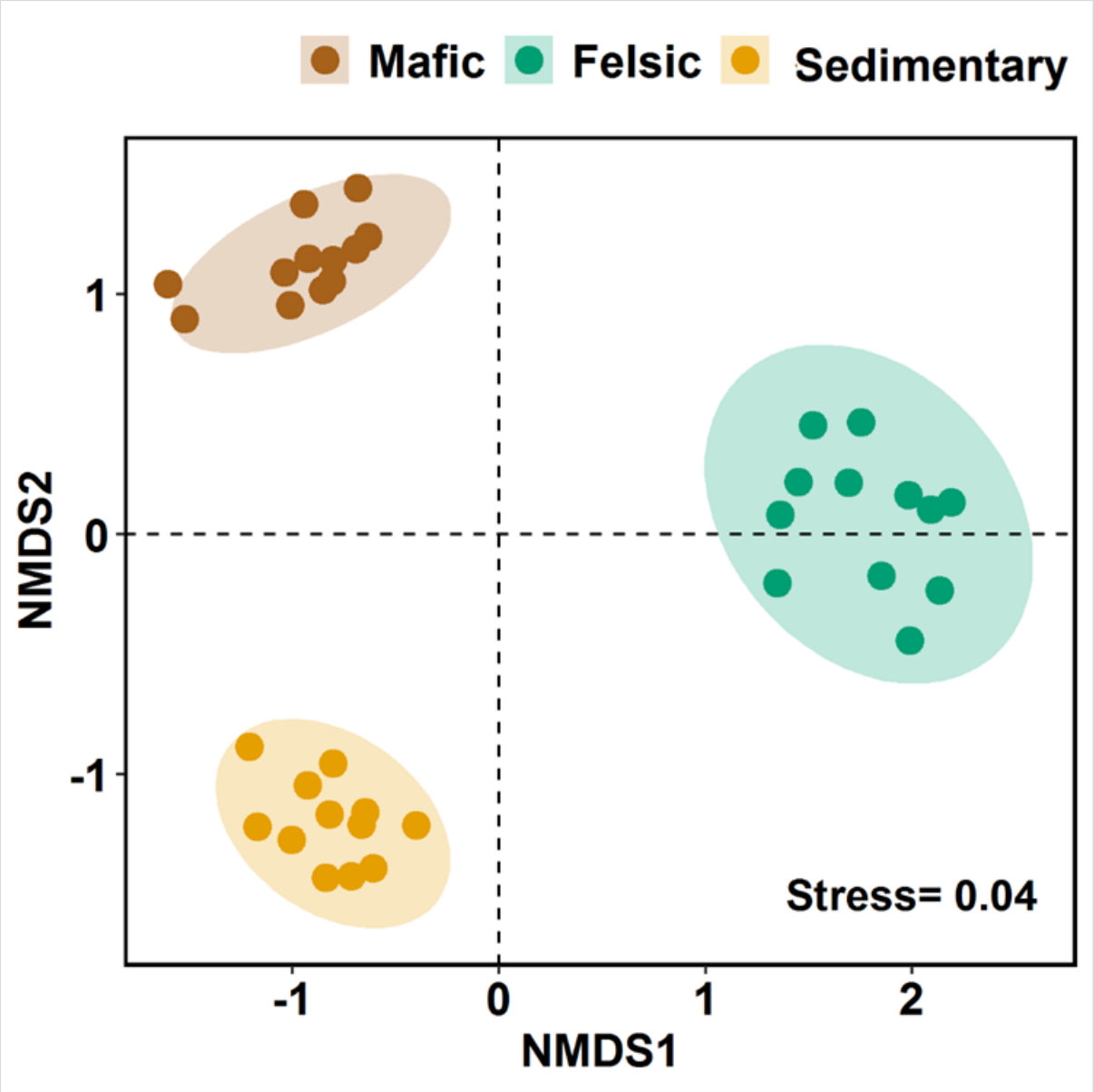

Figure S3.2. Species composition and similarities across geochemical regions. Non-metric multidimensional scaling (NMDS) on the inventory data to assess (dis)similarities and the separation of species composition and abundance for the felsic, mafic and sedimentary geochemical regions n = 12; 12; 12 for mafic, felsic and sedimentary, respectively. Forest tree species abundance of each plot are defined in a two-dimensional space with NMDS1 and 2 representing variables after dimension reduction of data derived from the first forest inventory. Values on X and Y axes are rank-based scores indicating ordination distance (similarity) between points and regions. Points represent plotID(s) and shaded ellipses represent regions. Points that are more similar to one another are ordinated closer together.

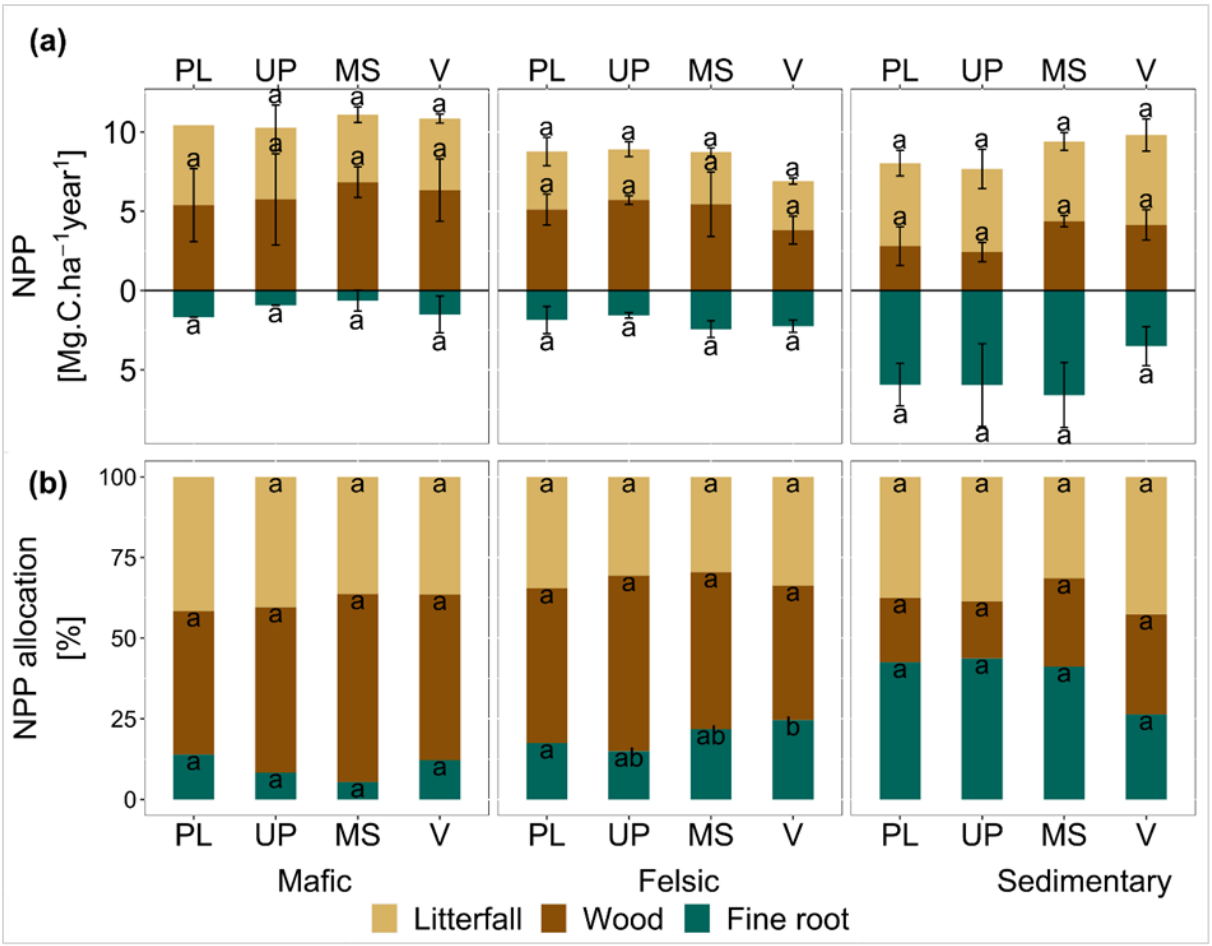

Figure S3.3. NPP and NPP allocation for three components across geochemical regions and along topographic positions (a) NPP of litterfall, wood, and fine roots across the mafic, felsic and sedimentary geochemical regions (mafic, felsic and sedimentary) and along topographic positions (PL: plateau, UP: upper slope, MS: middle slope and V: valley), (b) Relative C allocation for NPP of litterfall, wood and fine roots across the felsic, mafic and sediment geochemical regions and along four topographic positions (mean ± SD). Different letters on top of the stacked bars indicate significant differences in NPP and C allocation between topographic positions following Kruskal-Wallis tests and pair-wise comparison using Dunn's test (p-value ≤ 0.05). Tests were conducted for each component and geochemical region separately.

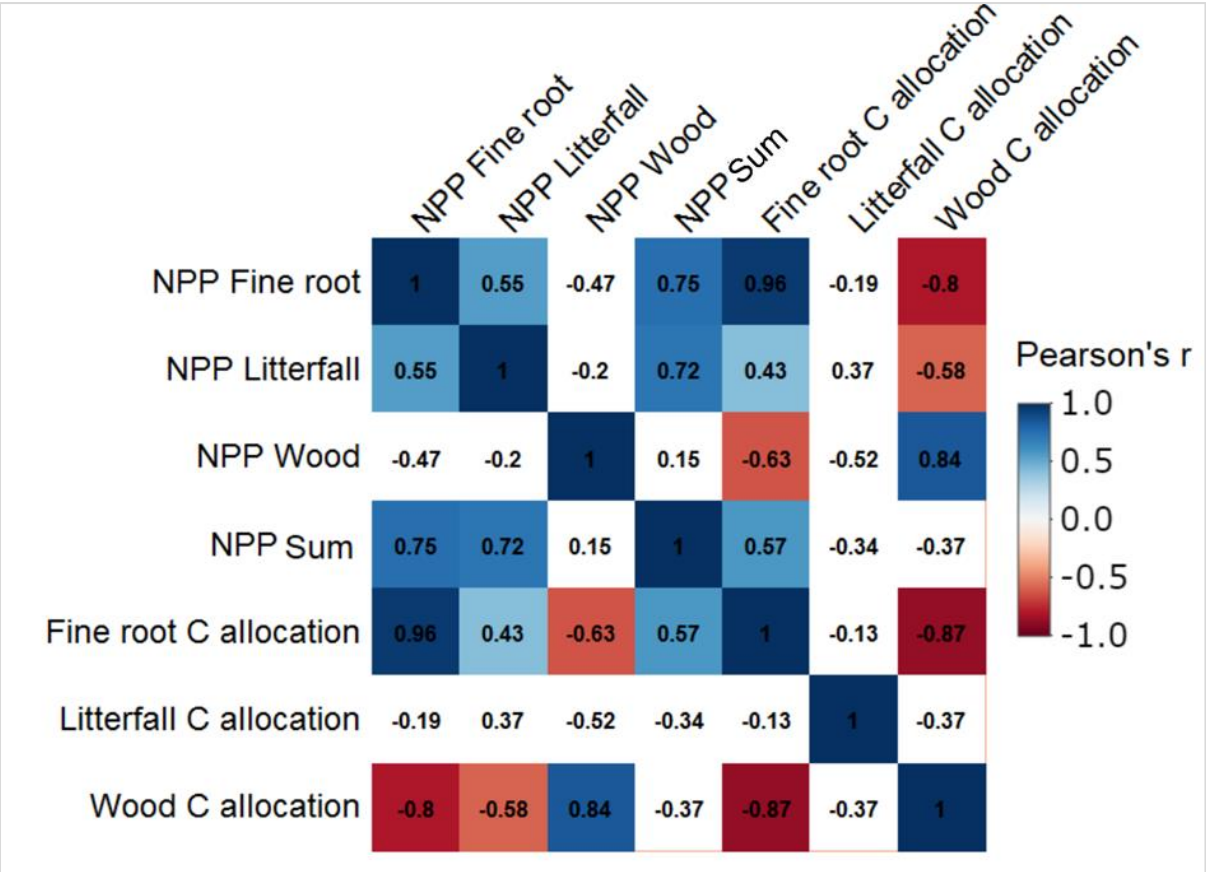

Figure S3.4. Correlations between NPP and NPP allocation. Pearson correlations between NPP components (fine roots, litterfall, wood, and total), and the corresponding relative NPP C allocation used in our analyses as response variables. White cells indicate non-significant correlations, p-value ≤ 0.05.

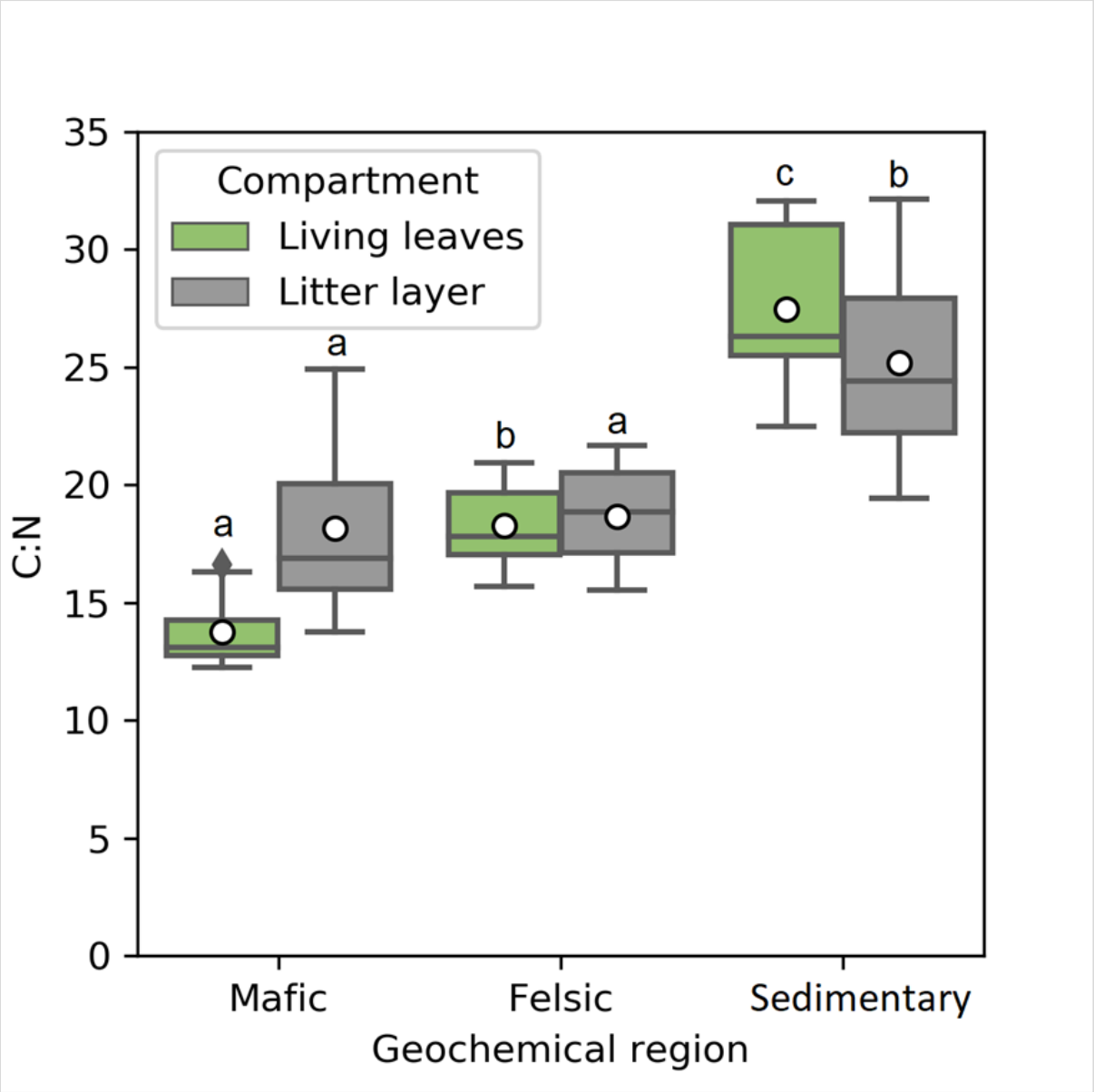

Figure S3.5. C:N ratio of living leaves and litter layer for the three geochemical regions. Plot based community weighted C:N ratio of living canopy leaves and mean C:N ratio of the L horizon litter layer across the three geochemical regions (n=12 per region). Different letters on top of boxplots indicate significant differences in C:N ratio between regions following Kruskal-Wallis tests and pair-wise comparison using Dunn's test (p-value ≤ 0.05). The lower and upper T-shape whiskers indicate the minimum and maximum C:N ratio respectively. The distance between the lower and upper end of the box represents the interquartile range. Horizontal line in the middle of the box represents the median C:N ratio and the white dot represents the mean C:N ratio. The tests were conducted separately for living canopy leaves and the litter layer.

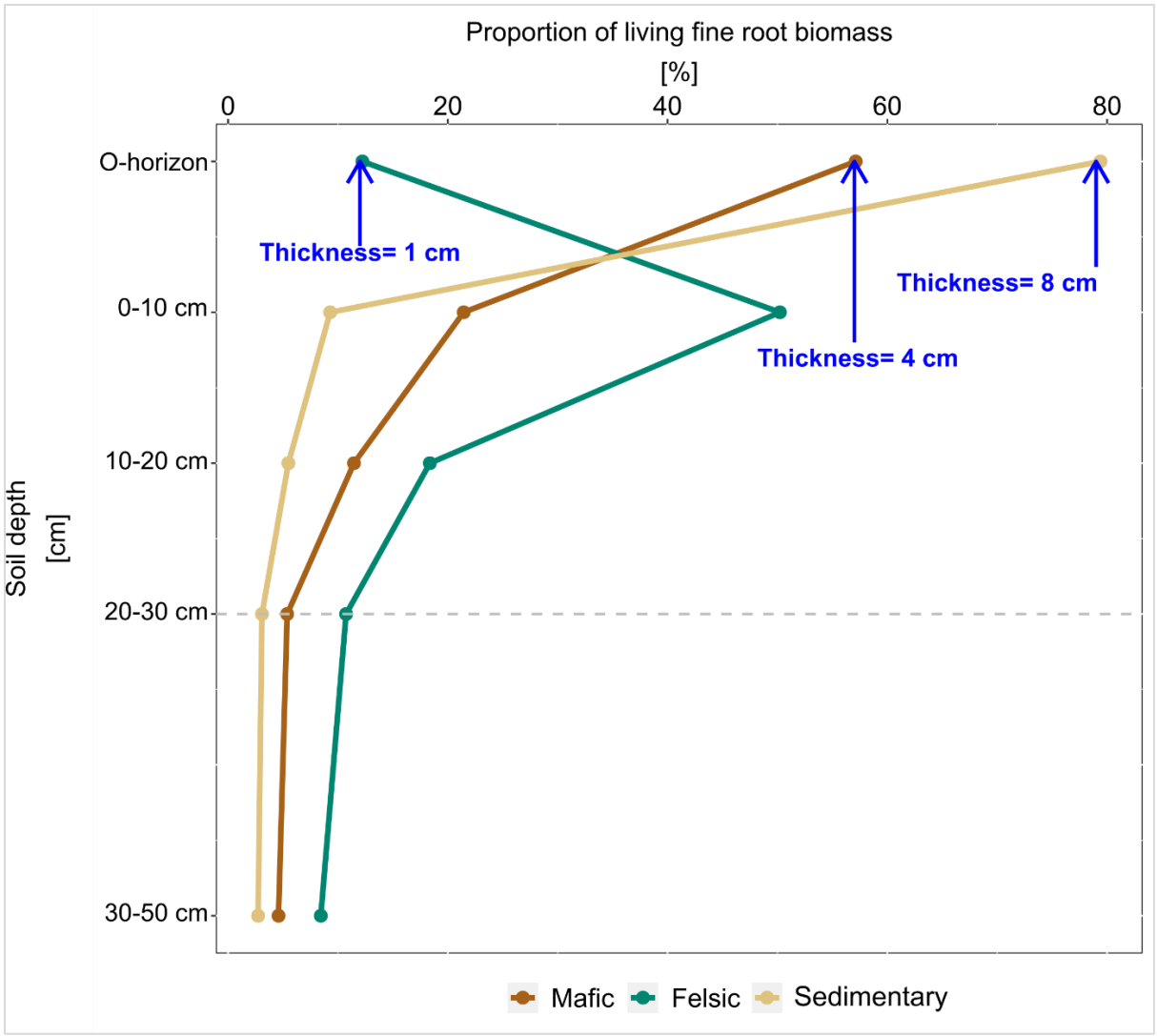

Figure S3.6. Relative root biomass along soil depth for the three geochemical regions. Means of relative root biomass along soil depth for O-horizon and the top 50 cm of mineral soil for the mafic, felsic and sedimentary regions expressed as proportion (%) of total root biomass. The horizontal gray dashed line indicates the cumulative 90 % root biomass in the assessed soil volume as basis for the selected geochemical soil properties used in the analyses. Number of observations aggregated for each point equal n = 8; 12; 12 for mafic, felsic and sedimentary respectively. Data taken from Doetterl *et al.* (2021c). Note that the thickness indicates the average thickness of O-horizon at each site.

Table S3.1. Mineral soil properties of the three geochemical regions. Chemical composition of the top 30 cm of mineral soils layers representing the three geochemical regions. Values presented are mean ± standard deviation (n=129). Mafic (Kahuzi-Biéga forest), felsic (Kibale forest), and sedimentary (Nyungwe forest). Source: Project TropSOC Database Version 1.0 (Doetterl et al., 2021a,c).

Variables	Units	Mafic	Felsic	sedimentary
Clay	%	42.7±11.1	33.0±5.5	32.5±13.9
Sand	(%)	42.4±16.2	55.6±5.2	48.4±17.4
Silt	(%)	13.2±3.2	11.4±2.7	20.2±9.6
pH_{KCL}	-	3.93±0.6	5.3±0.6	3.4±0.4
Total Nitrogen	%	0.4±0.2	0.2±0.1	0.2±0.2
C:N	-	10.3±5.9	12.5±6.3	56.4±70.3
Bio-P	mg kg^{-1}	17.9±28.5	31.2±25.7	5.5±35.9
Bases in CEC	%	16.0±20.5	73.0±18.1	8.8±14.5
CEC	cmol kg^{-1}	38.4±5.5	17.6±4.5	15.3±11.8
Bases in ECEC	%	48.2±23.2	84.3±17.8	8.2±15.2
ECEC	cmol kg^{-1}	12.1±4.1	14.4±4.7	7.1±3.1
Exchangeable Mg^{2+}	cmol kg^{-1}	1.9±0.9	2.3±0.8	0.2±0.6
Exchangeable Ca^{2+}	cmol kg^{-1}	5.1±4.2	11.2±4.4	0.4±2.3
Exchangeable K^{+}	cmol kg^{-1}	0.3±0.2	0.5±0.1	0.1±0.1
Total Ca	mg kg^{-1}	1600±1200	3000±900	100±1000
Total K	mg kg^{-1}	2800±400	2600±300	400±400
Total Mg	mg kg^{-1}	900±900	1400±700	500±1200
Total P	mg kg^{-1}	1800±700	700±400	500±700

Table S3.2. General plot information. General plot information, unique identifier of each plot where data were collected, international country code (Democratic Republic of the Congo = DRC; Uganda = UG; Rwanda = RW), latitude and longitude in decimal degree (WGS 1984; Projection EPSG 4326), topographic positions, dominant soil type based on the World Reference Base for Soil Resources, geochemistry of the parent material, and sampling date.

PlotID	Country	Latitude	Longitude	Position	Soil type	Geochemistry
KBPL14	DRC	-2.31249	28.7526	plateau	Mollic Nitisols (Ochric)	mafic magmatic rock
KBPL13	DRC	-2.31379	28.75295	upper slope	Mollic Nitisols (Ochric)	mafic magmatic rock
KBPL6	DRC	-2.31398	28.7524	upper slope	Alic Nitisols (Ochric)	mafic magmatic rock
KBPL15	DRC	-2.31159	28.75269	Middle slope	Mollic Nitisols (Ochric)	mafic magmatic rock
KBPL16	DRC	-2.31153	28.75294	Middle slope	Mollic Nitisols (Ochric)	mafic magmatic rock
KBPL10	DRC	-2.31439	28.75246	valley	Mollic Nitisols (Ochric)	mafic magmatic rock
KBPL11	DRC	-2.32866	28.72988	valley	Mollic Nitisols (Vetic)	mafic magmatic rock
KBPL12	DRC	-2.32768	28.72956	valley	Mollic Nitisols (Vetic)	mafic magmatic rock
UPL1	UG	0.46225	30.37403	plateau	Haplic Lixisols (Nitic)	felsic metamorphic
UPL2	UG	0.46245	30.37347	plateau	Haplic Lixisols (Nitic)	felsic metamorphic rock
UPL3	UG	0.46271	30.37291	plateau	Haplic Lixisols (Nitic)	felsic metamorphic rock
UPL4	UG	0.46078	30.37271	upper slope	Haplic Lixisols (Nitic)	felsic metamorphic rock
UPL5	UG	0.46083	30.37356	upper slope	Sederalic Nitisols (Ochric)	felsic metamorphic rock
UPL6	UG	0.46021	30.37396	upper slope	Sederalic Nitisols (Ochric)	felsic metamorphic rock
UPL7	UG	0.48398	30.35252	middle slope	Haplic Lixisols (Nitic)	felsic metamorphic rock
UPL8	UG	0.4838	30.35238	middle slope	Haplic Lixisols (Nitic)	felsic metamorphic rock
UPL9	UG	0.48337	30.35179	middle slope	Haplic Lixisols (Nitic)	felsic metamorphic rock
UPL10	UG	0.45994	30.37355	valley	Luvic Nitisols (Endogleyic)	felsic metamorphic rock
UPL11	UG	0.46054	30.37317	valley	Luvic Nitisols (Endogleyic)	felsic metamorphic rock
UPL12	UG	0.46028	30.37242	valley	Luvic Nitisols (Endogleyic)	felsic metamorphic rock
NPL1	RW	-2.4645	29.10346	plateau	Alic Nitisols (Ochric)	sedimentary rock
NPL2	RW	-2.46337	29.09542	plateau	Acric Ferralsols (Vetic)	sedimentary rock
NPL3	RW	-2.46328	29.09489	plateau	Acric Ferralsols (Vetic)	sedimentary rock
NPL4	RW	-2.4623	29.09644	upper slope	Acric Ferralsols (Vetic)	sedimentary rock
NPL5	RW	-2.46254	29.09666	upper slope	Acric Ferralsols (Vetic)	sedimentary rock
NPL6	RW	-2.46823	29.10455	upper slope	Acric Ferralsols (Vetic)	sedimentary rock
NPL7	RW	-2.46401	29.10335	middle slope	Haplic Alisols (Nitic)	sedimentary rock
NPL8	RW	-2.46319	29.10213	middle slope	Haplic Alisols (Nitic)	sedimentary rock
NPL9	RW	-2.46381	29.09542	middle slope	Haplic Alisols (Nitic)	sedimentary rock
NPL10	RW	-2.46391	29.10289	valley	Acric Ferralsols (Gleyic)	sedimentary rock
NPL11	RW	-2.46366	29.1031	valley	Acric Ferralsols (Gleyic)	sedimentary rock
NPL12	RW	-2.46321	29.10369	valley	Acric Ferralsols (Gleyic)	sedimentary rock

Table S3.3. Forest stands characteristics across the three investigated geochemical regions Forest stands characteristics across the three investigated geochemical regions. Species richness and Shannon indices, BA: species weighted tree basal area, DBH: tree diameter at breast height, average tree height, average wood density, the average number of trees per hectare, RGR: relative tree growth rate, τ_{wood}: wood C turnover rate, $\tau_{fineroot}$ is the fine root C turnover rate MAP: mean annual precipitation, MAT: mean annual temperature, slope inclination, slope length and altitude in terms of elevation above sea level. Values presented are (Mean ± SD) and the range along topographic positions. Letters in brackets for each stand characteristic indicate significant differences following Kruskal-Wallis tests and pair-wise comparison using Dunn's test (p-value < 0.05) performed to assess differences between geochemical regions. Kruskal-Wallis tests were performed on each stand separately. Source: Project TropSOC Database Version 1.0 (Doetterl et al., 2021a,c).

		Mafic		Felsic		Sedimentary	
Parameter	Unit	Mean±SD	Range	Mean±SD	Range	Mean±SD	Range
Species richness	-	10.1±1.9 (a)	6.6-13.3	12.7±2.0 (b)	9.5-15	10.2±1.2 (a)	8.3-12.1
Shannon	-	2.2±0.3 (ab)	1.6-2.6	2.3±0.3 (b)	1.8-2.6	2.0±0.2 (a)	1.6-2.3
BA	$m^2.ha^{-1}$	37.0±10.3 (a)	25-67	35.4±9.71 (a)	16-51	51.3±10.0 (b)	38-69
DBH	cm	25.0±2.6 (a)	10-232	27.8±3.7 (ab)	10-157	30.1±2.9 (b)	10-138
Tree height	m	13.1±2.3 (a)	10-31	16.4±2.1 (b)	5-30	16.7±2.2 (b)	5-32
Wood density	$g.cm^{-3}$	0.5 ± 0.1(a)	0.2-0.8	0.6±0.1(a)	0.2-0.8	0.6±0.1(a)	0.2-0.8
Tree density	$Number.ha^{-1}$	546.9±102.9 (b)	275-706	427.1±140.0 (a)	200-713	513.0±103.4 (ab)	331-700
RGR	%	7.0±2.0 (c)	2-9	5.0±1.0 (b)	3-6	2.0±0.5 (a)	1-2
τ_{wood}	$year^{-1}$	0.06±0.01	0.02-0.08	0.04±0.009	0.03-0.06	0.02±0.005	0.006-0.02
$\tau_{fineroot}$	$year-^{1}$	0.3 ± 0.2	0.1-0.7	0.3 ± 0.1	0.1-0.4	0.5 ± 0.1	0.3-0.6
MAP	mm	1924		1702		1697	
MAT	°C	15.3	14-17	19.2	19-22	16.7	16 -17
Slope	%	21±20	3-60	21±20	3-55	31±30	3-60
Slope length	m	70 ± 56	50-170	149 ± 125	55-374	101 ± 103	55- 339
Altitude	(m) a.s.l	2220 ± 38	1919-2224	1324 ± 60	1271–1424	1909 ± 22	1891-2395

Table S3.4. Rotated principal components and their mechanistic interpretation. Rotated principal component analysis for four principal components (RC) that were retained with Eigenvalues >1 and proportion variance >10 %. Upper part of the table shows eigenvalues, proportional, cumulative variance and mechanistic interpretation of specific RCs. Bottom part represents loadings with bold marked values showing highly correlated loadings (> 0.5 or < -0.5) of each RC that was used as part of the interpretation of each variable. Blank cells indicate that variables are not represented by the corresponding RCs and the loadings of those variables onto the RC are near zero.

Rotated component		RC1	RC2	RC3	RC4
Eigenvalue		6.9	4.4	3.7	2.6
Proportion Variance (%)		33.0	21.0	17.7	12.4
Cumulative Variance (%)		33.0	54.0	71.0	84.1
Mechanistic interpretation		Soil exchangeable cations	Soil base cation stocks	Soil C:N:P stocks & NP availability	Soil texture
Independent variables	Units				
CEC	0.01 me g^{-1}	**0.5**	-0.3	**0.7**	-0.2
ECEC	0.01 me g^{-1}	**0.9**	0.2	0.2	-0.1
Exhang. potassium	0.01 me g^{-1}	**0.6**	**0.5**	0.3	0.1
Exhang. calcium	0.01 me g^{-1}	**0.9**	0.4		
Exchang. magnesium	0.01 me g^{-1}	**0.8**	0.2	0.3	-0.3
Base saturation in CEC	%	**0.9**	0.4	0.1	-0.1
Available phosphorus	mg kg^{-1}	0.3	0.4	**0.5**	0.4
Total potassium	%	0.4	**0.9**		
Total calcium	%	**0.5**	**0.8**		0.1
Total magnesium	%	**0.5**	**0.7**	0.4	0.2
TRB	%	**0.5**	**0.8**	0.2	0.2
Total phosphorus	%	-0.1	0.2	**0.8**	-0.2
pH		**0.8**	**0.5**	-0.1	
C:N		**-0.8**	-0.4		-0.2
SOC	Mg ha^{-1}	0.2	0.1	**0.9**	
Ammonium	mg kg^{-1}	**0.7**	0.2	**0.5**	
Nitrate	mg kg^{-1}		**-0.5**		0.2
Total nitrogen	%		0.1	**0.9**	0.3
Clay content	%	0.4	-0.1		**-0.8**
Silt content	%	**-0.6**			**-0.6**
Sand content	%				**1.0**

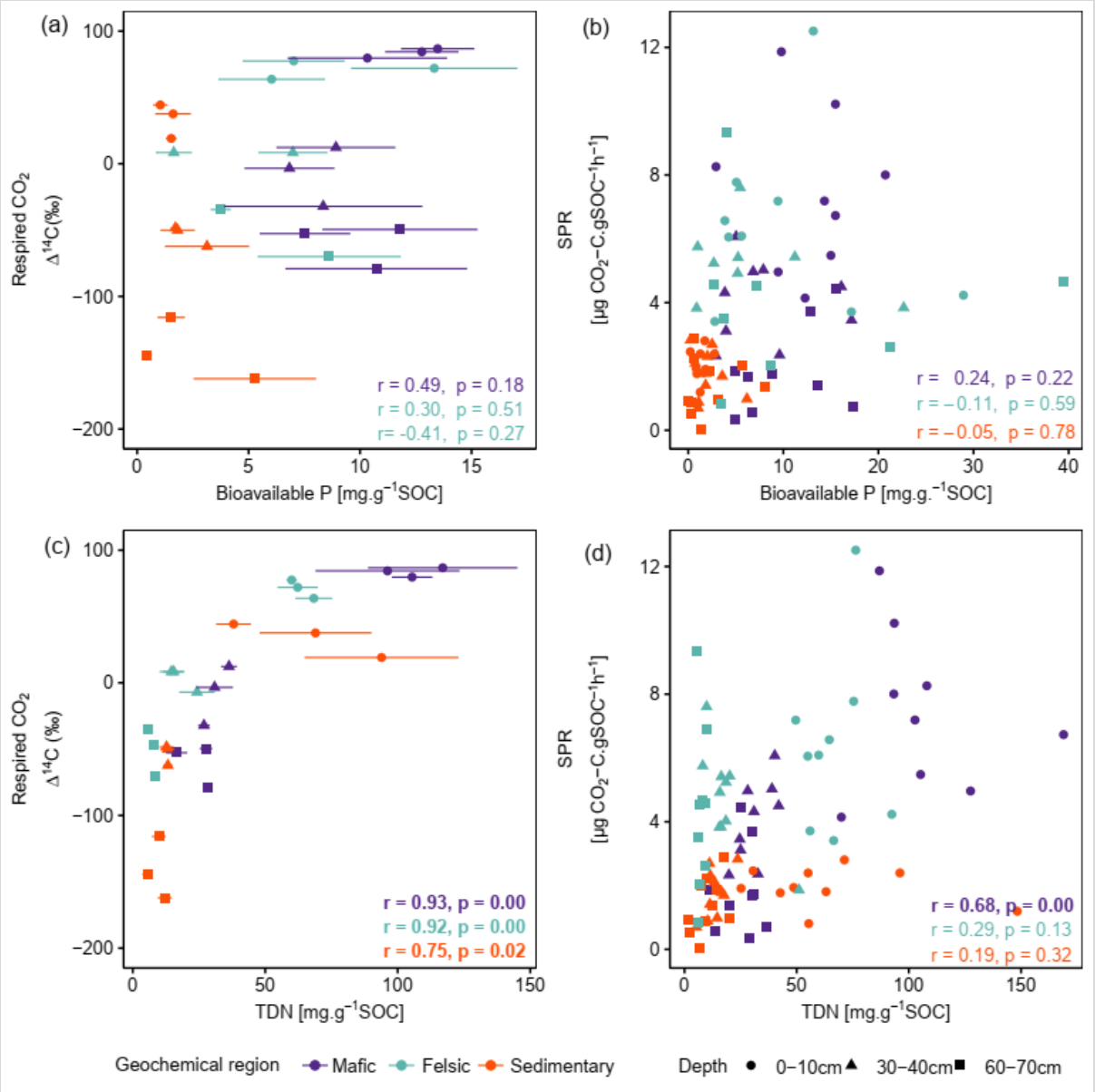

Figure S4.1. Pearson correlation between the composite of corresponding replicates of Δ14C of respired CO2 and SPR to P- (a, b) and N- (c, d) available nutrient data, reported by Doetterl et al. (2021b), normalized to SOC content for non-valley positions. Data displayed in panels (a) and (c) are averages plus standard errors of three field replicates. Panels (b) and (d) show all individual field replicates. Note that two outliers (artefacts) with high bioavailable p-values in subsoil were removed from panels (a) and (b). p-values in bold indicate significant results at $p < 0.05$. Bioavailable P is Bray P, and TDN is total dissolved nitrogen.

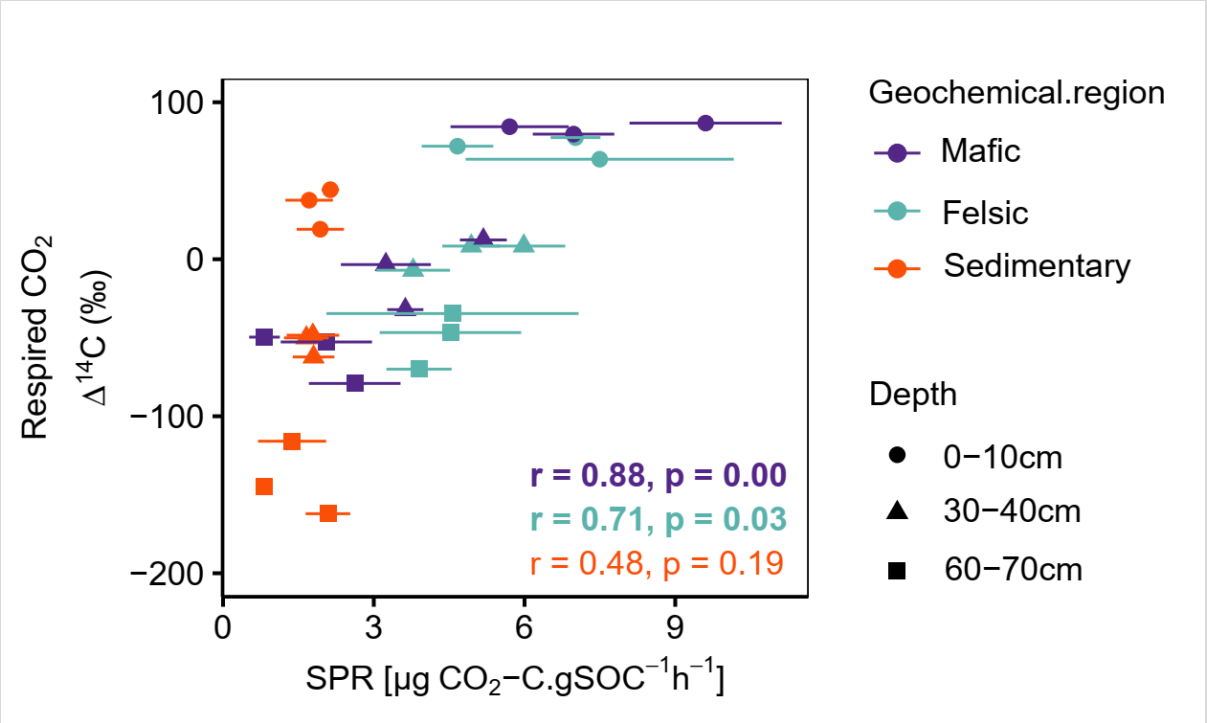

Figure S4.2. Pearson correlation between Δ14C of respired CO2 and SPR for non-valley positions. Data displayed are averages plus the standard error of three field replicates (n=85). p-values in bold indicate significant results at $p < 0.05$.

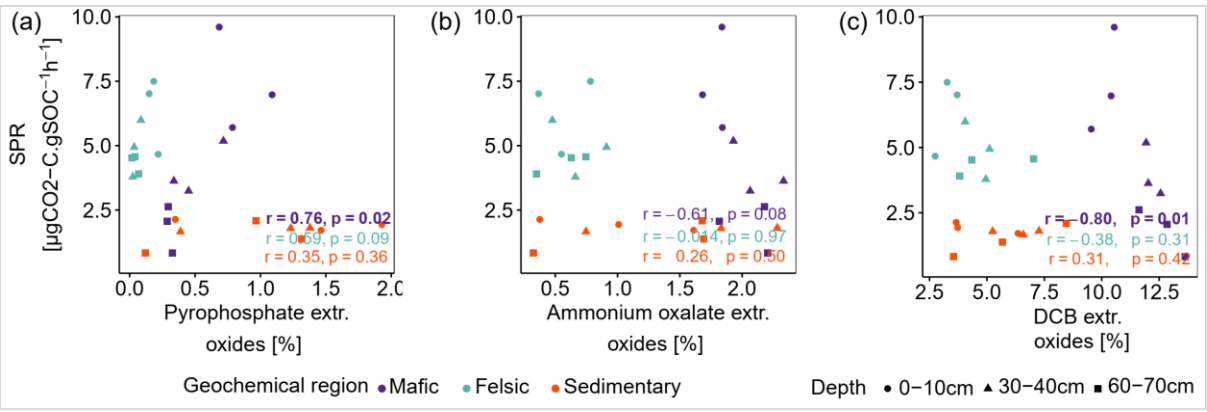

Figure S4.3. Pearson correlation between SPR and sum of pedogenic oxides (Al, Fe and Mn). (a) Sodium pyrophosphate extractable oxides, (b) ammonium oxalate-oxalic acid extractable oxides and (c) dithionite-citrate bicarbonate extractable oxides. p-values in bold indicate significant results at $p < 0.05$. Data reported by Reichenbach *et al.* (2021).

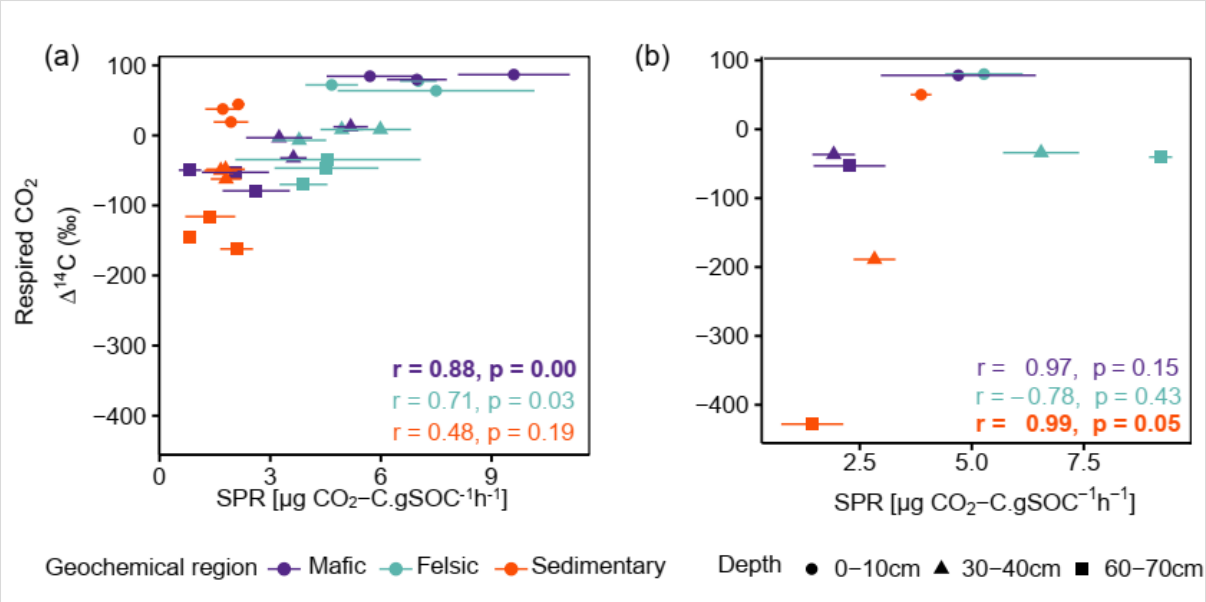

Figure S4.4. Pearson correlation between Δ14C of respired CO2 and SPR for (a) for non-valley positions and (b) for valley positions. Data displayed are averages plus the standard error of three field replicates (non-valleys n=85 and valley position n=27). p-values in bold indicate significant results at $p < 0.05$.

Table S4.1. Rotated principal component analysis for six principal components (RC) retained with eigenvalues > 1 and proportional variance > 5 %. The upper part of the table shows eigenvalues, individual and cumulative variance and mechanistic interpretation of specific RCs. The lower part represents loadings with values in bold showing the highest loadings of each RC (r > 0.5). CEC is potential cation exchange capacity, and ECEC is effective cation exchange capacity. POM is particulate organic matter.

	Rotated component		RC1	RC2	RC3	RC4	RC5
	Eigenvalue		8.0	7.5	3.4	2.6	2.4
	Proportion variance (%)		25.0	23.6	10.5	8.0	7.5
	Cumulative variance (%)		25.0	48.6	59.1	67.1	74.5
	Mechanistic interpretation		SOM and microbial activity	Soil solution chemistry	Texture	Aggregation	C:N and O horizon
	Independent variables	Units					
Microbial activity	Carbon enzymes	$nmol.g^{-1}.h^{-1}$	**0.6**	-0.1	-0.1	0.2	0.0
	Phosphorus enzymes	$nmol.g^{-1}.h^{-1}$	**0.7**	0.0	0.1	0.0	0.0
	Nitrogen enzymes	$nmol.g^{-1}.h^{-1}$	**0.6**	0.4	0.0	0.1	0.0
	Microbial biomass carbon	$mg.kg^{-1}$	**0.5**	0.3	-0.3	0.2	0.0
Nitrogen	Total dissolved nitrogen	$mg.kg^{-1}$	**0.9**	0.1	0.1	0.1	0.0
	Ammonium	$mg.kg^{-1}$	**0.9**	0.3	0.0	0.2	0.0
	Nitrate	$mg.kg^{-1}$	0.3	-0.1	0.2	0.0	0.0
	Nitrogen content	%	**1.0**	0.0	0.0	0.2	-0.1
Soil carbon	Dissolved organic carbon	$mg.kg^{-1}$	**0.8**	-0.3	-0.1	0.0	-0.1
	Carbon content	%	**0.9**	-0.2	0.1	0.1	0.0
	Soil organic carbon stock	$Mg.ha^{-1}$	**0.9**	-0.1	0.1	0.1	0.2
	C:N		-0.1	-0.1	0.0	-0.3	**0.8**
Carbon fractions	Microaggregate/silt and clay	%	0.2	0.2	0.0	**0.9**	-0.1
	Relative amount of POM	%	0.0	0.1	**0.6**	0.1	0.2
	Relative amount of microaggregate	%	0.2	0.1	-0.3	**0.8**	-0.3
	Relative amount of silt and clay	%	-0.1	-0.1	-0.2	**-0.8**	0.1
Soil fertility	Exchangeable acidity	$me.100g^{-1}$	0.3	**-0.9**	0.0	0.0	0.0
	Exchangeable bases	$me.100g^{-1}$	0.3	**0.9**	0.1	0.1	-0.1
	Cations exchange capacity	$me.100g^{-1}$	**0.7**	-0.2	-0.4	0.2	-0.3
	Effective cations exchange capacity	$me.100g^{-1}$	**0.6**	**0.7**	0.1	0.1	-0.1
	Base saturation in ECEC	%	0.0	**0.9**	0.1	0.1	-0.3
	Base saturation in CEC	%	0.0	**1.0**	0.2	0.0	-0.1
	pH		-0.1	**0.9**	0.0	0.1	-0.1
	Plant available phosphorus	$mg.kg^{-1}$	**0.5**	**0.3**	0.0	-0.2	-0.3
Clay activity	pH:Clay		0.0	**0.5**	**0.8**	0.0	0.0
	Base saturation in ECEC/ Clay		0.0	**0.9**	0.3	0.1	-0.2
	Base saturation in CEC/clay		0.0	**0.9**	0.3	0.0	-0.1
Texture	Clay	%	-0.1	-0.2	**-0.9**	0.1	-0.2
	Silt	%	0.1	-0.3	-0.1	-0.1	**0.9**
	Sand	%	0.0	0.3	**0.9**	0.0	-0.3
Carbon input	O horizon C stock	$Mg.ha^{-1}$	0.0	-0.5	0.2	-0.2	**0.6**

Table S4.2. Overview of soil properties and fertility indicators for the three geochemical regions and depth intervals. $Base_{exc}$ is the sum of exchangeable bases, CEC is potential cation exchange capacity and ECEC is effective cation exchange capacity. pHKCl is the soil pH measured with potassium chloride, and bio-P is bioavailable phosphorus (Bray P method). Values reported are averages plus standard deviations (n=85). Source: Project TropSOC Database Version 1.0 (Doetterl et al., 2021b).

Geochemical region	Depth [cm]	$Base_{exc}$ [me.100g^{-1}]	CEC [me.100g^{-1}]	ECEC [me.100g^{-1}]	pH_{KCl}	Bio-P [mg.kg^{-1}]	TDN [mg.kg^{-1}]	Clay [%]	Silt [%]	Sand [%]
	0-10	17.2±3.6	19.3±3.4	18.1±3.8	5.3±0.6	20.1±13.5	141.0±21.7	35±4	10±2	54±5
Felsic	30-40	6.5±1.5	12.3±1.8	7.6±1.2	4.7±0.7	13.8±19.1	14.4±7.5	41±11	8±2	51±10
	60-70	5.1±2.2	11.2±2.5	6.5±1.5	4.4±0.7	9.6±13.9	3.8±1.3	49±9	7±3	44±8
	0-10	7.2±7.3	42.6±8.2	12.1±4.9	3.6±0.6	30.8±12.4	263.8±100.1	54±9	14±4	33±11
Mafic	30-40	2.6±2.7	32.6±2.8	7.6±1.3	3.6±0.3	11.3±6.5	44.7±13.9	66±7	14±4	20±4
	60-70	1.1±0.7	31.7±4.1	6.7±1.0	3.5±0.2	11.0±5.2	26.2±5.9	67±3	13±4	20±3
	0-10	0.3±0.1	23.1±9.6	8.3±1.5	3.0±0.2	2.9±1.9	140.8±87.5	36±12	20±9.	44±18
Mixed	30-40	0.2±0.1	14.8±5.5	4.9±0.9	3.6±0.2	3.4±2.9	20.1±6	49±14	19±8	32±14
	60-70	0.2±0.1	12.5±6.7	3.8±0.7	3.7±0.1	2.5±3.19	10.6±5.8	50±14	21±13	29±14

Scientific contributions

Bukombe B, Bauters M, Boeckx P, Cizungu LN, Cooper M, Fiener P, Kidinda LK, Makelele I, Muhindo DI, Rewald B, Verheyen, K., Doetterl, S. 2022. Soil geochemistry – and not topography – as a major driver of carbon allocation, stocks, and dynamics in forests and soils of African tropical montane ecosystems. *New Phytologist* 236: 1676–1690. https://doi.org/10.1111/nph.18469.

Bukombe B, Fiener P, Hoyt AM, Kidinda LK, Doetterl S. 2021. Heterotrophic soil respiration and carbon cycling in geochemically distinct African tropical forest soils. *SOIL* 7: 639–659. https://doi.org/10.5194/soil-7-639-2021.

Doetterl S, Asifiwe RK, Baert G, Bamba F, Bauters M, Boeckx P, Bukombe B, Cadisch G, Cooper M, Cizungu LN, Hoyt, A., Kabaseke, C., Kalbitz, K., Kidinda, L., Maier, A., Mainka, M., Mayrock, J., Muhindo, D., Mujinya, B.B., Mukotanyi, S.M., Nabahungu, L., Reichenbach, M., Rewald, B., Six, J., Stegmann, A., Summerauer, L., Unseld, R., Vanlauwe, B., Van Oost, K., Verheyen, K., Vogel, C., Wilken, F., Fiener, P. 2021a. Organic matter cycling along geochemical, geomorphic, and disturbance gradients in forest and cropland of the African Tropics -- project TropSOC database version 1.0. *Earth System Science Data* **13**: 4133–4153. https://doi.org/10.5194/essd-13-4133-2021.

Doetterl S, Bukombe B, Cooper M, Kidinda L, Muhindo D, Reichenbach M, Stegmann A, Summerauer L, Wilken F, Fiener P. **2021c**. TropSOC Database. V. 1.0. *GFZ Data Services*. https://doi.org/10.5880/FIDGEO.2021.009.

Kidinda LK, Doetterl S, Kalbitz K, Bukombe B, Babin D, Mujinya BB, Vogel C. 2023. Relationships between geochemical properties and microbial nutrient acquisition in tropical forest and cropland soils. *Appl. Soil Ecol.*181: 104653. https://doi.org/10.1016/j.apsoil.2022.104653.

Kidinda LK, Olagoke FK, Vogel C, Bukombe B, Kalbitz K, Doetterl S. 2022. Microbial properties in tropical montane forest soils developed from contrasting parent material—An incubation experiment. J. Plant Nutr. Soil Sci. 185, 807–820. https://doi.org/10.1002/jpln.202100274.

Summerauer L, Baumann P, Ramirez-Lopez L, Barthel M, Bauters M, Bukombe B, Reichenbach M, Boeckx P, Kearsley E, Van Oost K, Vanlauwe, B., Chiragaga, D., Heri-Kazi, A.B., Moonen, P., Sila, A., Shepherd, K., Bazirake Mujinya, B., Van Ranst, E., Baert, G., Doetterl, S., Six, J. 2021. The central African soil spectral library: a new soil infrared repository and a geographical prediction analysis. *SOIL* 7: 693–715. https://doi.org/10.5194/soil-7-693-2021.